

Selected insulin-like peptides influence *Caenorhabditis elegans* locomotion in different ways

Nele VAN HOUT

Supervisor: Prof. Dr. W. Schafer
Animal physiology and Neurobiology

Co-supervisor: Prof. Dr. L. Temmerman
Animal physiology and Neurobiology

Mentor: B. Cockx
Animal physiology and Neurobiology

Thesis presented in
fulfillment of the requirements
for the degree of Master of Science
in Biology

Academic year 2020-2021

© Copyright by KU Leuven

Without written permission of the promoters and the authors it is forbidden to reproduce or adapt in any form or by any means any part of this publication. Requests for obtaining the right to reproduce or utilize parts of this publication should be addressed to KU Leuven, Faculteit Wetenschappen, Celestijnenlaan 200H - bus 2100, 3001 Leuven (Heverlee), Telephone +32 16 32 14 01.

A written permission of the promoter is also required to use the methods, products, schematics and programs described in this work for industrial or commercial use, and for submitting this publication in scientific contests.

Host lab information page

Master theses performed in the Temmerman lab comply with following house rules:

1. Maximal education and scientific self-empowerment of students

Students are encouraged to learn from their mistakes through dialogue, rather than by simply being corrected by their supervisors. All writing in this document is the result of this process.

Students get two feedback moments with respect to their writing process. One from their daily supervisor, who will advise them on format and content (e.g. scientific language, proper representation of results and structure of their interpretations). For this, daily supervisors interact either in person with the student, or via comments added to the manuscript. Under no circumstances do they rephrase sections of the text, which is entirely the student's wording. A second feedback session includes comments from (co)supervisors and only focuses on content. This implicates additional input with regards to the student's findings and the final discussion of results. The student's interpretation of this feedback is integrated in the final version of this manuscript, as it is presented here.

2. Authenticity in science

Potential plagiarism was verified using TurnItIn. This work overall scored 19% of potential plagiarism. Sections underlying this result were manually verified by the daily supervisor, as such supporting the authenticity of this work.

ACKNOWLEDGEMENTS

During this project, working in the Laboratory of Functional Genomics and Proteomics, I got the chance to develop myself as a scientist and deepen my interest for scientific research. Neurobiology has always been one of the disciplines that drew my attention. Now, putting it into practice has been really interesting and educational for me. Therefore, I am very grateful for everyone that made this journey possible and guided me along.

In the first place, I would like to thank my promoter Prof. Dr. William Schafer and co-promoter Prof. Dr. Liesbet Temmerman for their guidance and advice during this entire year. Although the practical arrangements of the project were not evident and changed throughout the year due to the COVID-19 pandemic, their support and direction ensured a proper course. Special thanks go out to my daily supervisor Bram. For the statistical support and critically reviewing my work, but mainly for his support in the lab, as he was always ready to answer any of my questions.

I cannot forget to thank all the other students in the lab, for the daily catch-up, and my roommates. My sisters Jo and Kaat, being always ready to talk, laugh, have some fun, or just chill with each other. Thanks Jo, for the weekly lunches and numerous chats, having more and more to talk about every time. And Kaat, for your playlists that I devoured the last months. Also, a big thank you to Kaat DC for always checking in with me even though it was so hard to see each other in real life.

Very special thanks go out to my parents, for their support during my whole master's degree. Thanks for all the advice when I needed to make hard decisions, the understanding when I changed those decisions, the freedom you gave me, and the trust you both put in me. This year was the final hurdle, but I could not have done it without all those relieving talks in the car, the numerous dinners that were set apart for me, the office space that I could casually call mine, the willingness to listen to me about the same things repeatedly, and the flexible environment you provided. I am very grateful for your unconditional support and perspective.

And last but not least, thank you Matthijs, for putting up with my chaotic brain at times, for listening to me when I was overwhelmed, for your reassurance, and most importantly, for every smile you brought to my face.

TABLE OF CONTENTS

ACKNOWLEDGEMENTS	I
TABLE OF CONTENTS	II
ABBREVIATIONS	V
SUMMARY	VII
INTRODUCTION	1
1. GENERAL INTRODUCTION OF INSULIN.....	1
1.1. <i>Insulin functioning</i>	1
1.2. <i>Insulin superfamily</i>	3
1.3. <i>Insulin in invertebrates</i>	5
1.4. <i>Structure conservation</i>	5
2. <i>C. ELEGANS</i> AS A MODEL ORGANISM.....	6
2.1. <i>Life cycle of C. elegans</i>	7
2.2. <i>Neuropeptides in C. elegans</i>	8
2.3. <i>Neuropeptide processing</i>	8
2.4. <i>Neuropeptide release</i>	10
3. INSULIN-LIKE PEPTIDES IN <i>C. ELEGANS</i>	11
4. FUNCTIONS OF INSULIN-LIKE PEPTIDES IN <i>C. ELEGANS</i>	12
5. MOLECULAR PATHWAYS CONNECTED WITH ILP SIGNALLING	13
6. DAUER STAGE IN <i>C. ELEGANS</i>	15
6.1. <i>Dauer characteristics</i>	16
7. NICTATION BEHAVIOUR IN <i>C. ELEGANS</i>	16
RESEARCH OUTLINE	19
MATERIALS AND METHODS	20
1. GENERAL <i>C. ELEGANS</i> TECHNIQUES	20
1.1. <i>Strains and growth conditions</i>	20
1.2. <i>Culturing of C. elegans on Nematode Growth Medium</i>	21
1.2.1. Preparation of NGM plates	21
1.2.2. Preparation of liquid <i>E. Coli</i> OP50 culture.....	21
1.2.3. Seeding of NGM plates with liquid <i>E. Coli</i> OP50 culture	21
1.2.4. Culturing of <i>C. elegans</i> hermaphrodites	22
1.2.5. Culturing of <i>C. elegans</i> males	22
1.2.6. Management of contamination.....	22
1.3. <i>Synchronizing C. elegans populations by bleaching</i>	23
1.4. <i>Freezing and recovery of C. elegans stocks</i>	23
1.5. <i>Determining genotype by PCR and agarose gel electrophoresis</i>	24
2. NICTATION ASSAYS.....	25

2.1. Preparation of microdirt chips	26
2.2. Grow dauers by starvation.....	26
2.3. Male assay	27
2.4. Statistical analysis	27
2.5. COPAS	28
3. LOCOMOTION ASSAYS.....	28
3.1. Statistical analysis	29
4. LOCALIZATION	29
5. IN SILICO ANALYSIS.....	30
RESULTS	31
1. NICTATION BEHAVIOUR.....	31
1.1. Some of the selected INS peptides affect nictation behaviour in hermaphrodites.....	31
1.1.1. COPAS treatment does not affect nictation behaviour of hermaphrodites	41
1.2. Males do not display nictation like dauers do	41
2. LOCOMOTION IS NOT AFFECTED BY THE SELECTED INS PEPTIDES IN HERMAPHRODITES	42
3. INSULIN EXPRESSION	45
3.1. Localization of the selected INS peptides in L3 juveniles and dauers.....	45
3.2. In silico meta-analysis.....	48
DISCUSSION	50
1. BEHAVIOURAL PHENOTYPES IN HERMAPHRODITES.....	50
1.1. Nictation behaviour.....	50
1.1.1. Dauer development and COPAS handling.....	50
1.1.2. Antagonists versus agonists	51
1.2. Locomotion behaviour.....	52
1.3. Insulin expression patterns	52
CONCLUSION.....	54
REFERENCES	56
APPENDICES.....	I
1. RISK ANALYSIS	I
2. BUFFERS AND SOLUTIONS	III
3. INSULIN EXPRESSION PATTERNS.....	V
3.1. Neuron expression expressed in percentages.....	V
4. POST-HOC ANALYSIS P-VALUES OF NICTATION ASSAYS	XI

ABBREVIATIONS

AIC	Akaike information criterion
Akt	Serine/threonine kinase 1
ASNA-1	Arsenite-translocating ATPase-1
BBB	Blood-brain barrier
bp	Base pairs
CAPS	Calcium-dependent activator protein
CGC	<i>Caenorhabditis</i> Genetics Centre
CNS	Central nervous system
COPAS	Complex object parametric analyser and sorter
DAF	Abnormal dauer formation
DMSO	Dimethylsulfoxide
EDTA	Ethylenediaminetetraacetic acid
FLP	FMRFamide (Phe-Met-Arg-Phe-NH ₂)-related peptide
FOXO	Forkhead box O
GABAergic	Gamma-aminobutyric acid-ergic
gDNA	Genomic DNA
GFP	Green Fluorescent Protein
GH	Growth hormone
GPCR	G protein-coupled receptor
IGF	Insulin-like growth factors
IGF-1	Insulin-like growth factor 1
IGFR	Insulin/IGF-1 transmembrane receptor
IIS	Insulin/insulin-like growth factor signalling pathway
ILP	Insulin-like peptide
INS	Insulin-like peptide
IRS	Insulin receptor substrate (family of scaffold proteins)
kb	kilobase
KO	Knock-out
LB	Lysogeny Broth
MAPK	Mitogen-activated protein kinase
mRNA	Messenger RNA
NGM	Basal Nematode Growth Medium

NLP	Neuropeptide like peptide
OD	Optical density
OE	Overexpression
PC	Proprotein convertases
PCR	polymerase chain reaction
PDK	Phosphoinositide-dependent kinase
PDMS	Polydimethylsiloxane
PI3K	Phosphoinositide 3-kinase
PIP2	Phosphatidylinositol 4,5-bisphosphate
PIP3	Phosphatidylinositol 3,4,5-trisphosphate
RER	Rough endoplasmic reticulum
TAE	Tris-acetate-EDTA
TCA	Tricarboxylic acid cycle
TF	Transcription factor
TOR	Target of rapamycin

SUMMARY

Insulin-like peptides (ILP) are widely distributed in phylogeny and have highly conserved roles in physiology and development throughout the animal kingdom. The *C. elegans* genome encodes 40 insulin-like peptides, primarily expressed in the nervous system. The large amount of ILPs present in *C. elegans*, compared to 10 insulin-like peptides in human, suggests some functional diversification. In *C. elegans* ILPs are known to be key modulators in diverse processes. They function as both agonists and antagonists of the insulin/insulin-like growth factor (IIS) pathway, which in turn regulates numerous biological activities including dauer formation, lifespan, reproduction and more. But all these peptides are thought to bind to just one receptor, the tyrosine kinase receptor DAF-2. However, these ILPs show broad regulatory and functional diversification in *C. elegans*, resulting in a unique and context-dependent set of functions for each insulin-like peptide.

In this thesis project we wanted to unravel more functions of the ILPs in *C. elegans*. To do this, we focused on a behaviour specific for the alternative developmental stage of *C. elegans*, the dauer stage. The dauer stage itself is a developmental arrest that occurs in harsh environmental conditions and can be triggered by a multitude of signals. Genomic analysis of dauer arrest has already elucidated an important role for pathway crosstalk in dauer regulation. One of the pathways regulating the dauer stage is the IIS pathway. Together with the knowledge that a lot of neurons that sense the triggering signals for dauer development express ILPs, research focusing on this stage could possibly clear up ILP functioning some more.

The IIS pathway is also known to affect nictation, which is a characteristic behaviour for dauers. In our experiments we tested the effect of different ILP mutants on this behaviour, to discover possible roles of insulin genes in its behaviour. Nictation ratio, nictation initiation and the average duration of nictation were quantified for knockout strains of *ins-1*, *ins-4*, *ins-6*, *ins-17* and *ins-19*, and insulin overexpression strains of *ins-15*, *ins-17*, *ins-19*, *ins-21*, *ins-36*, *ins-37*, *ins-38*, and *ins-39*. The locomotion of these strains was also tested to rule out any underlying deficits that could influence the results of their nictation assays. To link the presence of these ILPs in specific neurons to probable functions, cellular localization experiments were carried out.

The elucidation of ILP functioning can further resolve the regulation of the dauer stage and IIS functioning itself. Thereby leading to insights in *C. elegans*' complex neuronal and molecular pathways underlying its behaviour.

INTRODUCTION

This thesis project tries to elucidate the functioning of *Caenorhabditis elegans* insulin-like peptides. First, a general overview of insulin is given, where the functioning of insulin in humans and other vertebrates is reviewed. Because insulin-like peptides are also present in invertebrates, the next section talks about this subject, and how that these different insulin peptides in vertebrates and invertebrates are related with each other. We then elucidate further on the invertebrate *C. elegans*, as this is the model organisms used for our experiments. The general anatomy and life cycle of *C. elegans* are explained, as are the processing and release of its neuropeptides, such as the insulin-like peptides. The functioning of these insulin-like peptides and their molecular pathways are then discussed. Finally, the focus lies on a specific alternative stage of *C. elegans* development, the dauer stage. This stage has some specific characteristics, one of them being a specific behaviour. It is this behaviour that was used to score phenotypes in our experiments.

1. General introduction of insulin

The discovery of insulin in 1922 by Banting and Best represented a milestone in clinical medicine, where it was used in the treatment of diabetes. It was the first protein whose primary amino acid sequence was determined (Ryle, Sanger, Smith, & Kitai, 1955), the first hormone whose 3-D crystal structure was solved (Adams et al., 1969) and proinsulin was the first hormone precursor discovered (Steiner, Cunningham, Spigelman, & Aten, 1967). Hence, gaining knowledge on insulin also contributed extensively to the fields of molecular and comparative endocrinology.

1.1. Insulin functioning

Insulin is a phylogenetically old molecule, most known for its hormonal function in the mammalian body, regulating carbohydrate metabolism. Here, the peptide is released in the bloodstream by the beta cells of the islets of Langerhans in the pancreas upon elevated blood glucose levels. It acts primarily to stimulate glucose uptake in the adipose tissue, muscle cells and liver, all tissues important in the metabolism and storage of nutrients (Norris & Carr, 2013; Utiger, 2020). This hypoglycaemic response is only one of the effects insulin has on storage and mobilization of energy. It will also promote the use of sugar as an energy source, reduce gluconeogenesis, stimulates the storage of excess carbohydrates as glycogen, reduce the usage of fat as an energy source and promote its storage. Further, it will promote the formation of proteins from amino acids and reduce the use of protein as an energy source, making it the main anabolic hormone of the body (Barrington, 2020; Norris & Carr, 2013).

Although liver, muscle and adipose tissue are most sensitive to insulin, almost all other cell types are also responsive. In the brain, insulin receptors are widely expressed and distributed. Although they share a high resemblance with the peripheral receptors, brain insulin receptors have a slightly lower molecular weight and do not show a downregulation after exposure to high insulin levels (Duarte, Moreira, & Oliveira, 2012). Insulin itself can be transferred from the bloodstream to the cerebrospinal fluid in the central nervous system (CNS) via the blood-brain barrier (BBB). Here, the active transport of the hormone is mediated by insulin receptors in the endothelial cells of the barrier system (Duarte et al., 2012; Gerozissis, 2003). In the peripheral and central nervous system

insulin acts as an important neuromodulator and can reach high levels, exerting long-term trophic effects on the CNS neurons (Duarte et al., 2012; Schechter et al., 1992; Schulingkamp, Pagano, Hung, & Raffa, 2000). Brain insulin levels change during development, being the highest in fetal and neonatal stage and decreasing in the adult brain (Schechter et al., 1992). In the central nervous system insulin plays a major physiological role, contributing to the control of nutrient homeostasis, reproduction, cognition, memory and mood as well as to neurotrophic, neuromodulatory, and neuroprotective effects (Blázquez, Velázquez, Hurtado-Carneiro, & Ruiz-Albusac, 2014; Gerozissis, 2003; S. H. Lee, Zabolotny, Huang, Lee, & Kim, 2016). Disturbances in insulin functioning are involved in certain neurodegenerative diseases such as Alzheimer's disease (Blázquez et al., 2014). Moreover, insulin promotes neurite outgrowth and stimulates axon growth by stabilization of tubulin mRNA levels, overall regulating axonal growth, development and regeneration in the central and the peripheral nervous system (Lázár, Jancsó, & Sántha, 2020). The source of insulin in the brain, however, is still under discussion as it can be explained by *de novo* synthesis in the brain itself, crossing of the BBB, or both (Blázquez et al., 2014; Gerozissis, 2003).

Insulin is a conserved protein with only a few amino acid substitutions located at critical sites related to its own structure and biological activity. The peptide is composed of two chains, the A chain and the B chain, linked together by disulfide bonds (Fig.1). However, it is first synthesized as a single-chain precursor, preproinsulin, whose proteolytic processing is coupled to trafficking between cellular compartments (Weiss, Steiner, & Philipson, 2014). First, a 24-residue signal peptide directs preproinsulin to the rough endoplasmic reticulum (RER). Here, the signal peptide is cleaved off and proinsulin is formed in its correct conformation with three newly formed disulfide bonds. Next, proinsulin is transported to the trans-Golgi network where it undergoes maturation into active insulin. During this maturation process the connecting (C) domain, that lies within the A chain, of proinsulin is removed by a specialized set of endoproteases and a carboxypeptidase. The remaining insulin peptide thus consists of two peptide chains, the A and B chains, linked by two disulfide bonds. Vertebrate insulin A chains consist of 21 or 22 amino acids, and B chains of 31 to 38 amino acids. When insulins of different vertebrate classes are compared, the B chain is more variable in its number of amino acids (Weiss et al., 2014).

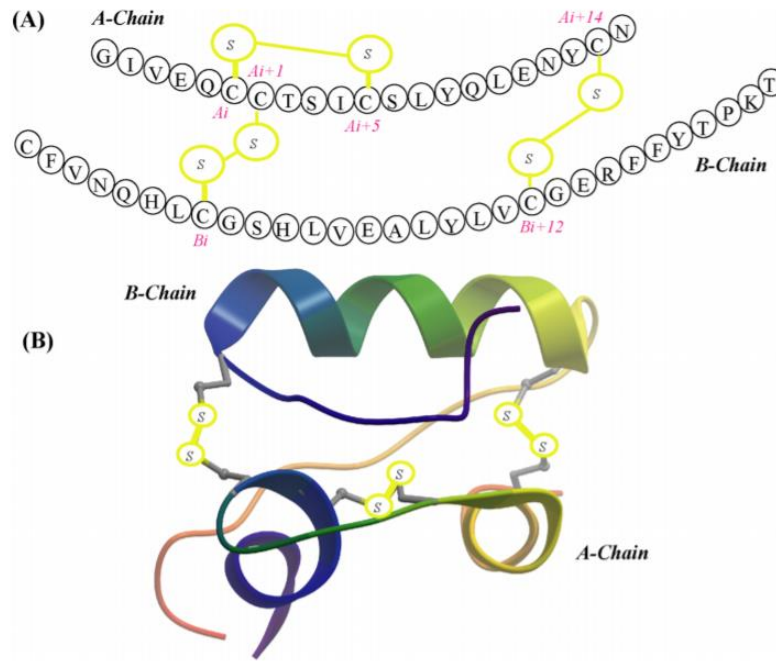


Figure 1: (A) Primary structure of human insulin showing the disposition of the two disulfide bonds between the A and B chain. (B) The tertiary structure of human insulin. Adopted from (Hossain & Wade, 2017)

1.2. Insulin superfamily

There are peptides that exhibit sequence and structure similarity to insulin, specifically to its disulfide bond distribution. This suggests a common ancestral gene and the term 'insulin superfamily' is used to describe all its presumed descendants (Schwabe & McDonald, 1977; Separovic, Wade, & Shabanpoor, 2009). In humans, relaxin was the first hormone to be structurally linked to insulin (Schwabe & McDonald, 1977). Relaxin is important for reproduction and the cardiovascular system (Bani, 1997). Later, insulin-like growth factors (IGF) were also assigned to the human insulin superfamily. Although these are single chain peptides, they are also crosslinked by 3 disulfide bridges and have a high binding affinity for the insulin receptor (Annunziata, Granata, & Ghigo, 2011). Besides their structural similarity to insulin, IGF's also have insulin-like actions in some tissues (Utiger, 2011). They function downstream of growth hormone (GH) promoting tissue growth and maturation through the upregulation of anabolic processes. They are mainly synthesized and secreted by the liver, but their receptors are distributed in almost all tissues. Local synthesis is also possible in some tissues, including the brain, bone and adipose tissue (Annunziata et al., 2011; Utiger, 2011). IGF-II is an highly regulated and important primary growth factor in early development, and its secretion decreases after the fetal stage (Chao & D'Amore, 2008). IGF-I on the other hand is a major growth factor in adults stimulating cell proliferation and inhibiting cell death (Laron, 2001). It also regulates neural development and has a role in brain development and aging (Ishii, 1993; Wrigley, Arafa, & Tropea, 2017). Overall the human insulin superfamily consists of ten members: insulin, insulin-like growth factors I and II, and a relaxin subfamily that comprises relaxin-1, -2 and -3 and four other insulin-like peptides (INSL 3, 4, 5 and 6) (Hossain & Wade, 2017). Although they all share a similar structure (Fig. 2), their functioning and biological activity is diverse, varying from metabolic control to cardiovascular biology, and collagen homeostasis (Separovic et al., 2009).

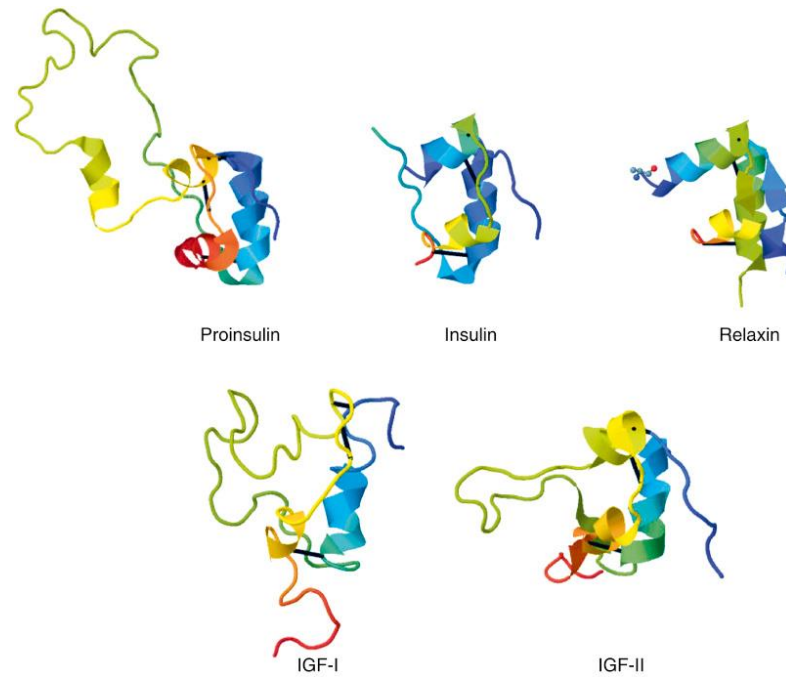


Figure 2: Colorized representation of insulin superfamily peptides in human (amino terminus in blue, carboxy terminus in red). Disulfide bonds are indicated by the thick black lines. Peptides modelled by protein data base structures (human pro-insulin, code 2KQP; human T insulin, code 1MSO; human relaxin, code 6RLX; human IGF-I, code 1BQT; human IGF-II, code 1IGL). Adopted from (Norris & Carr, 2013).

This large protein family is not constricted to humans or mammals. After its discovery, it was soon discovered that the hormone was widely distributed in phylogeny. By the mid-1970s, insulin had been isolated and sequenced in all classes of vertebrates, even in the class Agnata, or the jawless vertebrates which are considered to be the most evolutionary ancient vertebrates (Chan & Steiner, 2000). The insulin protein structure has been highly conserved during vertebrate evolution, together with its gene organization, which contains three exons and two introns in almost all vertebrates (Chan & Steiner, 2000). Over time, insulin-like peptides were also found in cephalochordates, mollusks, insects, nematodes and even in unicellular organisms (Csaba, 2013; Guo, Qiao, & Feng, 2008). Although these peptides have certain physiological activities similar to insulin, their secretion sites are different, and they possess various functions. Whereas the primary function of insulin is to maintain constant blood glucose levels, essential for normal central nervous system activity, the functioning of insulin in nonmammalian vertebrates is less well characterized (Chan & Steiner, 2000). However, the essence of their functioning seems to be conserved to regulating the anabolic switch. Overall, these findings suggest that the insulin superfamily is an evolutionary ancient and omnipresent group of peptides with varied physiological activities found throughout the animal kingdom.

1.3. Insulin in invertebrates

The first invertebrate insulin-like peptide was discovered in *Bombyx mori* (Linnaeus, 1758), the silkworm, and named bombyxinA2 (Nagasawa et al., 1986). The peptide showed the typical insulin structure of two nonidentical peptide chains crosslinked highly conserved cysteine residues forming disulfide bonds. Although bombyxinA2 only shared 40% sequence identity to human insulin, these structural similarities indicated that the peptide belonged to the insulin superfamily (Nagamatsu, Chan, Falkmers, & Steiner, 1991; Nagasawa et al., 1986).

In invertebrates, insulin-like peptides are not single copy genes but instead typically belong to gene families with several members. The reason for this expansion in gene numbers is unknown (Chan & Steiner, 2000). Moreover, invertebrates' insulin-like peptides function as neuroendocrine hormones promoting mitotic growth and development. In vertebrates, IGF-I and -II take on the role for mitotic growth, while insulin has acquired the primary function of a metabolic regulatory hormone. This functional divergence could take place due to a gene duplication event early in the vertebrate evolution. When comparing the structure and function of vertebrate insulin and IGF and invertebrate insulin-like peptides, a dichotomy emerges. The invertebrate insulin-like peptides generally have a two-chain structure, characteristic for the vertebrate insulin, but their described functions are more reminiscent of the single-chain IGF, acting as mitotic growth factors (Chan & Steiner, 2000).

1.4. Structure conservation

The discovery of insulin-like peptides in invertebrates confirms the hypothesis of an early origin and widespread evolution of the insulin superfamily. The amino acid sequence of insulin itself has been determined for around 100 vertebrate species, showing a highly conserved structure during its vertebrate evolution (Conlon, 2001; Ebberink, Smit, & Van Minnen, 1989). However, the sequence conservation is low with only 16 amino acids being conserved during vertebrate evolution. These conserved amino acids are all related to structure, receptor interaction or maintaining receptor-binding conformation (Conlon, 2001). The sequence similarity between vertebrate and invertebrate insulin-like peptides is low. Their structure, however, is also conserved in the same manner as it is in vertebrate evolution. With the conservation of amino acids related to structure (Ebberink et al., 1989). Still all these peptides are considered part of one superfamily because of a common amino acid sequence characteristic that is absolutely conserved, the insulin structural motif. This structural motif consists of six cysteine residues and a glycine residue (Fig. 3) (Ebberink et al., 1989; Guo et al., 2008; Separovic et al., 2009).

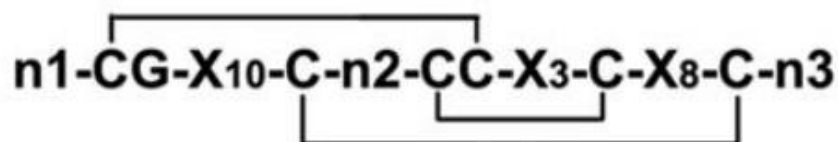


Figure 3: the putative insulin structural motif. Adopted from (Guo et al., 2008).

The conserved cysteine residues will form three disulfide bridges, one intramolecular cross-link within the A-chain, and two intermolecular between the A- and B- chains (fig. 1). These bridges are crucial for the native structure of the protein and responsible for conveying an overall similar tertiary structure (Guo et al., 2008; Separovic et al., 2009). So overall, the insulin structural motif, a shared identical cysteine-distribution pattern, is the basis of the identical disulfide linkage, similar tertiary structures and even of common characteristics in the *in vitro* folding pathways of the members of the insulin superfamily (Guo et al., 2008).

2. *C. elegans* as a model organism

This thesis project focuses on insulin-like peptides in the model organism *C. elegans*. Here, this organism is first introduced to then continue introducing current knowledge on insulin-like peptide signalling in *C. elegans*.

A multitude of insulin-like peptides have been found in the model organism *C. elegans*. This nematode is a small, free-living roundworm measuring about 1mm in length and 80µm in diameter (Altun & Hall, 2009a). In the wild, it can be found worldwide in rich soils or compost, predominantly in humid temperate areas. Here, *C. elegans* feeds and reproduces itself in decomposing plant materials rich in bacteria, such as fruits, flowers and stems (Frézal & Félix, 2015).

C. elegans was introduced by Sydney Brenner as a model organism in 1965, when he used it to study the nervous system and embryonic development (Corsi, Wightman, & Chalfie, 2015). The worm has two sexes, hermaphrodite, and male, and whereas hermaphrodites can self-fertilize, they can also mate with males. These nematodes can quickly reproduce themselves as their life cycle only encompasses 3.5 days (Corsi et al., 2015). Although *C. elegans* has a simple body plan, consisting of exactly 959 somatic cells in adults. The worm possesses many of the tissues found in architecturally more complex animals (e.g. muscles, nervous system, gonads, epidermis and gastrointestinal tract), but each radically simplified (Jorgensen & Mango, 2002); this is also true for its nervous system, which comprises only 302 neurons (Kosinski & Zaremba, 2007). Many of the molecular signals controlling its development are also found in other organisms, like humans (Yokoyama, 2020). Together with their large offspring quantities, these qualities make *C. elegans* an appealing model organism for genetic and developmental research. So, over the years, numerous genetic research tools were developed. *C. elegans* was also the first multicellular organism to have its genome fully sequenced (Jorgensen & Mango, 2002). Also, the connectome, or the pattern of neuron connections, has been completely mapped (Cook et al., 2019; Watts & Strogatz, 1998; White, Southgate, Thomson, & Brenner, 1986), containing a degree of information about neural connectivity unparalleled in any organism. Moreover, in *C. elegans* this mapping extends to all the cells. Additionally, there have been observations showing that *C. elegans* has the ability to recognize and react to things that have their preference, suggesting to a level of complex behaviour (Yokoyama, 2020).

C. elegans can be easily maintained within a laboratory environment. They can be cultured on agar plates seeded with *E. coli* as a food source. Or, when constant culturing is not needed, strains can be frozen for a long period of time (Frézal & Félix, 2015). The worm is completely transparent, making it possible to follow its development under the light microscope. Therefore, *C. elegans*

presents itself as an important model system for fundamental biological research in many fields including genomics, cell biology, neuroscience and aging.

2.1. Life cycle of *C. elegans*

Like other nematodes, the life cycle of *C. elegans* includes an embryonic stage, four juvenile stages (L1-L4) and adulthood (Fig. 4). The end of each juvenile stage is marked with a molt, where a new stage-specific cuticle is synthesized and the old one is shed (Altun & Hall, 2009a). However, two alternative life stages have been described that affect progression through the life cycle, depending on environmental conditions. The first one is L1 arrest, where juveniles can reversibly arrest development in the first juvenile phase in response to starvation. This developmental arrest occurs without morphological modifications, but these juveniles do have an increased stress resistance. *C. elegans* eggs that hatch in absence of food and go in to L1 arrest are 'ageless', meaning that time spent in arrest does not affect adult lifespan (Baugh, 2013). The second developmental arrest is called the dauer stage and can occur under several, often a combination of, stressful conditions (further discussed below) (Baugh, 2013). Dauer is an alternative developmental stage to L3. But the decision for dauer development is made in between the late L1 to early L3 stage, where juveniles can enter a predauer stage (L2d). Dauer juveniles are resistant to various stresses and can survive for several months without food. When they again encounter favourable conditions, dauer juveniles will feed again and resume their development (Altun & Hall, 2009a; Frézal & Félix, 2015).

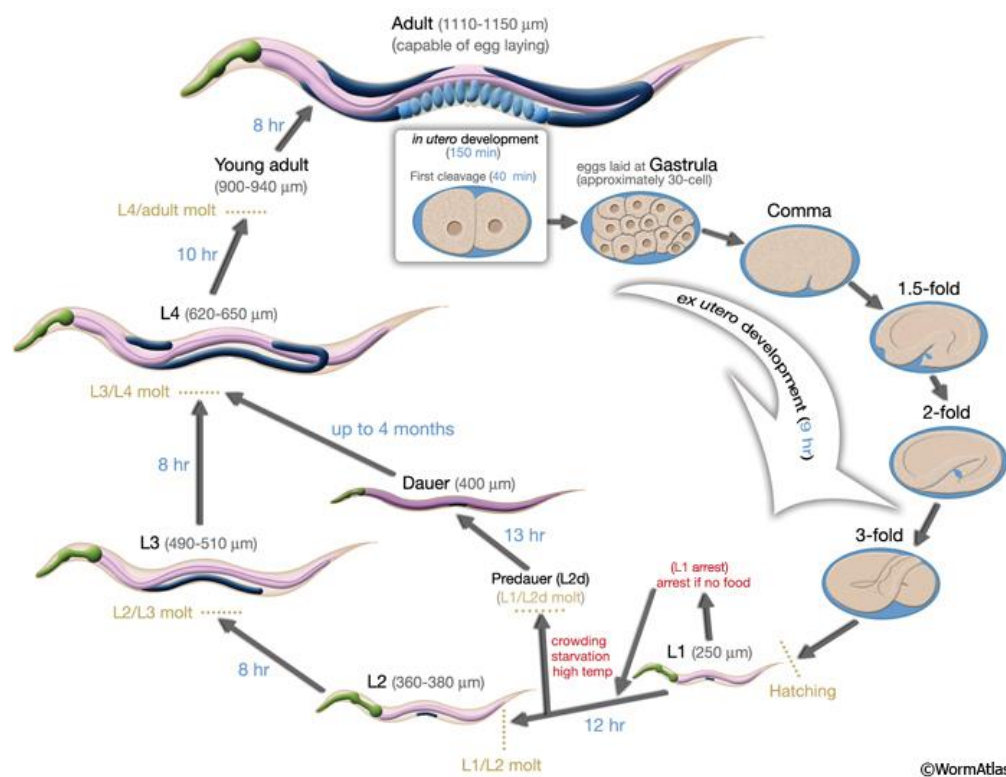


Figure 4: Life cycle of *C. elegans* at 22°C. Fertilization occurs at 0min. Numbers in blue give the approximate hours of time the animal spends at a certain stage. The length of the animal at each stage is marked in micrometers (μm). Adopted from (Altun & Hall, 2009a).

Life in the wild is characterized by “feast or famine” for *C. elegans*, and postembryonic development is governed by nutrient availability (Baugh, 2013). In this boom-and-bust lifestyle, there is a quick increase in population density when a bacterial bloom is encountered. However, when this resource is depleted, larvae will undergo developmental arrest until they encounter a novel food source (Frézal & Félix, 2015).

2.2. Neuropeptides in *C. elegans*

Neuropeptides are short sequences of amino acids that act as chemical signals, playing a critical role in synaptic signalling in all nervous systems. They regulate behaviour directly or indirectly by modulating synaptic activity. Or, they can be released as neurohormones to target distant cells and tissues, acting as a long-range signalling molecule (Chris Li, Kim, & College, 2008; Van Bael et al., 2018). So, by acting as neurohormones, neurotransmitters or neuromodulators, neuropeptides fine-tune the communication between specialized cells in response to a changing environment (Van Bael et al., 2018). Although the architecture of the *C. elegans* nervous system is extremely simple, this nematode has a notably large and diverse set of neuropeptide genes. So far, there have been 203 mature neuropeptides identified (Van Bael et al., 2018), in comparison to some over 100 known precursors in the human genome (Russo, 2017). This large family can be divided into 3 groups, the insulin-like peptides, the FMRFamide (Phe-Met-Arg-Phe-NH₂)-related peptides, or FLPs, and neuropeptide-like proteins or NLPs. The peptides of this last group only have little similarity among each other but make up the largest group, comprising 82 precursors. The insulin-like family contains 40 peptide precursor genes, whose products are involved in the regulation of development and reproductive growth. There are 34 FMRFamide-related precursor proteins, controlling locomotion, reproduction and social behaviour (C. Li, 2005; Van Bael, et al., 2018). Because of the small size of the neuropeptide genes and the small number of exons, it is difficult to identify all neuropeptide genes in the *C. elegans* genome based on sequence characteristics alone (C. Li, 2005). The short, mature neuropeptide sequences often entail the only evolutionary reasonably conserved regions in these precursor proteins, and are traditionally identified via mass spectrometry and/or cellular ligand-receptor binding assays (Edwards et al., 2019; Van Bael et al., 2018).

For many predicted neuropeptide genes found in the genome, expression patterns were also elucidated and all of them are likely to be expressed (C. Li, 2005; Van Bael, Zels, et al., 2018). Because of their widespread expression patterns, neuropeptides are likely to be involved in a multitude of behaviours in *C. elegans*, making it harder to identify their individual functions due to the overlap in expression patterns of different genes, which may also suggest some functional overlap. Besides, the similar sequences of many of these peptide genes and their binding to the same receptor are also factors making it more challenging to unfold the functionalities of individual neuropeptides. Up to date the most common strategy used to clear up a peptide’s function is to overexpress or inactivate its specific gene. Despite the caveats mentioned above, inactivation experiments have indicated that at least some of the neuropeptide genes have unique functions (Chris Li et al., 2008).

2.3. Neuropeptide processing

The biochemical pathway responsible for the generation of mature neuropeptides is highly conserved within the animal kingdom. All neuropeptides are encoded as larger, inactive precursor molecules, preproteins, that undergo posttranslational processing and modifications (Fig. 5). One

After cleavage of the signal peptide upon entry of the prepropeptide into the secretory pathway, the initial endoproteolytic cleavages occur C-terminal to dibasic residues, containing arginines and/or lysines, flanking the peptide sequence. Cleavages C-terminal to mono- or tribasic residues are also possible (Rosoff et al., 1992; Van Bael, Watteyne, et al., 2018). In neurons, multiple proprotein convertases (PC) are responsible for these cleavages, with most of the enzymes also needed to be cleaved to become active (Chris Li et al., 2008). The *C. elegans* genome encodes four PC genes that can execute this first step: *egl-3*, *kpc-1*, *bli-4*, and *aex-5*, where EGL-3 is the major PC needed for neuropeptide processing (Van Bael, Watteyne, et al., 2018). Once the precursor molecules are cleaved by proprotein convertases, carboxypeptidases E will remove the basic residues from the peptide sequence. In *C. elegans*, *egl-21* encodes a neural-specific carboxypeptidase E and is expressed in about 60% of the neurons (Jacob & Kaplan, 2003). Although EGL-21 seems to be the most important carboxypeptidase E, the *C. elegans* genome encodes two other carboxypeptidases: *cpd-1* and *cpd-2*. However, little is known about their functioning in the neuropeptide synthesis, as they are not as extensively studied as *egl-21* (Jacob & Kaplan, 2003; C. Li, 2005; Van Bael, Watteyne, et al., 2018). After cleavage post-translational modifications can occur whereas neuropeptides are commonly modified at the N- or C-terminus to protect them from degradation. Often, the modification also provides biological activity to the neuropeptide. In *C. elegans*, the most common modification is amidation, as there exists a redundant amidation mechanism (Van Bael, Watteyne, et al., 2018). Based on the presence of a C-terminal glycine, which donates an amino-group in the amidation process, all of the FLPs and many of the NLPs are likely to be amidated (Chris Li et al., 2008). The processing of INS neuropeptides in *C. elegans* is not as well-known, but ILPs could be processed via the same mechanisms. As the *ins* loci produce a single peptide from proinsulin through the enzymatic activity of *egl-3* and *kpc-1*, which is similar to human insulin and insulin-like growth factors (McCulloch, Zhou, & Jin, 2020).

2.4. Neuropeptide release

There are two main types of neuro-messenger containing vesicles: small, clear synaptic vesicles (containing neurotransmitters) and dense core vesicles (containing neuropeptides amongst other content). Their distribution pattern in the nerve endings also differs. Whereas small clear vesicles are localized at the synaptic zone, dense core vesicles are more diffusely scattered around the axon terminal (Salio et al., 2006). Although the exact mechanism for dense core vesicle movement to the cell membrane is not clear, it is believed that their neuropeptide release is dependent on a general calcium increase throughout the nerve terminal. This can occur after high levels of stimulation (Salio et al., 2006). Besides, some regulatory mechanisms may be shared between small clear and dense core vesicles in *C. elegans*. For example, UNC-104, is a kinesin necessary for the transport of small clear vesicles (Hall & Hedgecock, 1991) which can also function as the motor for dense core vesicles. Furthermore, UNC-13 is necessary to prime both types of vesicles for release (Sieburth, Madison, & Kaplan, 2006). A cytoplasmic protein specifically needed for dense core vesicle release is the calcium-dependent activator protein (CAPS). It promotes vesicle release by making a bridge between dense core vesicles and the plasma membrane (Grishanin et al., 2002). Similarly, *C. elegans* UNC-31 CAPS also promotes dense core vesicle release (Sieburth et al., 2006). Whereas in cholinergic ventral cord motor neurons PKC-1 is specifically needed for dense core vesicle release, in GABAergic motor neurons PKC-1 is not expressed, suggesting that there are other protein kinases at work in these motor neurons to regulate dense core vesicle release

(Chris Li et al., 2008; Sieburth et al., 2006). Unlike classical neurotransmitters, neuropeptides are not recovered from the synaptic cleft after release but need to be synthesized *de novo* in the cell body and transported down to the nerve terminal (C. Li, 2005).

3. Insulin-like peptides in *C. elegans*

The *C. elegans* genome encodes 40 insulin-like proteins (ILP's) which can be grouped into 3 families: alpha, beta and gamma (Duret, Guex, Peitsch, & Bairoch, 1998; Pierce et al., 2001) (Fig.6). ILP's in the gamma family contain three canonical disulfide bonds, two interchain bonds and one intrachain bond. The beta family has one additional interchain disulfide bond. The last class, the alpha family, contains different patterns of three disulfide bonds (Matsunaga, 2017).

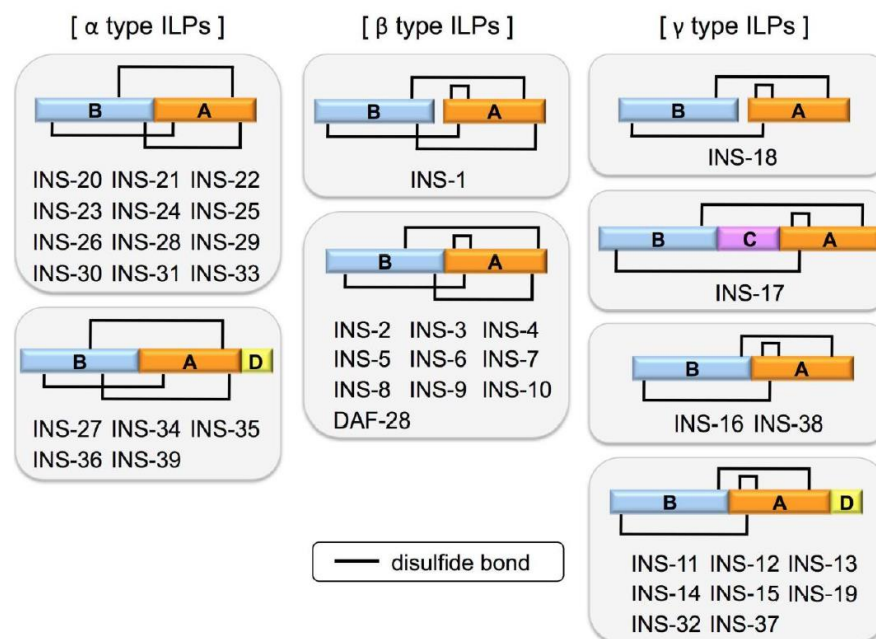


Figure 6: Schematic structures of the 40 putative mature insulin-like peptides in *C. elegans*. Adopted from (Matsunaga, 2017).

In *C. elegans*, the ILP's are primarily expressed in the nervous system. However, some ILP's are being secreted in the pseudocoel and are partly accumulating in coelomocytes. For example, both INS-35 and DAF-28, although respectively produced in the intestine and in neuronal cells, are secreted into the pseudocoel (Matsunaga, 2017). This fluid-filled body cavity lies inside the external body wall of the nematode and encompasses the internal organs. It is called a "pseudocoel" because it is not fully lined by mesodermal cells as it would be in the true coelomic cavity of vertebrates (Altun & Hall, 2009b). It was found that arsenite-translocating ATPase-1 (ASNA-1) positively regulates the excretion of neuropeptides. In mammals, ASNA-1 is expressed in the pancreatic cells, promoting insulin release (Kao et al., 2007), inferring an evolutionary conserved ILP transport function on ASNA-1. Because of this and other fundamental similarities in the ILP and insulin secretion mechanisms, the genetic and molecular pathways that control metabolism in *C. elegans* could be highly informative for analysis of human metabolic disease (Matsunaga & Kawano, 2018). It is possible that secretion of ILP's depends on the developmental state of the organism, or the growth conditions. It was found that the secretion polarity of INS-35 and INS-17 changes during dauer formation, an alternative developmental state. During normal development both proteins are secreted into the

basal side of the intestinal epithelial cells. This is changed to the apical side when the worm undergoes dauer formation. The ILP's are secreted towards the basal side again when the dauer larvae recover from diapause under favourable growth conditions (Matsunaga et al., 2016).

4. Functions of insulin-like peptides in *C. elegans*

The insulin-like peptides have highly conserved roles in physiology and development. The *C. elegans* genome encodes 40 ILP's, suggesting that there may be functional diversity among the nematode's insulin-like proteins. These proteins regulate diverse processes including longevity, development, reproduction and several specific stress responses, ultimately functioning as key modulators (Fernandes de Abreu et al., 2014a; Matsunaga & Kawano, 2018). However, all these peptides are thought to bind just one receptor, DAF-2, a cell-surface tyrosine kinase (Evans, Chen, & Tan, 2008). Binding this receptor promotes activation of downstream components to initiate biological effects. All ILP's are associated with the conserved insulin/insulin-like growth factor signalling (IIS) pathway. This pathway regulates numerous biological activities including dauer formation, lifespan, heat resistance, pathogen resistance, reproduction and many more (Matsunaga & Kawano, 2018; Zheng et al., 2019). Studies have shown that ILP's can either act as agonists or antagonists of DAF-2 to differentially affect multiple processes (Fernandes de Abreu et al., 2014a; Zheng et al., 2019). Overall strong agonists include *ins-3*, *ins-4*, *ins-6*, *ins-9*, *ins-19*, *ins-32* and *daf-28*. Strong antagonists include *ins-17*, *ins-37* and *ins-39*. However, there are also ILP's with a promoting or inhibiting function depending on the phenotype scored, meaning that their roles are context-dependent which contributes to functional specificities (Fernandes de Abreu et al., 2014a; Zheng et al., 2019).

Moreover, there is a broad regulatory and functional diversification in the ILP system, resulting in a unique set of functions for each insulin-like peptide. Many of the ILPs with detectable phenotypes are pleiotropic, indicating their diverse functions. Pleiotropy of genes allows the integration of multiple processes by these peptides, sacrificing specificity and independent regulation at the same time (Fernandes de Abreu et al., 2014a; Zheng et al., 2019). The diversification of *C. elegans* ILP's beyond functional redundancy also extends to their gene expression. ILP's can regulate each other transcriptionally to form a signalling network (Matsunaga, 2017). This network is organized into parallel circuits whose activities are affected by crosstalk, compensation, and feedback (Fernandes de Abreu et al., 2014a).

One of the processes regulated by the IIS pathway is lifespan. When solely looking at this phenotype, loss of function of *ins-6*, *ins-18* and *ins-23* results in prolonged lifespan, whereas *ins-11* functioning is necessary for a prolonged lifespan (Fernandes de Abreu et al., 2014a; Kawano, Nagatomo, Kimura, Gengyo-Ando, & Mitani, 2006). Also, both *ins-7* and *daf-28* are positive regulators of lifespan (Fernandes de Abreu et al., 2014a). Thermoregulation is negatively regulated by *ins-17*, *ins-1* and *ins-23*, where a knock-out results in a higher thermotolerance. For pathogen resistance, loss of function of *ins-27* and *ins-31* increased resistance. The opposite is true for *ins-20*: when deleted, pathogen resistance decreases. *ins-6*, *ins-13*, *ins-31* and *daf-28* all negatively regulate the reproductive period (Fernandes de Abreu et al., 2014a). The regulation of germ cell proliferation is controlled by both *ins-3* and *ins-33*, where loss of function results in a reduction in the number of germ cell proliferation (Matsunaga & Kawano, 2018).

The switch between reproductive growth and dauer arrest is also mediated by the IIS pathway. Here, development is controlled through stimulus regulated expression in different neurons. Different ILP's can encode different environmental information, to regulate dauer entry and dauer exit. On top of that, these two developmental switches of entry and exit can have different regulatory requirements. The environment will determine the developmental program, where the environmental cues for dauer entry are sensed by specific neurons that express a set of ILP's and the environment for dauer exit is sensed by a different set of neurons expressing a different pattern of ILP's. Thus, specific ILP's will generate precise responses to dauer-inducing cues and regulate development (Cornils, Gloeck, Chen, Zhang, & Alcedo, 2011). Multiple ILP's function in the regulation of dauer entry, including *ins-3*, *ins-4*, *ins-5*, *ins-6*, *ins-8*, *ins-10*, *ins-11*, *ins-12*, *ins-14*, *ins-17*, *ins-18*, *ins-21*, *ins-22*, *ins-23*, *ins-26*, *ins-33*, *ins-35* and *daf-28* (Cornils et al., 2011; Fernandes de Abreu et al., 2014a; Matsunaga, Gengyo-Ando, Mitani, Iwasaki, & Kawano, 2012; Matsunaga, Nakajima, et al., 2012). Specific studies on *daf-28* revealed that the expression in sensory neurons was downregulated under dauer-inducing conditions (W. Li, Kennedy, & Ruvkun, 2003). Also here a differential regulation between dauer entry and exit became evident as higher levels of *daf-28* are required to inhibit entry than to promote exit, whereas the opposite is true for *ins-6* (Cornils et al., 2011).

5. Molecular pathways connected with ILP signalling

The main signalling pathway used by ILP's in *C. elegans* is the canonical insulin/IGF-1 signalling (IIS) pathway. It connects nutrient levels to metabolism, growth, development, longevity, and behaviour. Like insulin-like peptides, the IIS pathway is also evolutionary conserved in metazoans (Claeys et al., 2002; Murphy & Hu, 2013).

The pathway is regulated by ILP's that bind the insulin/IGF-1 transmembrane receptor (IGFR) ortholog DAF-2, a tyrosine kinase cell-surface transmembrane receptor (Norris & Carr, 2013). The activated receptor will phosphorylate a variety of substrates, such as the insulin receptor substrate (IRS) family of scaffold proteins. Phosphorylated IRS proteins will recruit and activate multiple components of downstream cascades in their turn, such as the conserved phosphoinositide 3-kinase (PI3K)/Akt kinase cascade, Ras/MAPK (mitogen-activated protein kinase), and TOR (target of rapamycin) pathways. Activation of PI3K results in the regulation of a FOXO transcription factor, DAF-16, that governs most of the functions of the IIS pathway (Fig. 7). The serine/threonine kinases PDK-1, AKT-1, and AKT-2 first need to be activated, to phosphorylate DAF-16. Then, the phosphorylation of DAF-16 makes it possible for it to interact with proteins PAR-5 and FTT-2, which control DAF-16 subcellular localization. The DAF-18/PTEN lipid phosphatase and the serine/threonine phosphatase PPTR-1/PP2A counteract AGE-1/PI3K and AKT-1 signaling, respectively. DAF-16 also interacts with other factors in the nucleus, including SIR-2.1 and HCF-1, as well as additional transcription factors, such as HSF-1 and SKN-1 (Murphy & Hu, 2013).

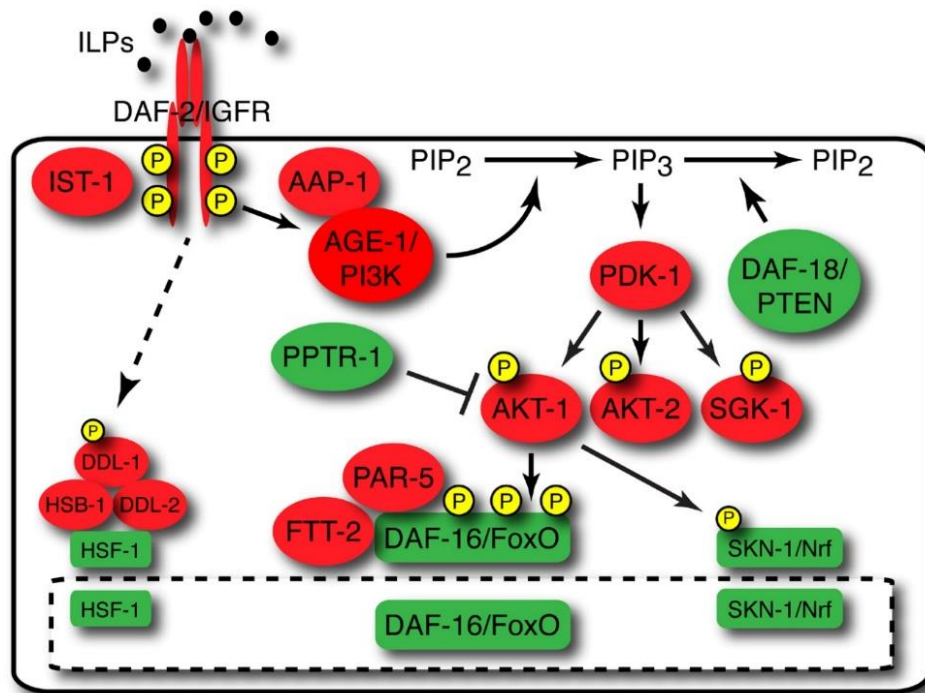


Figure 7: Schematic of *C. elegans* IIS. An active IIS pathway promotes the phosphorylation-dependent cytoplasmic seclusion of the transcription factors DAF-16, HSF-1, and SKN-1/Nrf. The insulin/IGF-1 receptor ortholog DAF-2 and other pathway components that promote IIS activity are coloured red, and molecules that either antagonize IIS or are antagonized by IIS are coloured green. Insulin-like peptides, which may either promote or antagonize DAF-2 activity, are coloured black. Adopted from (Murphy & Hu, 2013).

The DAF-2 receptor shares more than 30% amino acid identity with the human insulin, insulin growth factor-1 and insulin receptor-related receptors (Murphy & Hu, 2013). The mammalian insulin receptor is a homodimer, and each unit has an alpha chain outside the membrane and a membrane-spanning beta chain, this chain extends to the inside of the cell. The chains are linked by a disulfide bridge. The two alpha chains from the homodimer create a binding site for insulin, and the beta chains contain tyrosine protein kinase domains (Murphy & Hu, 2013; Norris & Carr, 2013). When insulin interacts with its binding site on the receptor, the two alpha chains move together and will close. This causes the beta chains to move closer together in their turn, enabling cross-autophosphorylation by their tyrosine kinase domains. The autophosphorylation creates a conformational change and will activate the insulin receptor kinase. The now phosphorylated tyrosine residues on the receptor function as attachment points for other proteins. Upon binding, these proteins, such as IRS, themselves are phosphorylated by the insulin receptor kinase (Norris & Carr, 2013). The *daf-2* locus encodes two alternatively spliced transcripts, but the specific functions of these DAF-2 isoforms is not known. The expression of DAF-2 is somewhat clear, as it is known to be highly expressed in the nervous system and the neuroendocrine cells, and weaker expressed in the hypodermis, intestine, and other tissues (Hunt-Newbury et al., 2007; Kimura, Riddle, & Ruvkun, 2011). The abundance of DAF-2 is modulated by nutritional status (Kimura et al., 2011).

The downstream DAF-16 transcription factor is a member of the FOXO family of Forkhead transcription factors. This family is known for being key regulators of stress responses, metabolism, growth, cell cycle control, and longevity in many organisms (Accili & Arden, 2004). The Forkhead DNA binding domain, DNA binding specificity, RxRxxS/T phosphorylation motifs, and 14-3-3 binding sites are conserved between *C. elegans* DAF-16 and mammalian FOXOs (Obsil & Obsilova, 2008). Cytoplasmic retention is caused by DAF-16 inhibition by the IIS pathway via phosphorylation at its

RxRxxS/T motifs (Lee, Hensch, & Ruvkun, 2001; Lin, Hsin, Libina, & Kenyon, 2001). Mutation of *daf-2*, *age-1*, *pdk-1* or *akt-1/2* will reduce DAF-16 phosphorylation, which leads to its nuclear translocation. Resulting in transcriptional regulation of DAF-16 target genes and IIS loss-of-function phenotypes. (Murphy & Hu, 2013).

6. Dauer stage in *C. elegans*

The functioning of all the insulin-like peptides of *C. elegans* is not fully known. In this thesis project, we wanted to elucidate some of these functions or interactions in the characteristic nictation behaviour of the specific dauer developmental stage. Here this alternative life stage is first discussed to then introduce the current knowledge on nictation behaviour of *C. elegans*.

C. elegans nematodes can undergo an alternative route to reproductive development in their lifecycle when encountering harsh environmental conditions. This so-called dauer stage is a stress resistant alternative to the third juvenile stage (Fig.4). Dauer developmental arrest can be triggered by a multitude of signals, among which the absence of food. However, the process of dauer formation itself also requires energy and therefore the presence of food in the environment. In fact, all post-embryonic developmental processes require energy. So, when L1 hatchlings encounter a starved environment, they immediately enter L1 arrest in response to starvation (Baugh, 2013). However, when the environment has limited food and a high population density, hatchlings can initiate post-embryonic development. But these conditions are not conducive for reproduction and population growth, triggering the juvenile into L2d development and subsequently dauer arrest (Wolkow & Hall, 2015) (Fig.4). The regulatory plasticity of *C. elegans* development leads to shifts in behaviour and metabolism, as well as to changes in development, growth, and reproduction, which are thought to improve the chances of survival and reproductive success (Fielenbach & Antebi, 2008; Hu, 2007).

Genomic analysis of dauer arrest has highlighted the role of pathway crosstalk in dauer regulation (Hu, 2007; Thomas, Birnby, & Vowels, 1993). The developmental decision for dauer formation can already occur late in the L1 larval stage and is a result of the integration of multiple environmental, genetic and internal signals, like population density, food supply and ambient temperature (Hu, 2007; Viney, Gardner, & Jackson, 2003). The population density is measured by the animals by sensing a constitutively synthesized pheromone which induces dauer arrest and prevents dauer recovery (Butcher, Fujita, Schroeder, & Clardy, 2007; Zwaal, Mendel, Sternberg, & Plasterk, 1997). Food availability is sensed by certain “food signals”, these inhibit dauer arrest and promote dauer entry, ensuring normal development in normal food conditions. While relative amounts of both these types of signals are considered, dauer arrest is also intrinsically dependent on the ambient temperature, an increased temperature enhances pheromone-induced dauer formation, and it is very strongly induced at 27°C (Ailion & Thomas, 2000). The sensory and dietary cues are further coupled to multiple conserved endocrine pathways governing the choice between reproduction and survival. These include the insulin/IGF, TGF-beta, serotonergic, and steroid hormone signal transduction pathway. Together with other pathways, they reveal a molecular basis for metazoan plasticity in response to extrinsic and intrinsic signals (Fielenbach & Antebi, 2008).

6.1. Dauer characteristics

Dauer larvae show distinct morphological and behavioural characteristics. These adaptations favour survival and dispersal of the worm in the harsh environmental conditions. Morphological characteristics of the dauer larvae include a radial constriction with shrunken tissues and a specialized cuticle. This thick cuticle covers the entire body and buccal cavity. It will protect the animal from environmental toxins and detergents. The thinner, stiffer body presumably helps in the performance of specialized dauer behaviours (Wolkow & Hall, 2015), their oral orifices are enclosed by an internal plug and their pharynxes are constricted and do not pump, preventing feeding of the dauer larva (Hu, 2007). Therefore, the larvae depend on intestinal and hypodermal lipid stores as an energy source (Wolkow & Hall, 2015). In good environmental conditions, *C. elegans* undergoes a metabolic shift between L1 and L2. Whereas L1 juveniles use the glyoxylate cycle to generate carbohydrates from lipid stores with the anaerobic conversion of isocitrate to malate, L2 larvae have a relative increase in TCA cycle activity where this conversion takes place aerobically. Dauers do not seem to undergo this metabolic change, as their transcription appears to be quiescent, but they have elevated levels of Hsp90, superoxide dismutase and catalase activity (Hu, 2007). This increased expression of protective enzymes makes them more resistant to high temperatures, oxidative stress and anoxia. Dauers also induce several stress-response pathways for desiccation tolerance (Wolkow & Hall, 2015).

Dauer-specific behaviours include a characteristic locomotion pattern and nictation, which is discussed below. Locomotion of dauer juveniles is focussed on the conservation of energy. Whereas non-dauers continuously explore their environment, dauers tend to lie motionless for long periods of time and then respond rapidly to stimuli (Wolkow & Hall, 2015). Both behaviours serve the goal of survival and dispersal.

7. Nictation behaviour in *C. elegans*

Nictation is a phoretic behaviour in which *C. elegans* stands on its tail and waves his head and body in three dimensions. There are two forms of nictation behaviour reported for *C. elegans* (Fig.8). During individual nictation, the nictating worms may wave or stay stationary. Nictation can also occur as a group, where the worms aggregate and stand together on a point-structured surface (Yang, Lee, Yim, & Lee, 2020). Nictation behaviour increases the probability that individuals will encounter other organisms, such as slugs, snails and isopods (Frézal & Félix, 2015). Thereby promoting phoresy dispersal of the dauer larvae, as they can climb on, or attach to other organisms and travel to a new niche. Dispersal is a crucial survival strategy for many animal species. Phoresy itself refers to a specific dispersal strategy, being the attachment to another, more mobile animal to facilitate dispersal. Thereby giving small organisms an opportunity to overcome their limited mobility and enabling them to increase the distance and efficiency in which they disperse (Yang et al., 2020). Nictation is a specific type of phoresy, as it promotes interactions between *C. elegans* worms and possible carrier animals (H. Lee et al., 2012). In harsh environments with a large population size, the numbers of dauers in the population will increase. Nictation allows these dauers to spread to a new niche via the exploitation a more mobile host. Once they encounter a more suited environment for development, the dauers will begin feeding again and their development will restart. This way, the individual can reproduce again and a new population can rise (Hu, 2007). When collected in the

wild, *C. elegans* are usually found in the dauers stage, suggesting that a large proportion of *C. elegans* exists as dauers in nature (Barrière & Félix, 2005). Dispersal by nictation in the dauer stage appears to have a great impact on the survival and evolution of nematode species (D. Lee, Lee, Kim, Lim, & Lee, 2017). Nictation behaviour can vary between nematode species, as other species exhibit other forms of nictation (Fig.8) (Yang et al., 2020).

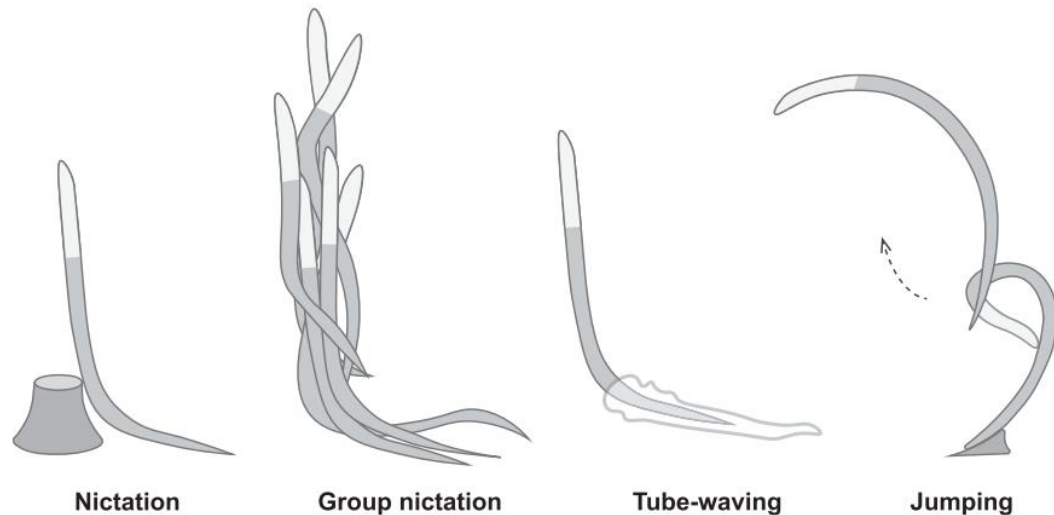


Figure 8: The diverse modes of nictation observed nematode species. *C. elegans* shows individual and group nictation. The other phenotypes such as tube-waving and jumping are observed in other nematode species. Adopted from (Yang et al., 2020).

Nictation behaviour is affected by several environmental factors. In *C. elegans*, for example, nictation was only observed on rough surfaces but not on flat surfaces. Therefore, tactile cues from the surface, sensed by mechanosensory neurons may promote nictation in dauers (H. Lee et al., 2012). The nictation ratio in *C. elegans* dauers is also known to increase as temperature increases (Yang et al., 2020) and the nictation ratio appears higher in covered petri dishes than in open dishes. So, high temperature and air movement seem to induce nictation, and humidity may also have an effect on nictation (Yang et al., 2020). When the surface is too moist, dauers will not be seen nictating. Probably because they cannot break the surface tension caused by the moisture, and thus cannot initiate nictation (Yang et al., 2020). Host sensing might also affect the nictation behaviour of *C. elegans*, as it can be connected with the induction of nictation behaviour by increased temperature and air movement, which could be the result of the presence of a host. Host sensing is already intensively studied in parasitic nematodes. The nictation responses for different host-specific chemicals differ between nematode species, as they interact with diverse hosts. CO₂ may be an example of a general cue signalling the presence of a host, because it was shown to be an aversive cue for adults but attracted dauers (Yang et al., 2020).

One of the known signalling factors that affect nictation is the insulin/IGF-1 signalling pathway. The activation of the IIS pathway inhibits nictation in *C. elegans*, since dauers with mutations in the *daf-2* receptor or other factors of the IIS pathway generally have a higher nictation ratio (D. Lee et al., 2017; Yang et al., 2020). Cell-specific rescue experiments showed that IIS regulates nictation via ASI and ASJ sensory neurons, which are also known to regulate dauer development and recovery (Bargmann & Horvitz, 1991; D. Lee et al., 2017). But more detailed analysis exposed distinctive regulation modes of IIS for dauer development and nictation. First, *daf-16*, the key

downstream regulator of IIS, has somewhat distinct function in dauer formation and nictation (D. Lee et al., 2017; Yang et al., 2020). Secondly, mutations in the insulin-like peptide genes *ins-28* or *ins-34* lowered nictation ratio, with little or no effect on dauer formation (Fernandes de Abreu et al., 2014a; D. Lee et al., 2017), suggesting that ligands for the DAF-2 receptor may be different for dauer development and nictation. Elucidation of the mechanism of nictation will contribute to an increased understanding of the conserved dispersal strategies in nematodes.

RESEARCH OUTLINE

With the known functions and pathways underlying ILP functioning made clear, we would like to research this more in depth, particularly ILP functioning during nictation behaviour.

Since several ILPs have an effect on dauer formation (Zheng et al., 2019) and are involved with sensing the environmental conditions that result in dauer formation (Fernandes de Abreu et al., 2014a; Honda, Tanaka, & Honda, 2008). We would like to test the role of some of these ILPs in nictation behaviour. By the use of overexpression and knock-out strains, we can look for differences in nictation behaviour of the mutant dauers. Due to the large amount of ILPs in *C. elegans* not all peptides can be tested during this project. Peptides of interest are therefore selected by their role in the IIS pathway and their influence on dauer development. After a first discovery analysis, ILPs with differing from the wild type are going to be tested again to create a more robust dataset and thus more reliable results.

By also testing the effect of the difference in gene expression on the locomotion of these strains, we hope to rule out any locomotory deficits that could possibly cause or influence differences in nictation behaviour. We aim to test for locomotion differences using speed assays.

Furthermore, we will also perform localization experiments both *in vivo* and *in silico* on some ILPs that showed differences in nictation behaviour. The presence of these peptides in specific neurons could then be possibly linked to their function. The cellular localization experiments will be done with GFP reporter strains of the different ILPs, in dauers and L3 juveniles. The same ILPs will also undergo an *in silico* analysis, to see whether the same neurons pop up.

MATERIALS AND METHODS

1. General *C. elegans* techniques

1.1. Strains and growth conditions

Throughout this project wild type worms, N2-Bristol, as well as various insulin mutant strains (Table 1) were used to search for behavioural phenotypes. Insulin overexpression strains were provided by the Chin-Sang lab, Queen's University Canada (Zheng et al., 2019), and deletion strains by Ch'ng lab, King's College London (Fernandes de Abreu et al., 2014b). Reporter strains were obtained from the *Caenorhabditis Genetics Centre* (CGC).

All strains were grown and maintained at 20°C on nematode growth medium (NGM), seeded with live *Escherichia coli* OP50 bacteria grown in lysogeny broth (LB) medium according to standard procedures (Stiernagle, 2006). All used buffers and solutions are described in Appendix 2.

Table 1: *C. elegans* mutant strains. Deletion: size in base pairs (bp) of the deleted region; N/A: not applicable.

Strain	Description	Deletion
HT1734	wwEx73 [ins-17p::GFP + unc-199(+)].	N/A
HT1741	wwls30 [ins-19p::GFP + unc-119(+)].	N/A
HT1809	wwEx84 [ins-39p::GFP + unc-119(+)].	N/A
HT2098	wwEx82 [ins-36p::GFP + unc-119(+)].	N/A
IC1545	zdsI5 I ; quEx601 [F25B3.3::ins-17] with ODR-1::RFP marker	N/A
IC1646	zdsI5 I ; quEx656 [F25B3.3::ins-39] with odr-1::RFP marker	N/A
IC1661	zdsI5 I ; quEx665 [F25B3.3::ins-15] with odr-1::RFP marker	N/A
IC1665	zdsI5 I ; quEx667 [F25B3.3::ins-36] with odr-1::RFP marker	N/A
IC1669	zdsI5 I ; quEX671 [F25B3.3::ins-21] with odr-1::RFP marker	N/A
IC1678	zdsI5 I ; quEx676 [F25B3.3::ins-37] with odr-1::RFP marker	N/A
IC1813	zdsI5 ; quEx770 (F25B3.3 driving ins-1)	N/A
IC1826	zdsI5 ; quEx783 (F25B3.3 driving ins-6)	N/A
IC1835	zdsI5 I ; quEx789 [F25B3.3::ins-19]	N/A
IC2225	quIs28 OC3X	N/A
PT31	nIs133 I ; him-5(e1490) [pkd-2p::GFP]	N/A
QL25	tm0790 - III	N/A
QL27	tm3620 - II	153bp
QL188	tm5155 - II	480bp
QZ80	nr2091 - IV	N/A
QZ81	tm2416 - II	316bp

1.2. Culturing of *C. elegans* on Nematode Growth Medium

General cultivation of *C. elegans* occurs on solid NGM agar plates seeded with a layer of *E. coli* OP50. The growth of the *E. coli* bacteria on the plate is limited by their auxotrophicity to uracil, making it easy to observe the worms. There are two methods that are generally accepted for *C. elegans* culturing, picking, and chunking. Both are based on the same principle of transferring worms from an old plate with depleted food source to a new plate with fresh food and are relatively inexpensive and simple. Fluorescent mutant strains were maintained by selectively picking fluorescent worms using a fluorescent microscope (Leica MZ 16 F). Plates were stored upside down in an incubator at 20°C.

1.2.1. Preparation of NGM plates

To prepare 1L of basal nematode growth medium (NGM) 17g of agar (Sigma-Aldrich), 3g of NaCl (Sigma-Aldrich) and 5g of Bacto Peptone (BD Biosciences) were dissolved in 800mL of AD water. This solution was autoclaved and allowed to cool down to 60°C before AD water was added to the foreseen volume of 1L. The subsequent steps were all performed under the laminar flow where 1mL of 1M CaCl₂ solution, 1mL of 1M MgSO₄ solution, 1mL of 5mg/mL cholesterol in ethanol solution, and 25mL of 1M phosphate buffer solution were added. The solution was gently swirled to allow mixing. Finally, depending on the experiment, a certain volume was poured into petri dishes of the desired size (Table 2) and left to solidify. When fully solid, the plates were inverted and placed at 4°C until ready for seeding. When large quantities of NGM needed to be prepared, Mediaclave was used.

Table 2: Volume of NGM and liquid *E. coli* OP50 culture used to seed for different Petri plate sizes.

Plate size (mm)	NGM volume (mL)	Culture volume (µL)
90	25	200
55	12	100
35	5	30

1.2.2. Preparation of liquid *E. Coli* OP50 culture

To prepare liquid LB medium, 20g of LB broth (Sigma-Aldrich) was first dissolved in 800mL of AD water and autoclaved after which it was diluted with AD water to 1L. From this LB medium 40mL was transferred to an autoclaved 50mL glass tube in the laminar flow cabinet and inoculated with a single colony from the *E. coli* OP50 streak plate. The tube was then placed in a shaking incubator at 37°C and allowed to grow overnight. The culture was ready to use the following day or could be stored at 4°C until ready for seeding.

1.2.3. Seeding of NGM plates with liquid *E. Coli* OP50 culture

The prepared NGM plates were seeded with bacteria under the laminar flow. Except when the plates were freshly poured, they were first left to acclimatize to room temperature. A certain volume of liquid *E. coli* OP50 culture (Table 2) was then pipetted onto the plates and evenly spread out in the middle of the plate with a sterilized glass spreader. The bacterial layer was not spread to the walls of the plate, preventing the worms from crawling up the sides which causes drying and death. The seeded plates were allowed to dry in the laminar flow cabinet. When dried, they were inverted and incubated at 37°C overnight. For 35mm plates, spreading of the bacteria and incubation at 37°C

was not necessary. They were just left at room temperature to grow overnight. The following morning the ready-to-use plates were stored at 4°C until needed.

1.2.4. Culturing of *C. elegans* hermaphrodites

For the general cultivation of *C. elegans* strains, worms need to be regularly transferred to freshly seeded NGM plates to keep them in good health. When the number of worms per plate becomes too great, the food becomes depleted, and the population is starved. Starved worms cannot be used in any experiments. In order to use them again for experimental purposes, at least three generations need to pass after the starvation to avoid any possible epigenetic modifications (Lim & Brunet, 2013). In general, the transfer of worms needs to occur every 1 to 3 generations and is dependent on the genotype, temperature, and the experiment for which they are used. In practice culturing needs to happen every two to three days and can be done using two methods 'picking' or 'chunking'. In both methods freshly seeded NGM plates were first allowed to acclimate to room temperature.

Picking makes it possible to transfer a specific number of worms to a fresh NGM agar plate. Here, a sterilized worm picker, a flattened platinum wire, was used to individually transfer worms. Using a stereomicroscope (Nikon C-DS SMZ 745), adult worms were located on an old plate, picked, and allowed to crawl onto a new plate. For medium sized Petri dishes, an average of 8 worms per plate was picked whereas large Petri dishes had an average of 10 transferred worms per plate.

Chunking can be used when plates are too starved to find enough adult worms for picking, or as a general technique. Here, a sterile scalpel is used to cut a small piece of agar containing worms and/or eggs out of an old plate. This chunk is then placed upside down onto the new plate, allowing worms to spread out on this new plate.

1.2.5. Culturing of *C. elegans* males

The culturing of *C. elegans* males required a slightly different procedure. After the acclimatization to room temperature of fresh NGM plates, one or two L4 hermaphrodites together with 8-20 males were picked using a sterilized worm picker and stereomicroscope and allowed to crawl onto a new plate.

1.2.6. Management of contamination

NGM plates could sometimes get contaminated by yeast, moulds, or other unwanted bacteria. Contaminated populations could not be used for experimental procedures. So, the contaminants needed to be eliminated to obtain a healthy stock again. In some cases, just picking worms from an uncontaminated area on the old plate could already solve the problem. But when the contamination proved to be more persistent, a bleaching solution was used in which only the eggs were preserved. This bleaching solution consisted of 5M NaOH and 5% household bleach in equal volumes. A small volume was pipetted on a new, freshly seeded NGM plate. Subsequently, adult worms, containing eggs, from the old plate were placed in the liquid. As the bleaching solution is left to dry, both the contaminants and living worms are killed off. When fully dried, the plates are again incubated upside down at 20°C for the eggs to hatch.

1.3. Synchronizing *C. elegans* populations by bleaching

To get a synchronized population, where all the worms have the same age, a hypochlorite treatment was performed, often referred to as bleaching. In this process adult worms erupt and release their eggs in the medium. The eggs can survive this hypochlorite treatment and will hatch in the medium where the worms will immediately go into L1 arrest because there is no food available. Once the worms are plated on food, they can all exit diapause at the same time, creating a synchronized population.

Worms were first collected in 15mL Falcon tubes. Approximately 9mL of S-basal was used to rinse two medium petri dishes of 55mmx15mm. The worms were allowed to settle before the supernatant was removed, leaving 3mL in the tube. A bleaching solution was prepared containing 1/3 of 5M NaOH and 2/3 of 5% household bleach. Two mL of this bleaching solution was added to the Falcon tube, after which it was vigorously shaken for 4min. Next, S-basal was added to 14mL and the tubes were centrifuged for 2 minutes at 1200rpm at 20°C. The supernatant was removed, and the worm pellet was resuspended in S-basal, added to 14mL again. This centrifuge and washing process was repeated a total of three times. After the last washing step, the remaining pellet was resuspended and S-basal was added to 10mL. The tube was placed in a rotator at 20°C overnight, or at least for 17 hours.

To seed the worms the next morning, they were first centrifuged for 2 minutes at 800rpm at 20°C. After the supernatant was removed, up to 500 worms were pipetted onto a medium NGM seeded plate. These plates were then incubated at 20°C for approximately 29 hours for the worms to reach the L3 stage. For young adults, the worms took approximately 50 hours to develop.

1.4. Freezing and recovery of *C. elegans* stocks

To create a long-term stock of the different *C. elegans* strains, worms were frozen at a temperature of -80°C. This way the strains with their desired phenotypes could be revisited in a later point in time without having to keep them in breeding. Or this could serve as a back-up when a problem arises with breeding the worms.

For long-term storage, worms were frozen using a liquid freezing solution. This solution contained 0.112g K₂HPO₄ (Sigma-Aldrich), 0.592g KH₂PO₄ (Sigma-Aldrich), 0.585g NaCl (Sigma-Aldrich) and 30mL glycerol (Sigma-Aldrich) per 100mL Milli-Q and was autoclaved before use. Two large, 90mm, uncontaminated and freshly starved plates were washed with a total volume of 3mL of S-basal. The plates preferably contained a lot of L1 larvae as they survive freezing the best. After the worms were collected in a 15mL Falcon tube with S-basal, an equal volume of liquid freezing solution was added. This volume was then aliquoted into 5 labelled 1.8mL cryo-vials (Thermo Scientific). The solution was gently pipetted up and down in between vials to make sure the worms were distributed evenly, preventing them to sink to the bottom. Next, the cryo-vials were encapsulated in a Styrofoam box, to allow slow freezing, and stored at a temperature of -80°C.

After 2 weeks one cryo-vial was thawed as a tester, to see if freezing was successful and living worms could be retrieved after thawing. The contents of the cryo-vial were spread over a seeded NGM plate at room temperature. After a couple of hours worms should start to move. If the worms were not able to recover, the whole freezing process was repeated. Because liquid freezing solution

was used, the whole contents of the vial needed to be thawed as the worms settle to the bottom of the cryo-vial when using this method.

1.5. Determining genotype by PCR and agarose gel electrophoresis

To check the genotypes of the different strains, a polymerase chain reaction (PCR) was performed together with an agarose gel electrophoresis. Different gene-specific primers were designed for each strain in line with general primer design guidelines. The genetic material was extracted from the worms during a worm lysis. Next, the gene of interest was amplified during a second PCR and finally the genotype was assessed with an agarose gel electrophoresis.

Primer design. Primers were designed with the online tool *Primer Wizard* in Benchling, conform to general primer design guidelines. Their length varied between 18bp and 24bp, they all had a GC content between 40% and 60%, their melting temperature varied between 55°C and 65°C, and the differences in annealing temperature of the primer pairs were less than 5°C.

Worm lysis. To extract gDNA from worms they were treated with proteinase K to lysate. The proteinase K (10 mg/mL, Tritirachium album, Sigma-Aldrich) was thawed on ice together with a PCR template buffer that served as a worm lysis buffer. 100µL of the PCR template buffer was added to 5µL of proteinase K. Next, 5µL of this mixture was aliquoted into different sample vials. Worms were picked using a sterilized picker and put in these sample vials. The number of worms per vial could differ, depending on the experiment. To check the genotype of a strain an average of 5 worms in each sample vial was used. These vials were placed at -80°C for 15 minutes to break open the cuticula of the worms. Next, a thermo cycles was used to extract the gDNA where the following PCR program was applied (Table 3).

Table 3: Specifics for the program used for worm lysis.

Release of genomic DNA	60 °C	60 min
Inactivation of Proteinase K	95 °C	15 min
Pause	4 °C	

Worm PCR. To amplify the gene of interest a second PCR program was used. First REDTaq ReadyMix PCR Reaction Mix (Sigma-Aldrich), forward and reverse primers (10µM) were thawed on ice, mixed together with Milli-Q up to a solution of 25µL. Then, 24µL of this solution was aliquoted into each sample vial of PCR 1. A PCR program was then applied (Table 4), where the annealing temperature could vary depending on the used primers. Often, a gradient PCR was performed when the optimal annealing temperature was not known. Or when different gDNA's were handled together.

Table 4: Specifics for the PCR program used for worm PCR.

Initial denaturation	95°C	2 min
Denaturation	95°C	1 min
Hybridisation	Annealing temp.	2 min
Extension	72°C	1 min
→ 30 cycles		
Final extension	72°C	5min
	10°C	

Agarose gel electrophoresis. A 1% agarose solution was prepared by adding 100mL of TAE buffer to 1g of agarose (Sigma-Aldrich) and heating the solution in the microwave until all the agarose was dissolved. A volume of 5 μ L GelRed (10000x in Dimethylsulfoxide (DMSO), Biotum) was added and the agarose solution was swirled gently to dissolve the GelRed. The agarose solution was poured into a gel casting tray with required comb and left to cool down. When solid, the gel was removed from its cast and the comb was carefully pulled out. For gel electrophoresis, the gel was submerged in TAE buffer in an electrophoresis chamber (Biorad PowerPac™ Basic). Next, 5 μ L of each sample was pipetted into the separate wells and 3 μ L of a 1Kb DNA ladder (Fermentas) was pipetted into the wells flanking the gel. The sample volume sometimes varied depending on the experiment. Finally, the gel electrophoresis was started, allowing the DNA fragments to separate, at 100V, 120mA. The current and time spent running could also vary depending on the experiment. After approximately 90 minutes the results were visualized with the ProXima 2500-T gel imaging system (Isogen Life Sciences).

2. Nictation assays

To determine differences in nictation behaviour of the various mutants, nictation assays were performed. The assays were carried out for all insulin overexpression and knockout strains. At first these strains were tested a total of three times. But when the results of strain-specific assays showed interesting data, more assays were conducted to get a total of 5 replicates per strain and a more robust dataset.

For the assay itself, approximately 50 dauers were placed on an acclimatised micro-dirt chip using a mouth-pipette with a little bit of S-basal. Fluorescent strains were assessed using a fluorescent microscope (Leica MZ 16 F), so that only those worms with the mutation and thus fluorescent signal would be used in the assay. The worms were left to acclimatise for 30 minutes on the chip in a covered petri dish. Next, up to 25 dauers were individually observed for 90 seconds, and the start and end of nictation was recorded using JWatcher. If a worm was still nictating when the 90 seconds ended, the recording was continued until the worm stopped nictating or the recording reached 2 minutes. To exclude quiescent dauers, nictation was only monitored for consistently moving worms. The whole experiment was conducted in a climate room where the relative humidity and temperature were kept stable at 40 and 20°C respectively. The data were analysed using a custom R script.

2.1. Preparation of microdirt chips

A silicone master chip containing arrays of posts with a 25 μ m radius, a 25 μ m height and a distance of 25 μ m between posts was previously used to create negative PDMS (18.18g polymer, Sigma-Aldrich) molds. The PDMS was prepared and degassed in a vacuum chamber for 1 hour to eliminate any air bubbles before use. A clean master chip was fixed with tape at the bottom of a petri dish before PDMS was poured over. This was cured at 60°C for 2 hours, after which the PDMS was carefully removed from the master chip. This new PDMS chip was then placed in a petri dish with its structures facing upwards, to function as a negative mold. A 4% agarose solution was prepared by adding 150mL of Milli-Q to 6g of agarose (Sigma-Aldrich). The solution was either heated in the microwave until all the agar was dissolved or autoclaved. After heating the evaporated portion of Milli-Q was calculated and added again to the solution to maintain the 4% agarose and create identical chips. The agar solution was allowed to cool down to about 60°C before it was poured over the PDMS chip. Air bubbles were removed by scraping over the PDMS with a glass slide. The agar was left to solidify at room temperature. The micro-dirt chip was then cut out from the petri dish with a scalpel, lifted from the negative mold, and placed structure-side up onto a petri dish. Finally, agar microdirt chip was placed at 37°C for 1 hour and kept at 4°C before use.

2.2. Grow dauers by starvation

Because food has a role in dauer formation and there are shown effects on metabolism of healthy and unhealthy food sources, an exact method was used to grow the food source for dauer generation. This way, the worms were always given the exact same food source.

First, a day culture was grown from a single colony of OP50 in 5mL of LB medium in a Falcon tube at 37°C in a shaking incubator. Once the bacteria reached their exponential phase and an OD₆₀₀-value of 0.8 was reached, a seeding culture was grown from this day culture. This step was crucial in creating a similar food source every time. The same number of bacteria were inoculated in the same volume every time. From the day culture 0.5mL was used and added to 4.5mL of LB medium. If the OD-value of the day culture was slightly different from 0.8, 0.4 was divided by this value to get the desired volume to add. Next, this seeding culture was grown at 37°C in a shaking incubator until it reached OD₆₀₀-value of 1.0. Then, 100 μ L of this culture was used to seed medium 55mmx15mm NGM plates, following general procedures. The OP50 was carefully spread using a sterilized glass spreader and the plates were left to dry under the laminar flow. The seeded plates were incubated for 16 hours at 37°C, and stored at 4°C. Every procedure with bacterial cultures was performed using sterile techniques in a laminar flow cabinet.

To generate dauers, 10 young adult worms were put onto these plates using a sterilized worm picker. The plates were inverted and incubated at 20°C for eight days. By then the population was starved and numerous L2 worms had made the developmental decision to go into dauer diapause because of the lack of food and the crowding of the plate. Dauers could then be visually recognized by their shape and darker intestines using a stereomicroscope (Nikon C-DS SMZ 745). Both quiescent and moving dauers were selected for the following nictation assay.

2.3. Male assay

A couple of experimental nictation assays for males were also conducted. None of them proven useful eventually. The earlier described nictation assay for dauers was not applicable to males. All the setups were tested both on food and off food.

A first test was conducted with cotton gauze, as this material was proven ideal to support the nictation behaviour of dauers in earlier in house testing. A 1cm² patch of cotton gauze was placed on a NGM plate with males and slightly pressed down using a worm picker. The nictation behaviour of the males was assessed after 30 minutes.

The following section of testing was all performed on 35mmx15mm babyplates, both on and off food and on dried plates without food. Cotton strings of 1cm, 2cm or 3cm were placed either parallel to each other, in a triangle or in a square on the plate and slightly pressed down using a worm picker. Males were then placed in the middle of this construction with a sterile worm picker and left to acclimatise for 30 minutes before being assessed on their nictation behaviour.

2.4. Statistical analysis

The data from JWatcher was processed using a custom R script. Multiple dependent variables were computed and normalized against the wild type. For this, recorded nictations that lasted less than 1 second were not included. The nictation ratio was calculated as the percentage of the total time that the individual spent nictating. The nictation initiation index was calculated as the frequency of nictation initiations during non-nictating time. The average duration of nictation calculated as the total time spent nictating by the individual divided by the number of nictation initiations. These parameters were computed for the original dataset and a dataset only containing nictating worms.

To test the influence of one or more independent variables on one dependent variable, an ANOVA type III was conducted. Multiple parameters for nictation behaviour were measured in different mutants for these assays, nictation ratio, nictation initiation and the average duration of nictation. The data was structured in such a way that each mutant strain was tested a specific number of times, being the experiment number. Because of the experimental design multiple mutant strains were always tested together as a set and thus nested. The independent variable of the mutant, being condition, was considered a fixed effect nested in the random effect set. The day that the experiment was conducted was also considered random. A linear mixed model was used for the analysis of the data in a custom RStudio script. AIC model diagnosis revealed that models with and without the random effect of set represented the dataset almost as well. Therefore, a model containing only the fixed effect of condition, random effect of the day and the random interaction effect was used for analysis. Although this extra layer of information was now removed from the model, the dataset was still equally good represented and the same model could be used for further analysis, enabling comparison. With the multi-way ANOVA, we could test for differences in nictation behaviour whilst simultaneously controlling for the random effect of the day of the experiment and the interaction effect. The assumption of normality of residuals was visually checked both with a histogram and qqplot, and with the Shapiro-Wilk's test. The assumption of homogeneity of variances is hard to test in R for mixed models with readily available packages. Therefore, the variation in observations from the different independent variables was visually checked using a boxplot, and with the rule of thumb that ratio of maximum variance to minimum variance should not exceed 5. A Dunnett post hoc

analysis was performed where the means of the experimental groups were compared against the control group to see if there was a difference. The significance level was set on $p < 0.05$ for all the statistical tests.

After a first discovery screen, mutant strains that gave interesting results were selected for further testing. Because of this, the strains were no longer tested in the same sets as before. The same linear mixed model could thus be used to analyse this data and was proven the most accurate after AIC model diagnosis of multiple model options. The previous post hoc analysis method was also still valid for this model, as were the methods for testing ANOVA assumptions.

2.5. COPAS

To test whether the COPAS (Complex Object Parametric Analyzer and Sorter) biosorting system could be used to select dauers in mutant strains with weak dauer formation, wild type worms were tested on nictation behaviour after COPAS sorting against the nictation behaviour of wild type worms after manual selection. Wild type dauers were grown following the previously described protocol. Then one population of dauers was washed of their plate with a total volume of 6mL S-basal and collected in a 50mL Falcon tube. The worms were allowed to settle before the supernatant was suctioned. Before the tube was coupled to the COPAS, the worms were diluted with S-basal to a concentration of approximately 1000 worms per 1mL. Dauers were then selected by the sorting system and dropped onto unseeded NGM plates. From here the dauers were transferred to a microdirt chip using a mouth-pipet with S-basal.

The analysis for these experiments was conducted using a custom R script. A linear mixed model was used. The condition, being manually selected or by the COPAS, was considered a fixed effect. Whereas the day of the assay was considered a random effect. The model also took the interaction effect of condition and day into account. ANOVA assumptions were checked, and the significance level was set on $p < 0.05$.

3. Locomotion assays

To check whether the mutant worms had defects in their locomotion, a tracking setup on solid plates off food was used, as defects in locomotion could affect, or be a source of, differences in nictation behaviour. With this assay several parameters could be extracted including speed, number of turns, number of pauses and the proportion of time the worms spend turning, running and pausing. Speed was used as the main parameter for locomotion. A custom Matlab script (version R2016a) for tracking worms was used to identify worms on the plate and trace their displacement through time. Centroid speed was used as a readout for overall locomotion, with speed either defined as the measured speed over all behaviours or as the measured speed solely while running. The whole procedure was performed in a climate-controlled room with a temperature of 20°C and relative humidity of approximately 40.

Synchronized L3 larvae, prepared as described in section 1.1.3. of *Material and methods*, were used for locomotion tracking. The worms were first washed of their plates with S-basal and collected in a 15mL Falcon tube. A little drop containing approximately 30-50 worms was pipetted on an already acclimatized large 90mmx15mm unseeded NGM plate. The transferred liquid was left to

evaporate, and the uncovered plate was placed under a camera for immediate recording. The locomotion of the worms was tracked using StreamPix software. At the beginning of each experiment the cameras were set to display 2/3 of the plates and the focus and contrast of each camera was manually adjusted for optimal results. There were no lights in the room excepts for the light source beneath the plates. Settings were saved to 2 frames per second and the exposure was held constant. Each plate was recorded for at least 30min. Fluorescent strains underwent an intermediate step where fluorescent worms were first sorted under the fluorescent microscope using a mouth-pipet with S-basal.

3.1. Statistical analysis

Each mutant strain was tracked a total of three times for 30min and each experiment took place on a different day. Using a custom Matlab script, the displacement of individual worms on the plate was divided in tracks of 30sec. For each of these tracks, the speed when running in this 30sec time interval and the overall speed over all behaviours was calculated. The data from Matlab was then processed using a custom R script. To test the influence of the independent variables on the dependent variable speed, an ANOVA type III was conducted. The independent variable of the strain, being condition, was considered a fixed effect. Whereas the independent variable of the day that the experiment was conducted was considered a random effect. Using AIC model diagnosis, multiple models were assessed. A linear mixed model also containing the interaction effect between condition and day of the experiment as a random factor represented the data the best and was used for analysis. The assumption of normality of residuals was visually checked both with a histogram and qqplot, and with the Shapiro-Wilk's test. The assumption of homogeneity of variances is hard to test in R for mixed models with readily available packages. Therefore, the variation in observations from the different independent variables was visually checked using a boxplot, and with the rule of thumb that ratio of maximum variance to minimum variance should not exceed 5. With a multi-way ANOVA, we could test for differences in speed whilst simultaneously controlling for the random interaction effect and the effect of the day that the experiment was conducted. A Dunnett post hoc analysis was performed where the means of the experimental groups were compared against the control group to see if there was a difference. A significance level of $p < 0.05$ was imposed for all the statistical assays.

4. Localization

Cellular localization of insulin peptides was done by imaging fluorescent reporter strains. The imaging of GFP reporter strains was done with the use of a confocal microscope (Olympus Fluoview FV1000). The images were taken at a magnitude of 20.0 with on objective lens NAvalue of 0.75.

First the worms were prepared and mounted on slides. A 2% agarose solution was heated until it reached boiling point. The agarose (Sigma-Aldrich) was dissolved in 100mL Milli-Q. A drop of this hot solution was placed on a glass slide. Another slide was put on top so that the agar would spread out, but there was no extra pressure applied. The agar was left to solidify after which the slides were pulled apart. To immobilize the worms a 6 μ L drop of 10mM Tetramisole was pipetted on the agarose after which 5 to 10 worms were placed in this drop with a sterile worm picker. A coverslip was used to cover the worms. This coverslip was fixed to the slide with Vaseline to prevent it from

sliding or slipping, as the microscope slides were placed upside down in the holder of the confocal microscope.

5. In silico analysis

An *in silico* analysis of the expression of all the insulin genes was performed. Here, data from both the CenGEN database and wormbase were compared. However, as the data from CenGEN was more complete and uniformly presented. The focus lied on data obtained from the CenGEN database.

RESULTS

1. Nictation behaviour

To discover possible roles of insulin genes in the regulation of nictation behaviour, nictation ratio, nictation initiation and the average duration of nictation were quantified for knockout strains of *ins-1*, *ins-4*, *ins-6*, *ins-17* and *ins-19*, and insulin overexpression strains of *ins-15*, *ins-17*, *ins-19*, *ins-21*, *ins-36*, *ins-37*, *ins-38*, and *ins-39*. Insulin mutant were selected for analysis regarding their role in the IIS pathway and their influence on dauer development. Selected insulin overexpression (OE) and knock-out (KO) strains were screened for nictation variants by a standardized nictation assay using a micro-dirt chip. Using ANOVA and Dunnet post-hoc analysis, we ultimately found 3 strains to have a significantly different nictation ratio compared to wild type (*ins-17* OE, *ins-19* OE and *ins-19* KO, Fig. 9-10, Table 1 in Appendix 4). Two strains were found to have a significantly different initiation index compared to the wild type (*ins-19* OE and *ins-36* OE, Fig.11, Table 1 in Appendix 4), and there were no strains found with a significantly different average duration of nictation (Fig.12, Table 1 in Appendix 4).

1.1. Some of the selected INS peptides affect nictation behaviour in hermaphrodites

A first discovery screen, consisting of three assays for each mutant, was carried out for all the selected insulin strains. Overall, overexpression strains of *ins-19* and *ins-39*, and knockout mutants of *ins-1*, *ins-6*, and *ins-17* showed differences in nictation behaviour.

Analysis of the nictation behaviour showed that there was a significant difference in nictation ratio for the different insulin strains ($F= 4.2164$) with a p-value of 0.0005976 (Fig.9). Post-hoc analysis revealed that the overexpression strains *ins-39* and *ins-19*, and the knockout strain of *ins-17* had a difference in nictation ratio compared to the wild type with a respective p-value of 0.00989, 0.02773, and 0.04976.

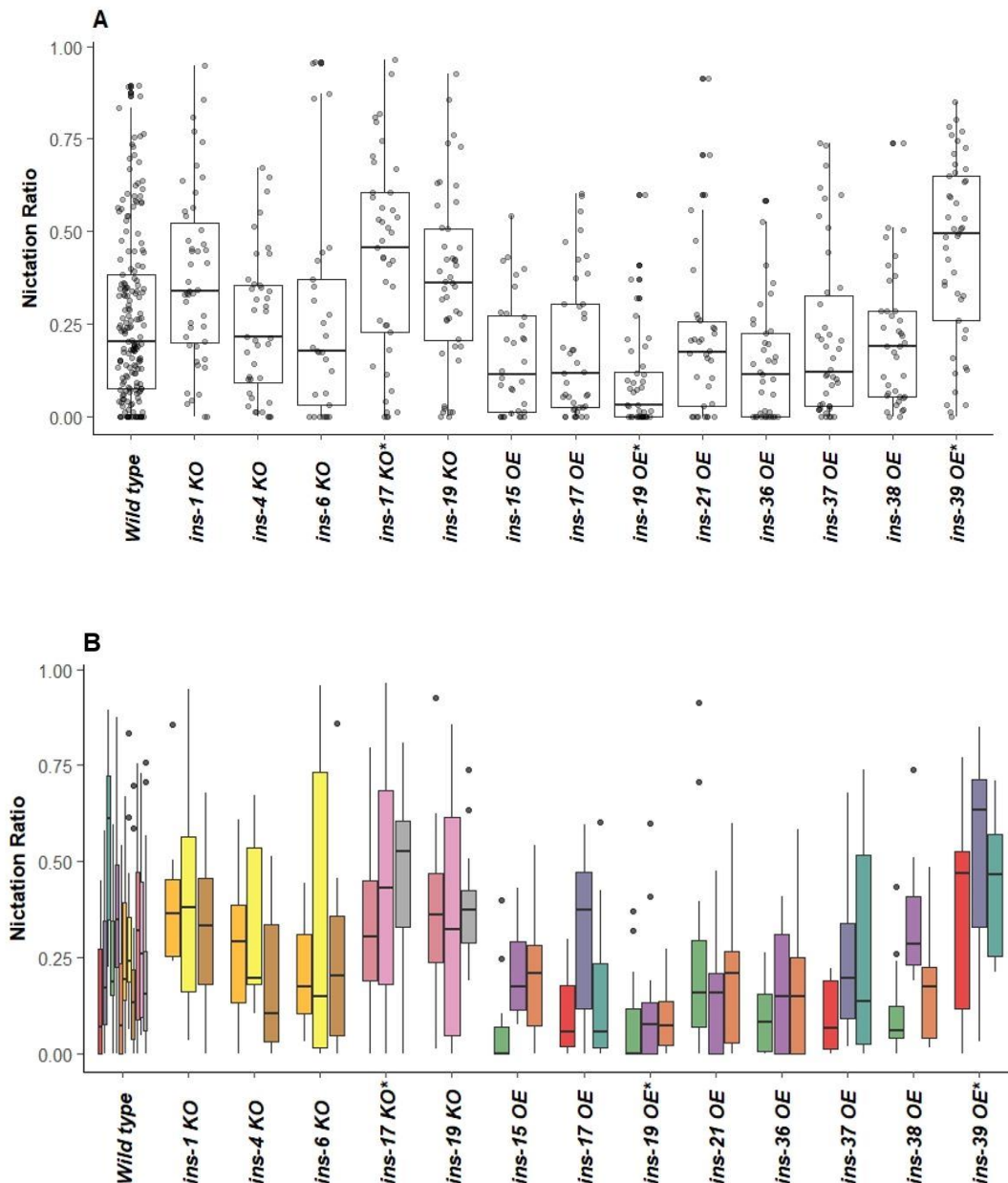


Figure 9: Nictation ratio of different insulin mutant strains, indicated by boxplots in different colours (A), and the same nictation ratio but then visualized for each different day per mutant strain by a boxplot where the different colours correspond to the different experimental days (B). Each strain was tested 3 times. Light grey points represent the nictation ratio of individual worms in A. Strains indicated with KO are knock-out mutants of this specific insulin gene, whereas strains indicated with OE are overexpression mutants. Mutants with a significant difference in nictation ratio when compared to the wild type, are marked with an asterisk.

The nictation ratio is calculated based on all the active worms in the assay, whether they are nictating or not. This parameter for nictation can be used to see the effect of the mutation on the decision to nictate or not. However, by excluding non-nictating worms, the nictation ratio gives a better view on the differences in actual nictation behaviour itself. A large number of non-nictating

worms present in the experiment could for example mask otherwise normal nictation behaviour. Therefore, the nictation ratio, only including actively nictating worms, can give a more complete view of the nictation behaviour.

When only the actively nictating individuals were included in the nictation ratio, the effect of the different strains stayed significant ($F= 4.0398$) with a slightly higher p-value of 0.0007968 (Fig.10). But only two strains remained significant in post hoc analysis when compared to the wild type, being the overexpression mutant of *ins-39*, and the *ins-17* knockout with p-values of 0.0301, and 0.0233, respectively.

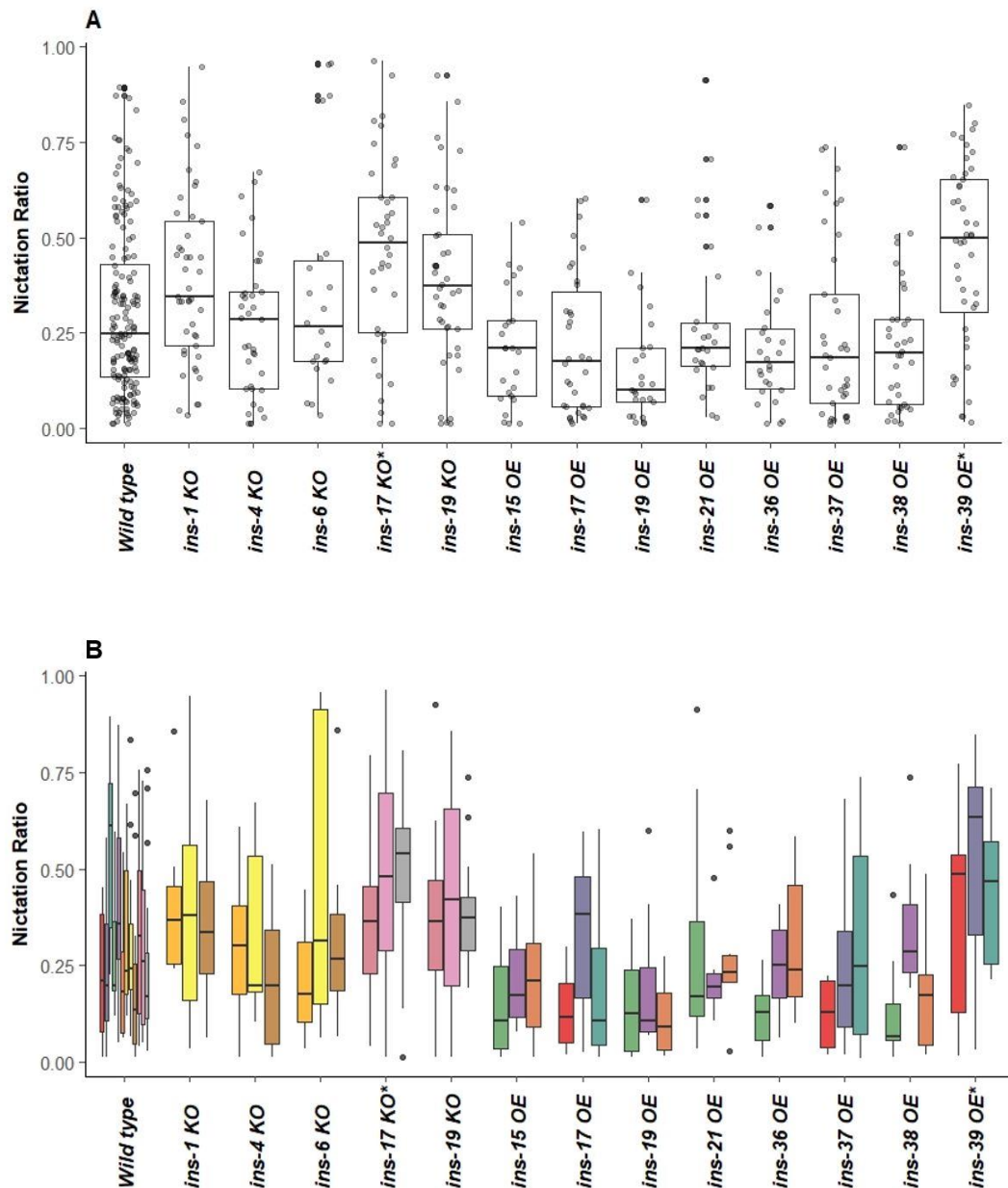


Figure 10: Nictation ratio of different insulin mutant strains only accounting actively nictating worms, indicated by boxplots in different colours (A), and the same nictation ratio but then visualized for each different day per mutant strain by a boxplot where the different colours correspond to the different experimental days (B). Each strain was tested 3 times. Light grey points represent the nictation ratio of individual worms in A. Strains indicated with KO are knock-out mutants of this specific insulin gene, whereas strains indicated with OE are overexpression mutants. Mutants with a significant difference in nictation ratio when compared to the wild type, are marked with an asterisk.

Nictation initiation was measured via the initiation index (Fig.11) and found significant when tested ($F= 3.0977$) with a p-value of 0.006113. No significant differences in nictation initiation were found in post hoc analysis with a p-value <0.05 when compared to the wild type. But both the overexpression mutants of *ins-39* and *ins-19* showed some noticeable results with relatively low p-values of 0.0898 and 0.0724.

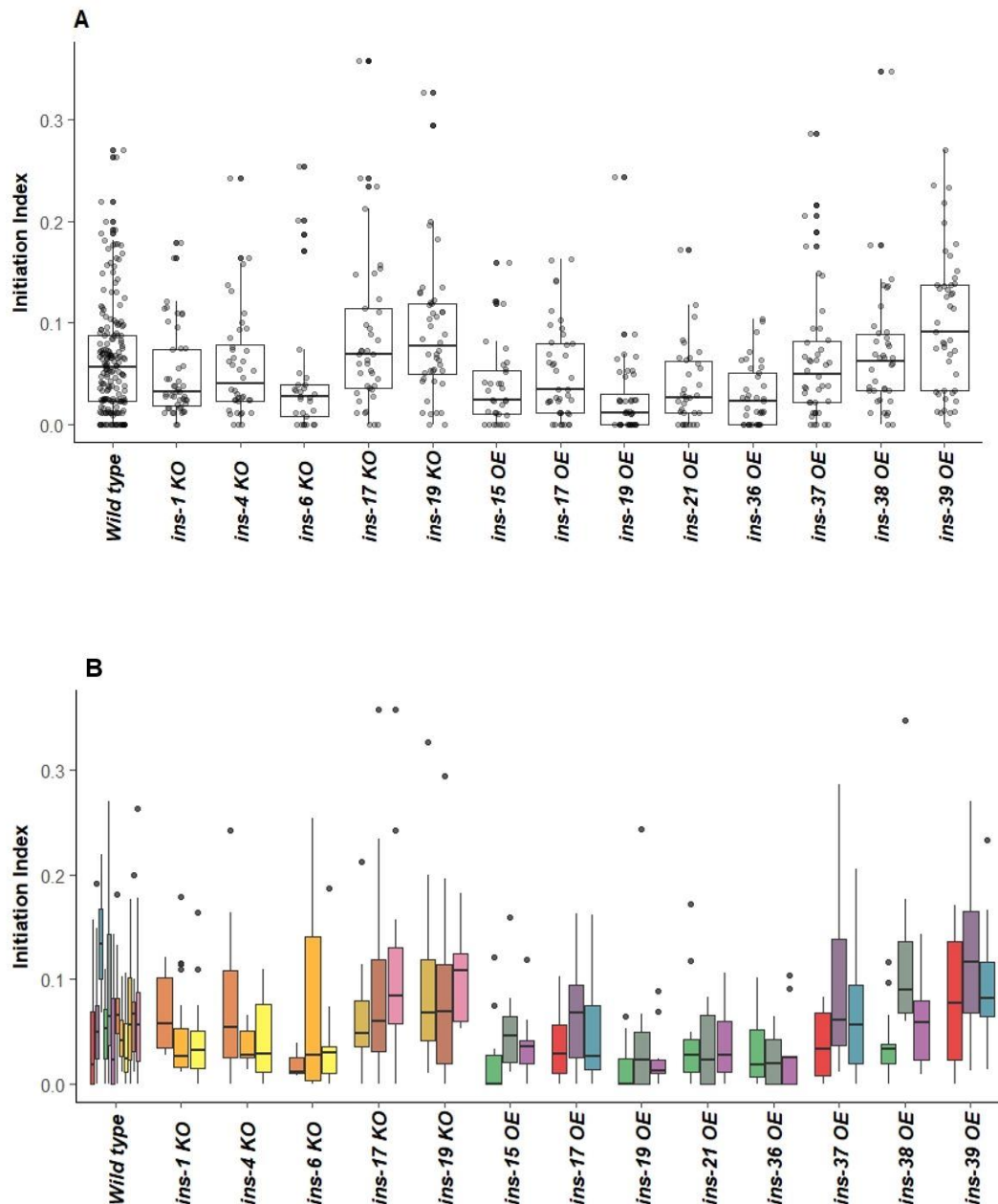


Figure 11: Nictation initiation index of different insulin mutant strains, indicated by boxplots in different colours (A), and the same nictation initiation index but then visualized for each different day per mutant strain by a boxplot where the different colours correspond to the different experimental days (B). Each strain was tested 3 times. Light grey points represent the nictation ratio of individual worms in A. Strains indicated with KO are knock-out mutants of this specific insulin gene, whereas strains indicated with OE are overexpression mutants. Mutants with a significant difference in nictation ratio when compared to the wild type, are marked with an asterisk.

When the average duration of nictation was quantified, there was a significant difference for the different insulin mutants ($F= 5.0162$) with a p-value of 0.000231 (Fig.12). Only deletion mutants revealed significant differences in average duration compared to the wild type in post hoc analysis, being *ins-17*, *ins-1*, and *ins-6* with respective p-values of 0.04171, <0.0001 and 0.00133.

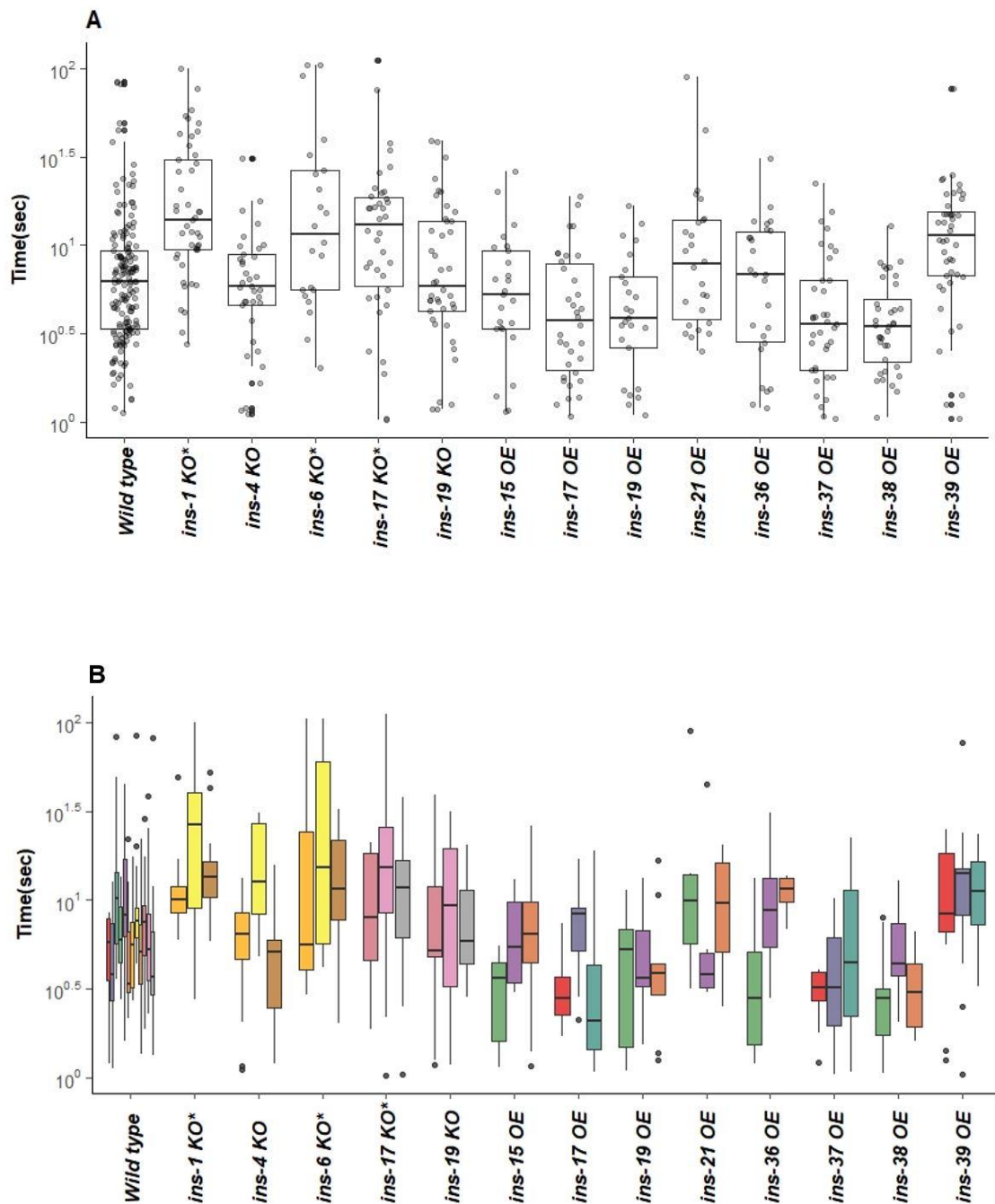


Figure 12: The average duration of nictation of different insulin mutant strains, indicated by boxplots in different colours on a log₁₀ scale (A), and the average duration of nictation but then visualized for each different day per mutant strain by a boxplot where the different colours correspond to the different experimental days (B). Each strain was tested 3 times. Light grey points represent the nictation ratio of individual worms in A. Strains indicated with KO are knock-out mutants of this specific insulin gene, whereas strains indicated with OE are overexpression mutants. Mutants with a significant difference in nictation ratio when compared to the wild type, are marked with an asterisk.

Based on these results, six strains were selected for further testing, aiming to create a more robust dataset for these interventions. These were both the overexpression and deletion strains of *ins-17* and *ins-19*, and the overexpression strains of *ins-36* and *ins-39*. These strains were tested another two times, to get a total of 5 experiments per strain. The overexpression mutants of *ins-19* and *ins-39* previously showed a difference in nictation ratio, as did the knockout mutant of *ins-17* (Fig.9 and Fig.10). *ins-17* overexpression and *ins-19* deletion strains were added to this analysis for conceptual completeness of the assay. *Insulin 36* overexpression did not present any differences in the previous analysis. But it was of interest to other research in the host lab, therefore, it was decided to incorporate it in the following experiments. Deletion strains of *ins-36* and *ins-39* were not available at the time of experiments and are thus not included in this work.

When the data were assessed for nictation ratio (note that 3/5 replicas are already included in Figures 9-12), there was a significant difference in nictation ratio for the different insulin mutants (F= 6.1913) with a p-value of 0.000318 (Fig.13). Post-hoc analysis showed a significant difference for *ins-17* overexpression in comparison to the wild type with a p-value of 0.0240. Both the deletion and overexpression mutant of *ins-19* also showed a difference in nictation ratio in comparison to the wild type with p-values of 0.0660 and 0.0837, respectively (*i.e.* below the significance level of $p < 0.05$).

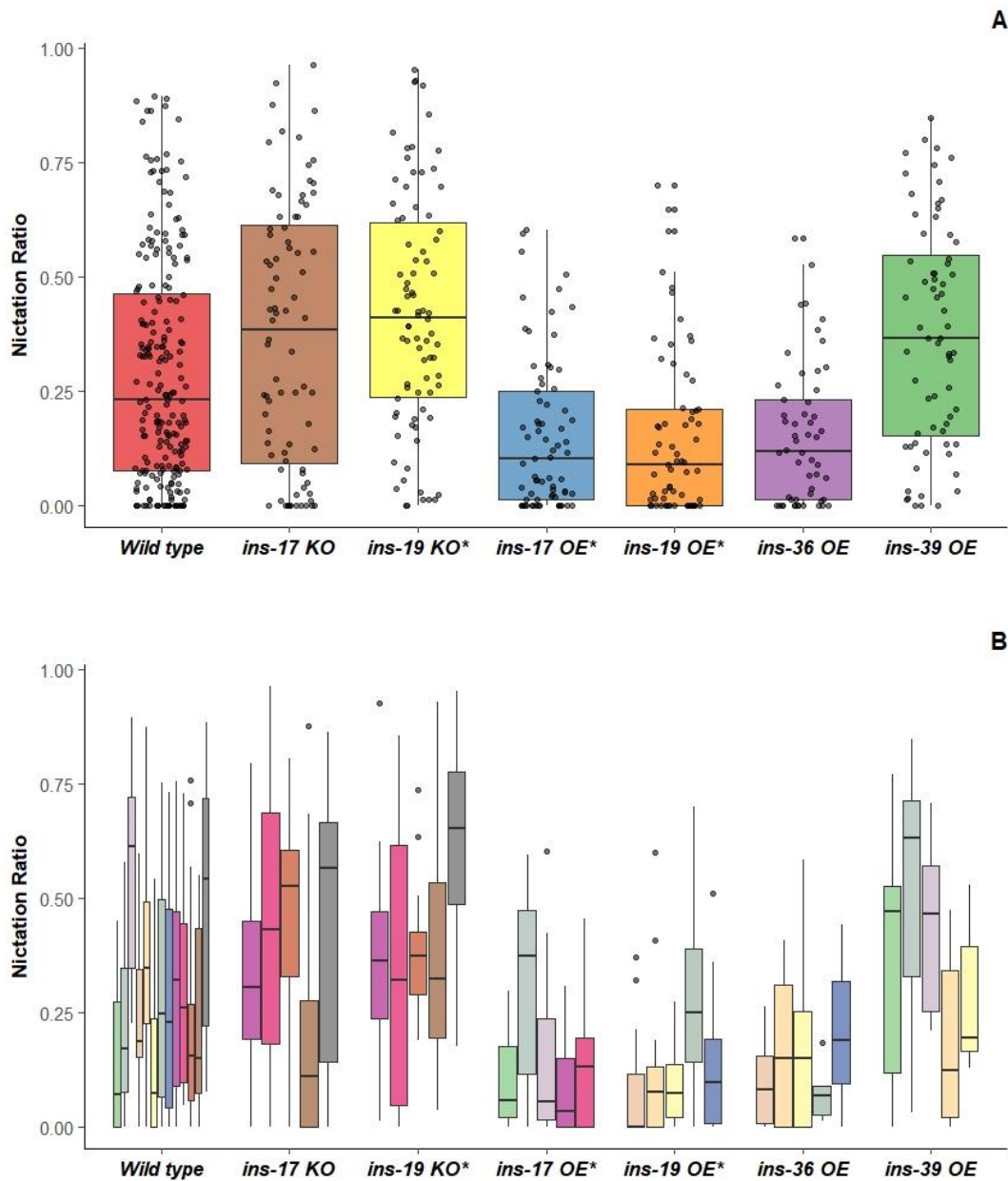


Figure 13: Nictation ratio of different insulin mutant strains, indicated by boxplots in different colours (A), and the same nictation ratio but then visualized for each different day per mutant strain by a boxplot where the different colours correspond to the different experimental days (B). Each strain was tested 5 times. Light grey points represent the nictation ratio of individual worms in A. Strains indicated with KO are knock-out mutants of this specific insulin gene, whereas strains indicated with OE are overexpression mutants. Mutants with a significant difference in nictation ratio ($p < 0.1$) when compared to the wild type, are marked with an asterisk.

The effect of the different strains stayed significant ($F = 5.8584$) with a p-value of 0.0004406 (Fig.14), when only the nictating individuals were included in the nictation ratio. Post hoc analysis revealed a significant difference in nictation ratio of *ins-17* overexpression when compared to the wild type, with a p-value of 0.0287. The noticeable difference in nictation ratio of *ins-19* mutants did not hold up when only nictating worms were included in the analysis, demonstrating the effect of non-nictating worms on the nictation ratio.

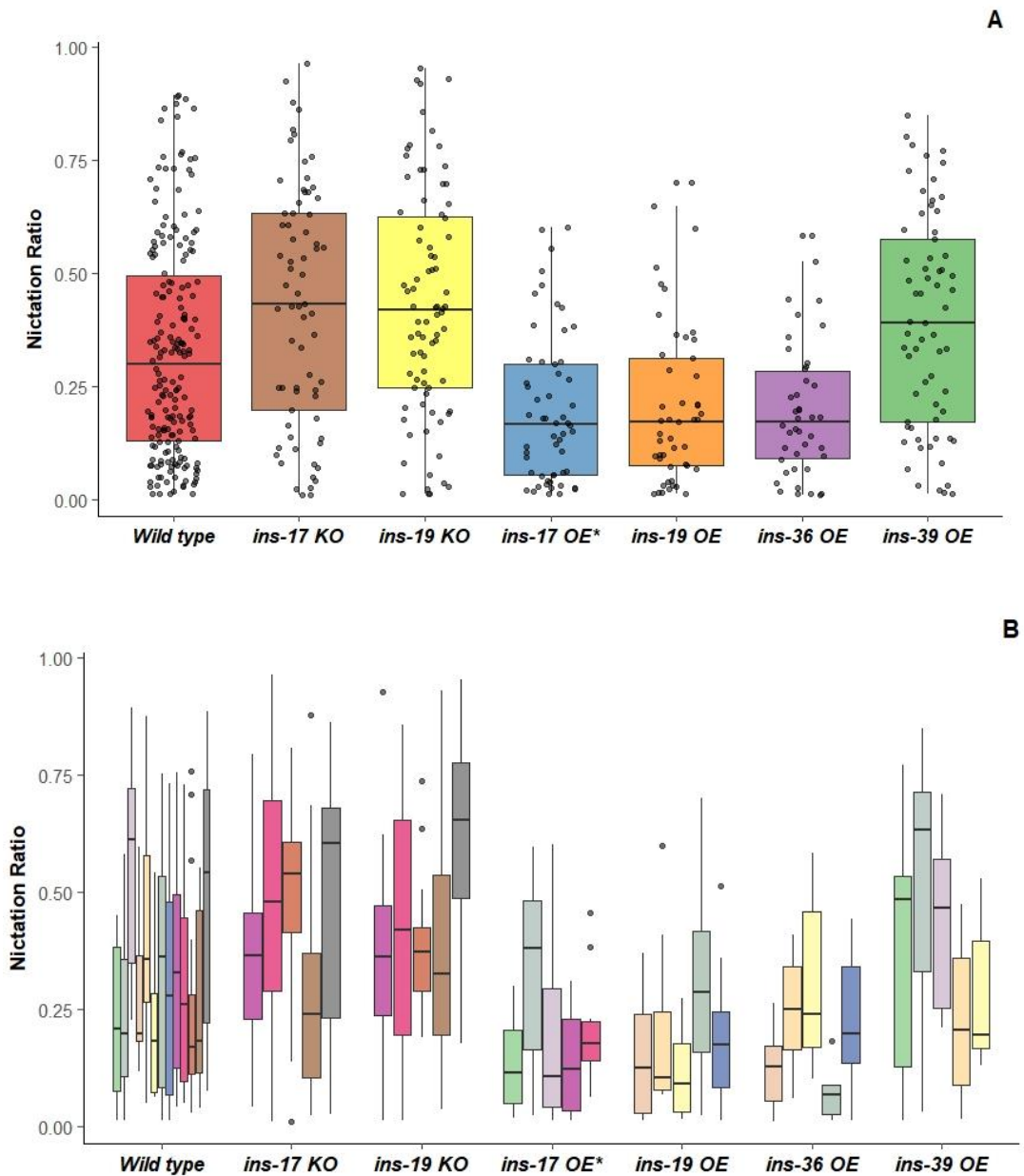


Figure 14: Nictation ratio of different insulin mutant strains, only accounting of actively nictating worms, indicated by boxplots in different colours (A), and the same nictation ratio but then visualized for each different day per mutant strain by a boxplot where the different colours correspond to the different experimental days (B). Each strain was tested 5 times. Light grey points represent the nictation ratio of individual worms in A. Strains indicated with KO are knock-out mutants of this specific insulin gene, whereas strains indicated with OE are overexpression mutants. Mutants with a significant difference in nictation ratio when compared to the wild type, are marked with an asterisk.

The initiation index was tested ($F= 5.1275$) and showed a significant difference in nictation initiation for the different insulin mutants with a p-value of 0.001018 (Fig.15). Post hoc analysis revealed two significant results. Overexpression of *ins-36* and *ins-19* were both found significant in initiation index with a p-value of 0.0346 and 0.0392, respectively. The deletion mutant of *ins-19* also showed a difference in nictation initiation in comparison to the wild type with a p value of 0.0892, but this did not meet the significance level of $p<0.05$. This was also the case for the overexpression mutant of *ins-17*, which had a p-value of 0.0723 for nictation initiation.

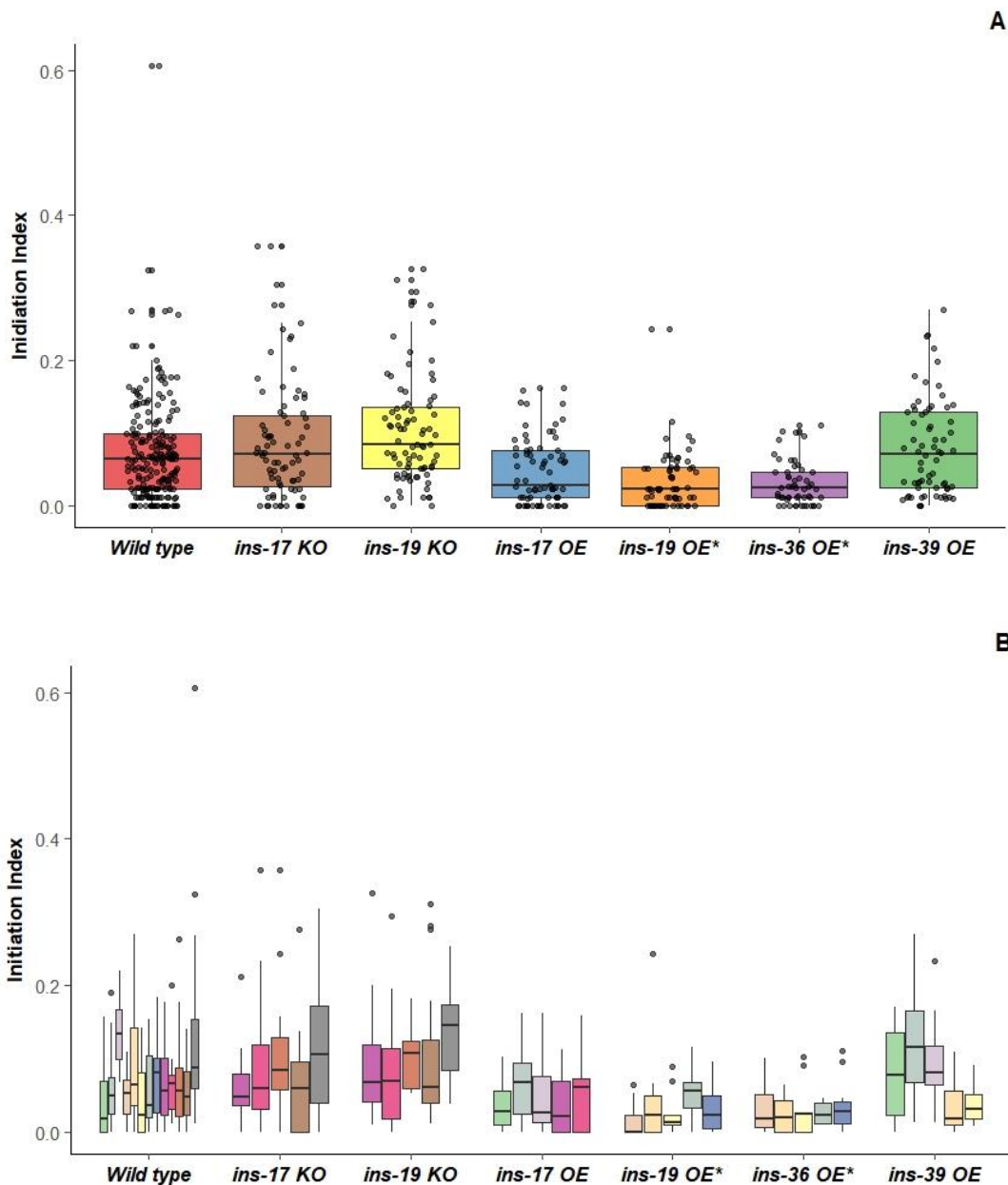


Figure 15: Nictation initiation index of different insulin mutant strains, indicated by boxplots in different colours (A), and the same nictation initiation index but then visualized for each different day per mutant strain by a boxplot where the different colours correspond to the different experimental days (B). Each strain was tested 5 times. Light grey points represent the nictation ratio of individual worms in A. Strains indicated with KO are knock-out mutants of this specific insulin gene, whereas strains indicated with OE are overexpression mutants. Mutants with a significant difference in nictation ratio when compared to the wild type, are marked with an asterisk.

There was an overall significant difference in average duration of nictation for the different insulin mutants ($F= 4.0176$) with a p-value of 0.004717 (Fig.16). But post-hoc analysis showed no significant strains at the significance level of $p<0.05$. The overexpression mutant of *ins-17* however did show reduction in duration of nictation behaviour, although with a p-value of 0.0982, considered not significant.

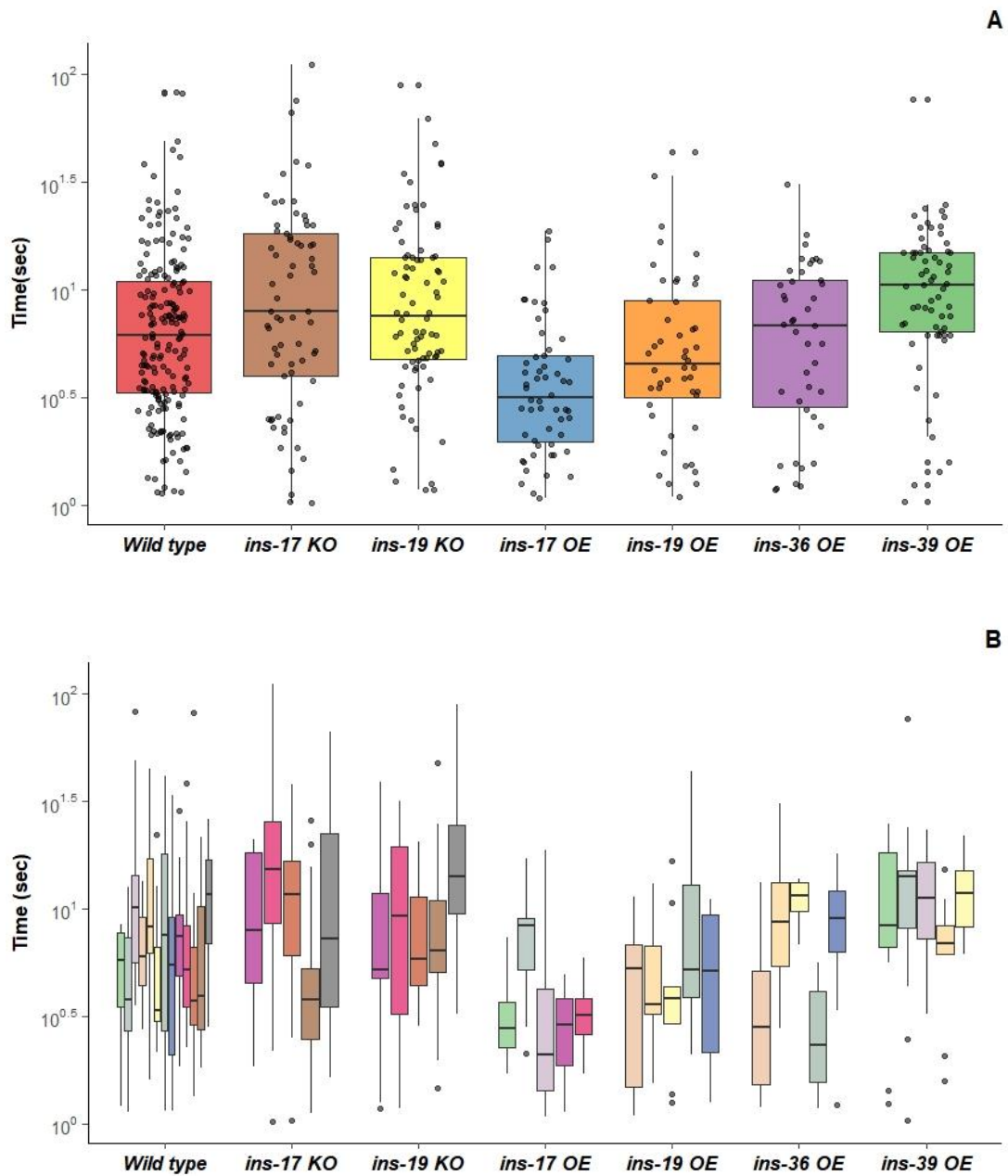


Figure 16: The average duration of nictation of different insulin mutant strains, indicated by boxplots in different colours on a \log_{10} scale (A), and the average duration of nictation but then visualized for each different day per mutant strain by a boxplot where the different colours correspond to the different experimental days (B). Each strain was tested 5 times. Light grey points represent the nictation ratio of individual worms in A. Strains indicated with KO are knock-out mutants of this specific insulin gene, whereas strains indicated with OE are overexpression mutants. Mutants with a significant difference in nictation ratio when compared to the wild type, are marked with an asterisk.

1.1.1. COPAS treatment does not affect nictation behaviour of hermaphrodites

During our experiments, not every strain would produce as much dauers after dauer induction by starvation (see 2.2 *Material and Methods*). The dauers would therefore be difficult to find and pick of their plates. The automatic COPAS biosorting system could be used to select dauers in strains with weak dauer formation. But this treatment is harsh to the worms and could thus possibly influence their behaviour. To see if worm selection and handling by the COPAS influenced nictation behaviour, the nictation behaviour of wild type dauers was assessed in both conditions (Fig.17). There was no significant difference in nictation ratio between both conditions ($F=0.3476$). When only the nictating worms were included in this analysis, there was again no significant difference found ($F=0.1537$). The same non-significance holds true for both the nictation initiation index ($F=0.1187$) and the average duration of nictation ($F=0.7317$), indicating that it is unlikely for the COPAS step to have significantly affected experimental outcomes.

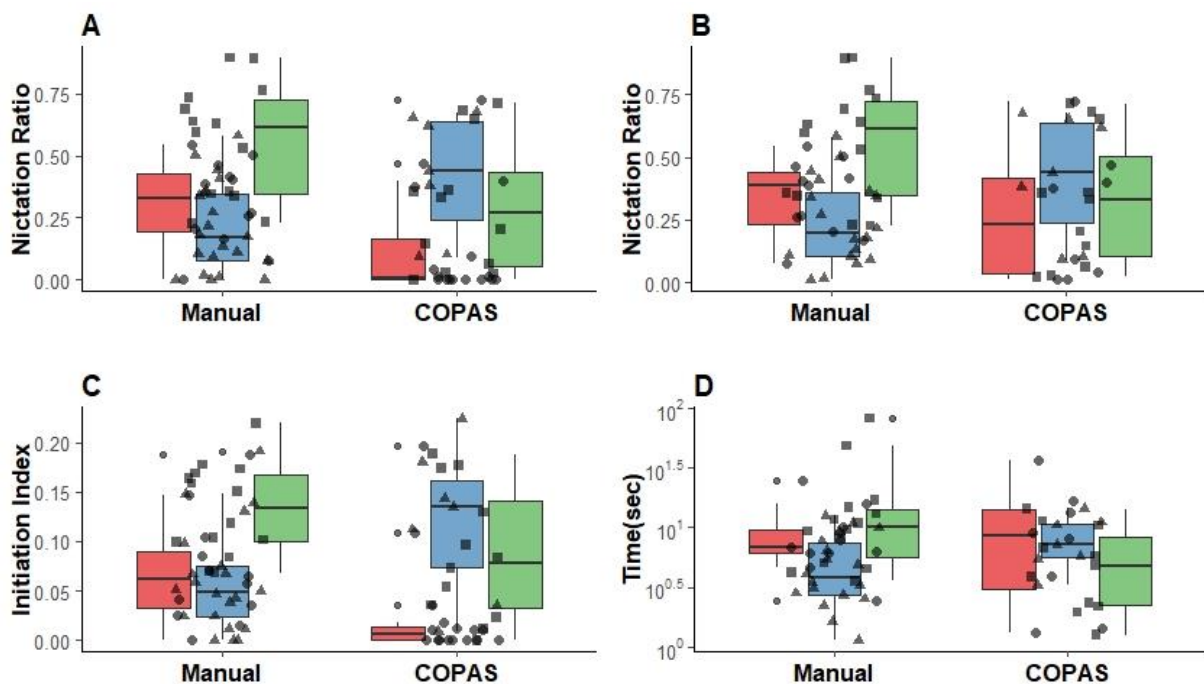


Figure 17: The three parameters used for the assessment for nictation behaviour; nictation ratio (A-B), nictation initiation (C) and average duration of nictation (D) are shown for wild type dauers that were selected manually vs automatically (by a COPAS large particle flow cytometer). A; nictation ratio based on all animals in experiment, B; nictation ratio only including actively nictating worms, C; initiation index, D; average duration of nictation on a \log_{10} scale, thus not including non-nictating individuals. The experiment was conducted trice, indicated by boxplots in a different colour for every experiment. Individual measurements per experiment are depicted as data points in different shapes (red & circle: experiment 1, blue & triangle: experiment 2, green & square: experiment 3).

1.2. Males do not display nictation like dauers do

The nictation behaviour of males could not be assessed with the experimental set-ups described in section 1.2.3. of *Material and methods*. But we did observe some sort of nictation behaviour, where males shortly raised their heads and turned them around. This behaviour was only present when there were special structures or other worms available for the males to push themselves off. This behaviour could maybe not be categorized as nictation behaviour, but more likely as phoretic or exploratory behaviour.

2. Locomotion is not affected by the selected INS peptides in hermaphrodites

While the aim of this work is to probe for insulin gene regulators of nictation, differences in baseline two-dimensional locomotion between interventions and control animals could already (indirectly) affect nictation behaviour. Hence, triaging animals with general locomotion deficits from those struggling with nictation behaviour only, is important. The same genes of interest were evaluated for overall locomotion abilities, being *ins-17*, *ins-19*, *ins-36*, and *ins-39*, but here we only quantified locomotion of overexpression strains because of time restraints. We used centroid speed as a readout for overall locomotion, with speed either defined as the measured speed over all behaviours or as the measured speed solely while running (see 3. *Material and Methods*).

There was no significant difference in speed while running for the different conditions ($F=0.7702$). Also, in post hoc analysis there were no significant differences found for the different insulin strains with respect to the wild type. It was noticeable that overexpression of *ins-19* affected the speed more, as its p-value ($p=0.474$) was much lower than that of the other strains, which resembled the wild type very accurately with p-values of 0.997 and higher. The same holds true for the speed over all behaviours. There was no significant difference found in speed for the different conditions ($F=0.7856$). Again, post hoc analysis did not show significant differences for the different insulin mutants with respect to the wild type. However, the earlier-discussed effect of *ins-19* overexpression was even more outspoken for the speed over all behaviours (*cf.* above). Indeed, while all data distributions are similar.

ins-19 overexpression seems to lead to shift towards the lower end of the range (Fig.18). Also, while we heeded inter-experimental variation and did observe lower speed measurements in one of our independent experiments (three in total, Fig.19), this random effect was not significant.

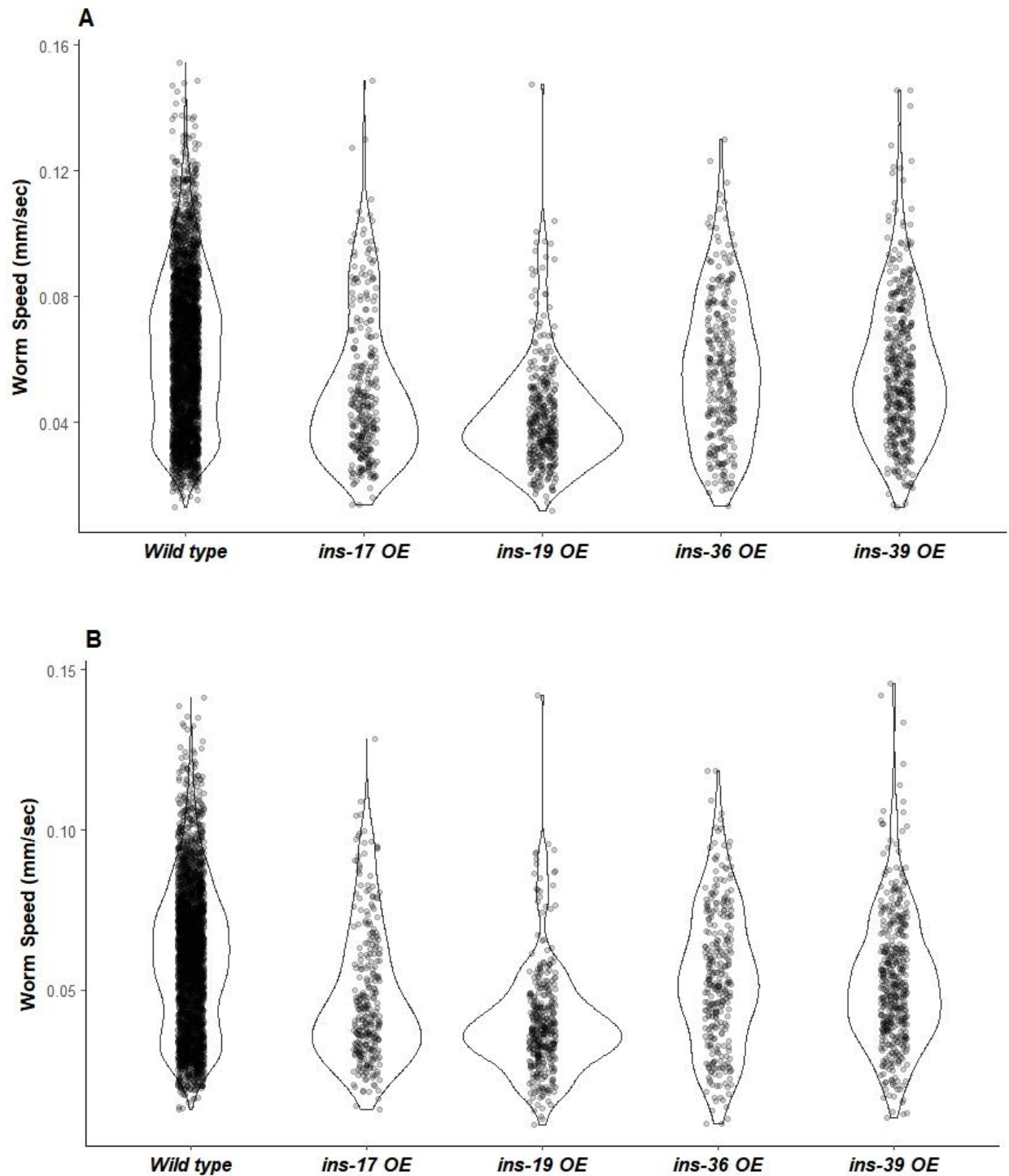


Figure 18: Average worm speed while running (A) and over all behaviours (B) for *ins-17* OE, *ins-19* OE, *ins-36* OE, *ins-39* OE, and wild type. Individual measurements are displayed as grey dots.

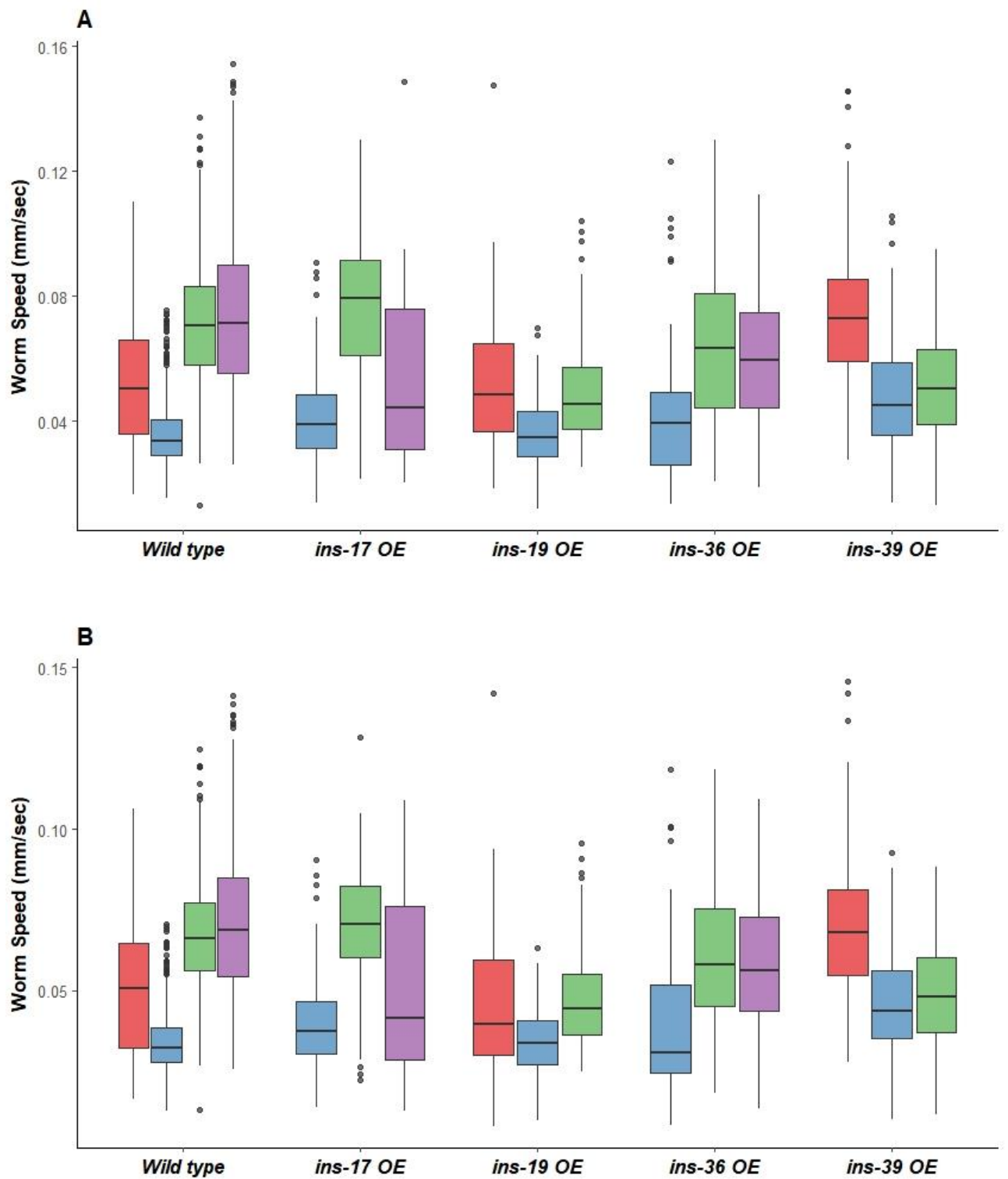


Figure 19: Average worm speed while running (A) and over all behaviours (B) for *ins-17 OE*, *ins-19 OE*, *ins-36 OE*, *ins-39 OE*, and wild type. Boxplots for different testing days are shown in different colours.

3. Insulin expression

Knowledge on insulin gene expression patterns could help reveal and define functional relationships of these peptides. Hence, next to the testing of actual behaviours, we also examined expression patterns of selected insulin-like peptides via *in vivo* experiments and an *in silico* meta-analysis.

3.1. Localization of the selected INS peptides in L3 juveniles and dauers

The expression of the four different insulin peptides of interest (see 1.1 *Results*) was visualized in dauers vs L3 juveniles via GFP reporter expression driven by gene-specific promoters. The four visualized peptides were *ins-17p*: Fig. 19, *ins-19p*: Fig. 20, *ins-36p*: Fig. 21 and *ins-39p*: Fig.22.

ins-17p (Fig.20) clearly drives expression in the head and tail of the dauer, where multiple cell bodies light up. The proximal part of the body also shows expression, where not only cell bodies but also axons or nerve cords light up. The L3 juvenile, however, only shows *ins-17p* expression in the head. Although multiple cell bodies light up, there is evidently less expression compared to the dauer.

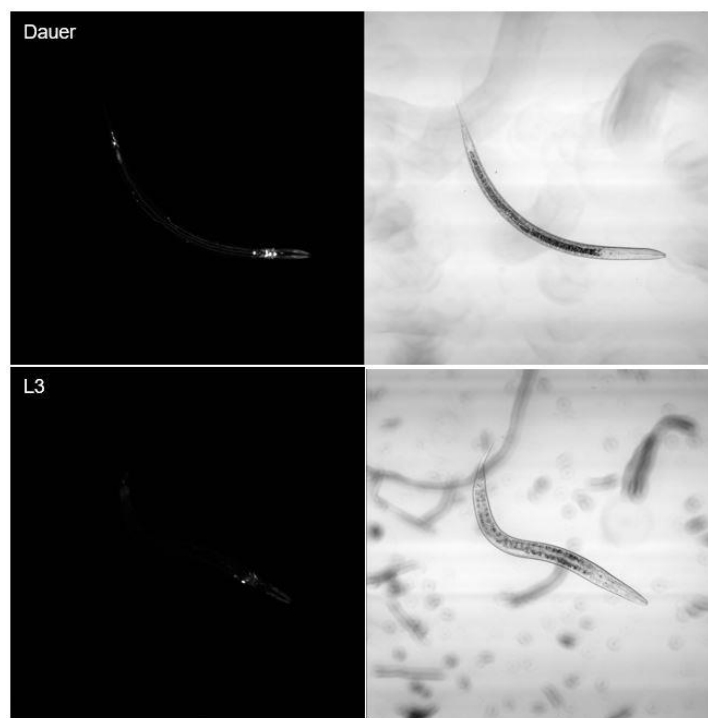


Figure 20: The fluorescently visualized expression of INS-17 peptide in both dauer and L3 larvae (right) compared to brightfield (left).

There is mostly, if not only, autofluorescence observed in *ins-19p*-driven GFP animals in the dauer and L3 alike (Fig.21). The assumedly autofluorescent signal was, however, more clear in the dauer than in the L3 juvenile.

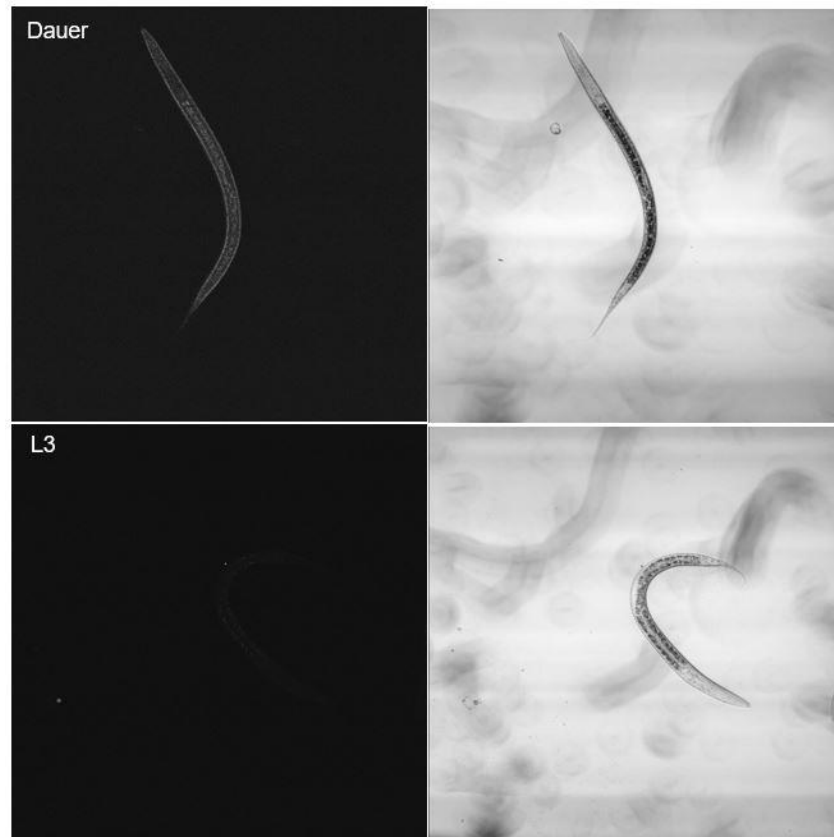


Figure 21: The fluorescently visualized expression of INS-19 peptide in both dauer and L3 larvae (right) compared to brightfield (left). The fluorescent signal in the dauer can be assigned to autofluorescence.

ins-36p reveals expression in the dauer head where multiple cell bodies light up (Fig.22). The image also contains some autofluorescence, making it more difficult to differentiate between the fluorescent signal excited by INS-36 peptides and the autofluorescence. Having said this, the dauer tail likely also shows some specific expression. The L3 larvae displays some expression in the intestine, the head, and the tail. Here, one cell body in the head clearly lights up, together with more distal expression of non-individually-recognizable cells.

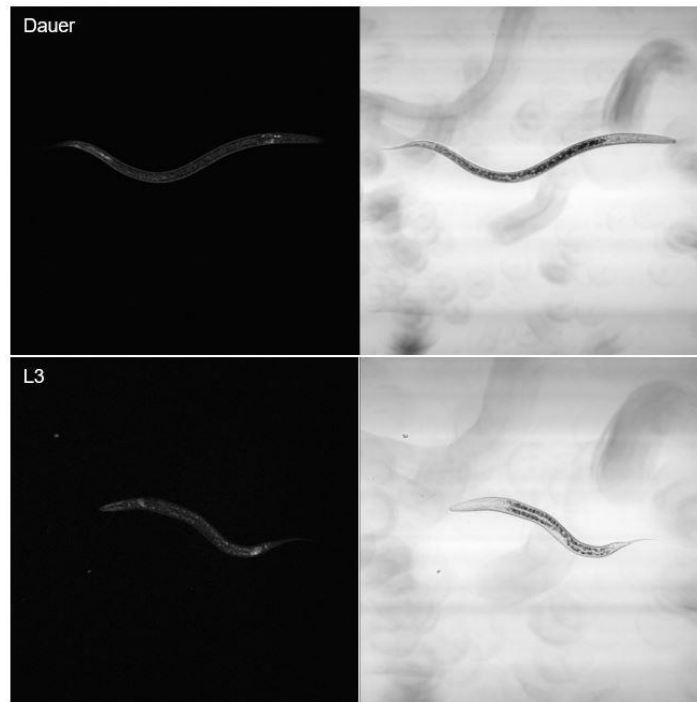


Figure 22: The fluorescently visualized expression of INS-36 peptide in both dauer and L3 larvae (right) compared to brightfield (left). Part of the fluorescence in both the dauer and L3 larvae is due to autofluorescence.

There is clear ins-39p expression in both the tail and head of the dauer (Fig.23). Multiple cell bodies light up in the head and there are two visible cell bodies present in the tail. The fluorescence also outlines the beginning of some axons or nerve cords in the dauer. L3 larvae mostly show expression in the intestines. One worm also presents a clear signal in its tail, but this was not observed in any other worms.

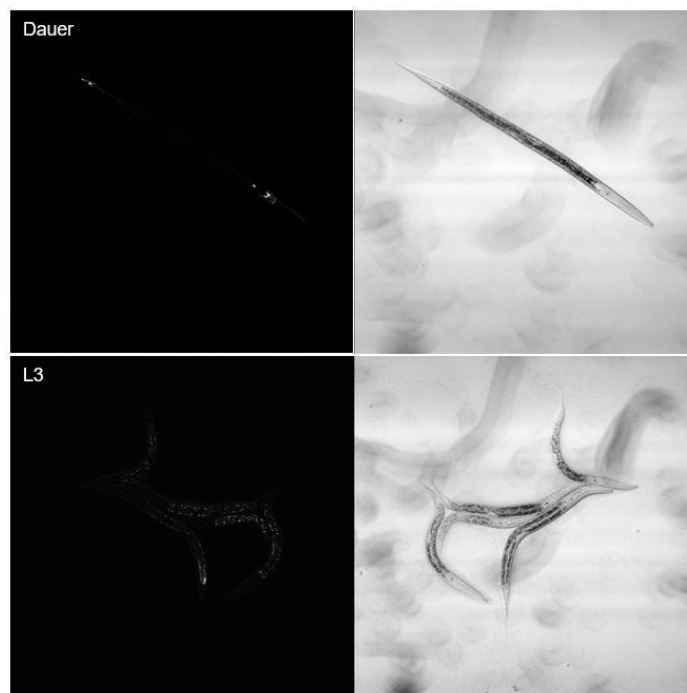


Figure 23: The fluorescently visualized expression of INS-39 peptide in both dauer and L3 larvae (right) compared to brightfield (left).

3.2. *In silico* meta-analysis

In addition to *in vivo* analysis of insulin expression patterns of *ins-17*, *ins-19*, *ins-36* and *ins-39*, an *in silico* analysis of possible expression sites of all insulin-like genes was performed. For this, the gene expressions by cell type were assessed for all insulin-like genes of the *C. elegans* Neuronal Gene Expression Network database (Taylor et al., 2020). Here, the expression patterns of the four insulin-like peptides of interest were assessed in L4-staged hermaphrodites without filtering by threshold (Table 5). The absolute values were converted to percentages per neuron and a gradient was added in red where the highest percentage per peptide was bright red. An overview of the expression of all the insulin peptides can be found in Appendix 3. There were no data available for *ins-8*, *ins-31*, and *ins-38*. When a more stringent threshold of 2 (True Positive Rate of 0.810) for expression was implemented, there was no expression of *ins-19*, *ins-20*, *ins-33*, and *ins-34* as these were now below threshold.

Table 5: The expression of *ins-17*, *ins-19*, *ins-36*, and *ins-39* in different cell types expressed in percentages.

	<i>ins-17</i>	<i>ins-19</i>	<i>ins-36</i>	<i>ins-39</i>		<i>ins-17</i>	<i>ins-19</i>	<i>ins-36</i>	<i>ins-39</i>		<i>ins-17</i>	<i>ins-19</i>	<i>ins-36</i>	<i>ins-39</i>
ADA	1%	0%	0%	0%	DA	0%	0%	0%	0%	PVQ	0%	0%	0%	0%
ADE	0%	0%	0%	0%	DA9	0%	0%	0%	0%	PVR	0%	0%	0%	0%
ADF	0%	0%	3%	1%	DB	0%	6%	0%	0%	PVT	0%	0%	0%	0%
ADL	0%	0%	3%	1%	DB01	0%	0%	0%	0%	PVW	0%	0%	0%	0%
AFD	0%	0%	0%	30%	DVA	0%	0%	0%	0%	RIA	0%	0%	0%	0%
AIA	0%	0%	0%	0%	DVB	0%	0%	0%	0%	RIB	0%	0%	0%	0%
AIB	0%	0%	0%	0%	DVC	0%	0%	0%	0%	RIC	0%	0%	0%	0%
AIM	0%	0%	0%	0%	FLP	0%	0%	0%	0%	RID	3%	0%	0%	0%
AIN	4%	68%	0%	0%	HSN	2%	0%	0%	0%	RIF	5%	0%	0%	0%
AIY	0%	0%	0%	0%	I1	0%	0%	0%	0%	RIG	0%	0%	0%	0%
AIZ	41%	0%	0%	0%	I2	0%	0%	0%	0%	RIH	0%	0%	2%	0%
ALA	0%	0%	0%	0%	I3	0%	0%	0%	0%	RIM	0%	0%	0%	1%
ALM	0%	0%	0%	0%	I4	1%	0%	0%	0%	RIP	0%	0%	0%	0%
ALN	3%	0%	0%	0%	I5	0%	0%	0%	0%	RIR	0%	0%	0%	0%
AQR	0%	0%	0%	0%	I6	0%	0%	0%	0%	RIS	0%	0%	0%	0%
AS	0%	0%	1%	0%	IL1	0%	0%	0%	0%	RIV	0%	0%	0%	0%
ASEL	0%	0%	0%	0%	IL2_DV	0%	0%	6%	0%	RMD_DV	0%	0%	0%	0%
ASER	0%	0%	9%	5%	IL2_LR	0%	0%	2%	0%	RMD_LR	0%	0%	0%	1%
ASG	0%	0%	6%	0%	LUA	2%	0%	0%	0%	RME_DV	0%	0%	0%	0%
ASH	0%	0%	6%	0%	M1	0%	0%	0%	0%	RME_LR	0%	0%	0%	0%
ASI	0%	0%	0%	0%	M2	2%	0%	0%	0%	RMF	1%	0%	0%	0%
ASJ	0%	10%	0%	17%	M3	0%	0%	0%	0%	RMG	0%	0%	0%	0%
ASK	0%	0%	0%	21%	M4	1%	0%	0%	0%	RMH	3%	0%	0%	0%
AUA	0%	0%	13%	0%	M5	1%	0%	0%	0%	SAA	0%	0%	0%	0%
AVA	0%	0%	0%	0%	MC	0%	0%	0%	0%	SAB	0%	0%	0%	0%
AVB	0%	0%	0%	0%	MI	3%	0%	0%	0%	SDQ	0%	0%	0%	0%
AVD	0%	0%	0%	0%	NSM	0%	16%	0%	0%	SIA	0%	0%	0%	0%
AVE	2%	0%	0%	0%	OLL	0%	0%	0%	0%	SIB	0%	0%	0%	0%
AVF	0%	0%	0%	0%	OLQ	0%	0%	0%	0%	SMB	8%	0%	0%	0%
AVG	2%	0%	0%	0%	PDA	0%	0%	0%	0%	SMD	0%	0%	0%	0%
AVH	0%	0%	0%	0%	PDB	0%	0%	0%	0%	URA	0%	0%	10%	0%
AVJ	0%	0%	0%	0%	PDE	0%	0%	0%	0%	URB	0%	0%	0%	0%
AVK	0%	0%	0%	0%	PHA	1%	0%	2%	0%	URX	0%	0%	1%	0%
AVL	0%	0%	0%	0%	PHB	1%	0%	11%	0%	URY	0%	0%	0%	0%

AVM	0%	0%	0%	0%
AWA	0%	0%	0%	0%
AWB	0%	0%	0%	0%
AWC_OFF	0%	0%	0%	1%
AWC_ON	0%	0%	0%	19%
BAG	0%	0%	2%	0%
BDU	0%	0%	0%	0%
CAN	0%	0%	0%	0%
CEP	0%	0%	0%	0%

PHC	0%	0%	17%	3%
PLM	0%	0%	0%	0%
PLN	6%	0%	1%	0%
PQR	0%	0%	0%	0%
PVC	0%	0%	0%	0%
PVD	0%	0%	0%	0%
PVM	0%	0%	0%	0%
PVN	0%	0%	0%	0%
PVP	0%	0%	0%	0%

VA	0%	0%	0%	0%
VA12	0%	0%	0%	0%
VB	0%	0%	0%	0%
VB01	0%	0%	0%	0%
VB02	0%	0%	0%	0%
VC	0%	0%	0%	0%
VC_4_5	0%	0%	0%	0%
VD_DD	0%	0%	1%	0%

Overall, *ins-36* displays a very broad expression pattern, as the highest expression of the gene in one neuron, being AVM, is only 17% of the overall tpm count of *ins-36*, with similar relative contributions for cells. Opposite to that is *ins-19* which is mostly expressed in AIN but does not seem of importance in many other neurons. Also, relative *ins-17* levels are particularly high in AIZ, next to lower percentages in PLN, AIN, RID, RIF, SMB and MI. Most of the expression of *ins-39* is divided over AFD, ASJ, ASK and AWC_ON.

DISCUSSION

1. Behavioural phenotypes in hermaphrodites

1.1. Nictation behaviour

The nictation behaviour of different insulin mutant strains was assessed in nictation assays. Initial testing showed multiple differences between these mutants and the wild type. Dauers that overexpressed *ins-39* or *ins-19* had a higher nictation ratio. The same insulin peptides demonstrated differences in nictation initiation, although not as distinct. Dauers that overexpressed *ins-39* initiated nictation more often than the wild type. Dauers that overexpressed *ins-19* however, initiated nictation less often. The deletion of *ins-17* gave a higher nictation ratio both when only the nictating worms were included and when all the active worms were included in the assay. The duration of nictation was only different in knock-out mutants. Both *ins-1*, *ins-6* and *ins-17* deletion mutants showed nictation behaviour that lasted longer.

When more experiments were carried out, creating a more robust dataset, there were some remarkable changes in the differences in nictation behaviour. As a lot of differences did not continue to apply and new ones arose. There were no longer differences found in the average duration of nictation. Instead of the expected lower significant result of deletion mutants *ins-1*, *ins-6* and *ins-17*, because of the more robust dataset. A new difference in average duration emerged, that of the overexpression of *ins-17*, which showed a shorter average duration of nictation. Although the deletion of *ins-17* gave a longer duration of nictation behaviour and the overexpression did the opposite, the fact that these results are not consistent between the different datasets raises concern. It can be stated that *ins-17* could affect nictation behaviour, specifically the duration of this behaviour. But caution must be drawn to the experimental design and the reliability of the assays. The same holds true for the assessed nictation ratio. First *ins-17* knockout mutants showed a higher nictation ratio, whereas later the overexpression mutants of *ins-17* gave a decreased nictation ratio. The first discovered difference in nictation ratio of *ins-39* overexpression mutants did not hold up in further testing. The difference found for *ins-19* overexpression mutants however was still present, although not as distinct. The decreased initiation of nictation in dauers that overexpressed *ins-19* first detected in initial testing, became more distinct in further analysis.

1.1.1. Dauer development and COPAS handling

Due to the large number of insulin peptides in *C. elegans*, it was practically not possible to test them all. Therefore, peptides were prioritized based on their supposed role in the IIS pathway (Zheng et al., 2019). Soon, a problem emerged as the overexpression of these peptides also affects dauer development (Fernandes de Abreu et al., 2014c). Overexpression strains of *ins-1*, *ins-4*, and *ins-6* for instance could not be tested because there were too few dauers present for manual selection. To overcome this problem, an automated approach was tested to select dauers.

A COPAS biosort instrument was used for dauer selection via large-particle flow cytometry, and although the worms that underwent selection by COPAS were handled more roughly than their

counterpart. There was no difference in nictation behaviour for manually selected dauers or dauers that were selected by the COPAS.

For further research automated selection could be considered in behavioural assays as a sorting tool. The COPAS could save time and provide a more randomly selected population for testing, ensuring unbiased treatment for every experiment. However, to establish automated biosorting as a given in behavioural assays, more testing should be done. As we here only tested for differences in nictation behaviour with a limited number of replicates.

1.1.2. Antagonists versus agonists

During this project, a total of 13 strains were tested on their nictation behaviour. Insulin overexpression strains included *ins-15*, *-17*, *-19*, *-21*, *-36*, *-37*, *-38* and *-39*. The deletion mutants covered *ins-1*, *-4*, *-6*, *-17* and *-19*. Most of these peptides can be classified as either a weak or strong agonist or antagonist of the IIS pathway (Zheng et al., 2019). Insulins 17, 37 and 39 are strong antagonists and downregulate the IIS pathway, increasing the length of L1 arrest life span, increasing dauer formation and fat accumulation for instance. Although these peptides are believed to have the same effect on the IIS pathway. Only insulin 39 showed a difference in nictation behaviour. Overexpression of *insulin 39* resulted in an enhancement of nictation initiation and ratio. Overexpression of *ins-37* and *ins-17* did not result in behavioural phenotypes of nictation. However, the deletion of *ins-17* gave an elongation of the duration of nictation behaviour. There were no assays conducted using the deletion counterparts of *ins-37* and *ins-39*. Although we probably do not expect to see a phenotype for *ins-37*, it would be interesting to see the results for *ins-39* knock-out. *Insulins 15*, *21*, *36* and *38* are weak antagonist of the IIS pathway. Here, only *ins-36* showed a difference in nictation behaviour which was interestingly the opposite of *ins-39*. Overexpression of *ins-36* resulted in a decrease of nictation initiation. Nictation assays with a knock-out mutant of *ins-36* were not conducted during this project but could also be complementary in future research.

Insulin peptides 4, 6 and 19 are agonists of the IIS pathway and thus their expression has the opposite effect to the expression of the antagonists concerning L1 arrest life span, dauer formation and fat accumulation. Our results suggest that this also holds true for nictation behaviour, at least concerning *ins-19*. Overexpression of *ins-19* resulted in a decrease in nictation ratio and nictation initiation and the deletion of *ins-19* gave an increase in nictation ratio. The deletion of *ins-4* did not result in any behavioural phenotypes for nictation. However, deletion of *ins-6* resulted in the same response as the deletion of the antagonist *ins-17*, being an elongation of nictation duration. Deletion of *ins-1* also gave an elongation of nictation duration. *Ins-1* is a weak agonist of the IIS pathway. Taking this into account, the duration of nictation seems randomly influenced and should not be used to draw conclusion as both weak agonist, strong agonist and strong antagonist deletion render the same result.

Our results suggest that an insulin its function in the IIS pathway is not a good criterium to predict nictation behaviour.

1.2. Locomotion behaviour

To confirm whether the nictation behaviours observed for overexpression strains of *ins-17*, *ins-19*, *ins-36* and *ins-39* are solely an effect of the insulin peptide on nictation behaviour and not a movement defect, their locomotion was assessed. Their speed was determined and compared to that of wild type worms. The assay was performed off food as this was more relevant to the behaviour in the nictation assay, which is also done without a food source. The results did not show significant differences in speed for any of the insulin overexpression mutants. Indicating that the observed differences in nictation behaviour are not the result of defects or differences in locomotion.

Although not significant, our data did show a slightly lower speed for overexpression of *ins-19* when compared to the wild type and the other insulin mutants. This observation was even more outspoken when the speed was measured over all the behaviours, and not only while running. The existing dataset could be re-assessed for other behaviours such as pausing or turning. As differences in these behaviours could explain the reduced speed of *ins-19*.

1.3. Insulin expression patterns

The expression of *ins-17*, *ins-19*, *ins-36*, and *ins-39* was visualized in the *C. elegans* dauer and L3 larvae. Our findings approach those of an earlier conducted study, using the same reporter strains (Ritter et al., 2013). Here, we compare these results and link the found expression patterns to the findings from our *in silico* analysis.

Insulin 17 expression was found in the head, tail, cell bodies in the body of the dauer and in nerve cords connecting these cells. The L3 larvae however, only showed *ins-17* expression in the head. Although multiple cell bodies expressed *ins-17*, there was evidently less expression compared to the dauer. Our findings approach those of Ritter et al., where *ins-17* expression was found in the rectum, intestines, body neurons, ventral nerve cord, vulva neuron, tail neurons, vulva muscle, head muscle, spermatheca and distal tip cell of the dauer. This study also reported *ins-17* expression in the L3 rectum, intestine, head neurons, body neurons, ventral nerve cord, tail neurons, head muscles and coelomocytes. During our analysis, the expression in the ventral nerve cord could have been overlooked due to a shortfall of images at multiple depths. *In silico* analysis revealed *ins-17* expression in a whole array of neurons: AIN, AIZ, ALN, AVE, AVG, HSN, LUA, M2, M4, M5, M1, PHA, PHB, PLN, SMB, RMH, RMF, RID, RIF. The highest expression was found in AIZ which is pair of interneurons with cell bodies situated in the lateral ganglia. AIZ neurons are the main integrating neurons for the receptors of the amphid sensilla. Their main function is thus the integration of information as it is part of the first layer of amphid interneuron pairs that receive and process synaptic output from the amphid sensory neurons towards a behavioural. Besides this, it also has functions in chemotaxis, thermotaxis and locomotion (Ino & Yoshida, 2009).

Insulin 19 expression was consistent with findings from Ritter et al., and showed no expression in either dauers or L3 juveniles. However, *ins-19* is known to have sex-enriched expression in males during the L4 larval phase (Ritter et al., 2013; Thoemke et al., 2005). Our *in silico* analysis also revealed expression of *ins-19* in four different neurons; ASJ, AIN, NSM and DB. But this expression is very minimal and did not surpass threshold two. A reason that this low expression was not picked up in visualisation experiments could be the reporter strain itself. As the reporter strain used in these experiments had a promotor of only <800bp. The majority of the expression found in the *in silico*

analysis was detected in the AIN pair of interneurons with cell bodies situated in the lateral ganglia. AIN is known to be presynaptic to the AFD neurons which are part of the amphid sensillum and have functions in thermotaxis, thermo sensing, thermonociception, locomotion, social feeding and CO₂ sensing (Bretscher et al., 2011). ASJ is another neuron pair that expresses *ins-19* and is part of the amphid sensilla, functioning to control dauer entry and exit, light sensation, and electro sensory navigation. *Insulin 19* expression was also found in two pharyngeal neurosecretory-motor neurons, NSM. These neurons were suggested to have neurohormonal function, signalling the presence of food and bacteria to the body. It is also suggested that NSM modulates the enhanced slowing response. Lastly, *ins-19* expression was also found in DB, a neuron class of seven motoneurons that innervate dorsal muscles and have cell bodies in the ventral cord. They have a function in forward locomotion and proprioception. Despite the low expression levels of *ins-19* in these neuron classes, overexpression of *ins-19* could activate their pathways, ultimately influencing nictation behaviour.

Insulin 36 was expressed in the dauer head and tail area, and in the intestine, tail, and head of the L3 larvae. Ritter et al., found that *ins-36* was expressed during all life stages in both the intestine and head neurons. Due to autofluorescence, the expression signal from the dauer intestine in could have been masked in our experiments. The same study also found *ins-36* expression in the rectum, ventral nerve cord, hypodermis, uterus, coelomocytes, and head muscles of the dauer. For the L3 larvae, they found expression of *ins-36* in the pharynx, rectum, head muscles, hypodermis, and coelomocytes in the L3 larvae. The fluorescent signal we found could thus probably originate from *ins-36* expression in the pharynx, head muscles, and head neurons. In silico analysis revealed *ins-36* expression in numerous neurons: ADF, ADL, AS, ASER, ASG, ASH, AUA, BAG, PLN, PHC, PHB, PHA, IL2_DV, IL2_LR, RIH, URA, URX, VD_DD. Some of them associated with the amphid sensillia (ADF, ADL, ASG, ASH) or part of the amphid neurons (ASER). The majority of the expression was reported in neurons with cell bodies situated in the lateral ganglia or lumbar ganglia.

Insulin 39 showed clear expression in cell bodies of the head and tail of the dauer in our experiments. Ritter et al. found *ins-39* expression throughout all life stages in the intestine and head neurons. During the dauer stage, they found additional expression in tail neurons, uterus, and the distal tip cell. This expression pattern is consistent with our findings. For the L3 larvae we found only found expression in the intestine, although Ritter et al. also found expression in the tail and head neurons. One worm does show expression in its tail, but there was no expression found in the head. During *in silico* analysis *ins-39* expression was reported primarily in neurons associated with, or part of the amphid sensilla, being ASJ, AWC_ON, ASK and AFD. RIM and RMD neurons can explain the other recorded expression found in the head, as they both innervate muscles in the head via NMJs in the nerve ring. Although their contribution to the overall expression is rather small. The reported tail expression could be the result of *ins-39* expression in PHC neuron, as this neuron has also been previously reported to express *ins-39*. Along with AFD and FLP neurons in the head, PHC neurons sense noxious temperatures and will induce a reflex-like escape reaction as a temperature avoidance response. The expression of *ins-39* in PHC also is quite small in comparison with the neurons associated with the amphid sensilla.

CONCLUSION

This thesis project contributed to shedding a light on a highly diverse, yet functionally redundant family of insulin-like peptides. As the *C. elegans* genome encodes 40 INS genes, more work will be needed to build a more coherent view. However, we can already conclude that insulin-17 is clearly involved in nictation behaviour, as both its overexpression and deletion mutants affected this behaviour. The gene is also widely expressed in the nematode body, suggesting a broad functionality. A precise function for *ins-17* cannot yet be pinpointed from our experiments, in part because of the high variability of nictation assays. Relevant to this, is that insulin-like peptides show high expression in the amphids, where environmental conditions are translated by the nervous system. Therefore, further development of more controlled nictation assays, in which the environmental conditions are better equalized (e.g. by reducing fluctuations in the environmental conditions and more replicates) is advisable to assess nictation behaviour without too many possible sensory disruptions.

Insulin-19 overexpression also showed to have an effect on the initiation of nictation, although its expression was not present in our localization experiments. This could suggest that the overexpression of *ins-19* recruits receptors, pathways and neurons that it otherwise would not. Actually expressing the phenotype of another, structurally related, insulin peptide. Precise structural comparison of all insulin peptides could find such peptide. Or further nictation assays of all the insulin peptides, in search for similar results could also lead to the find of such a peptide. *Insulin-19* is known to be expressed in males. Its effect on nictation behaviour could indicate a role of *ins-19* in the exploratory behaviour in males. To test this hypothesis, both overexpression and deletion male mutants of *ins-19* should be examined on their exploratory behaviour. Either a nictation assays for males can be developed. Or the exploratory behaviour of males can be assessed in a speed assay.

This work emphasizes the gap of knowledge in insulin functioning while underlining the importance of insulin redundancy and the effect of environmental conditions on *C. elegans* behaviour. But it also shows us that insulin-like peptides have an influence on nictation behaviour, although their effect is not (yet) predictable.

REFERENCES

- Accili, D., & Arden, K. C. (2004). FoxOs at the crossroads of cellular metabolism, differentiation, and transformation. *Cell*, *117*(4), 421–426. [https://doi.org/10.1016/S0092-8674\(04\)00452-0](https://doi.org/10.1016/S0092-8674(04)00452-0)
- Adams, M. J., Blundell, T. L., Dodson, E. J., Dodson, G. G., Vijayan, M., Baker, E. N., ... Sheat, S. (1969). Structure of Rhombohedral 2 Zinc Insulin Crystals. *Nature*, *224*(5218), 491–495. <https://doi.org/10.1038/224491a0>
- Ailion, M., & Thomas, J. H. (2000). Dauer formation induced by high temperatures in *Caenorhabditis elegans*. *Genetics*, *156*(3), 1047–1067.
- Altun, Z. F., & Hall, D. H. (2009a). Introduction. In *Wormatlas* (pp. 619–631).
- Altun, Z. F., & Hall, D. H. (2009b). Pericellular structures. In *Wormatlas*. <https://doi.org/doi:10.3908/wormatlas.1.20>
- Annunziata, M., Granata, R., & Ghigo, E. (2011). The IGF system. *Acta Diabetologica*, *48*(1), 1–9. <https://doi.org/10.1007/s00592-010-0227-z>
- Bani, D. (1997). Relaxin: A pleiotropic hormone. *General Pharmacology*. Elsevier Science Inc. [https://doi.org/10.1016/S0306-3623\(96\)00171-1](https://doi.org/10.1016/S0306-3623(96)00171-1)
- Bargmann, C. I., & Horvitz, H. R. (1991). Control of larval development by chemosensory neurons in *Caenorhabditis elegans*. *Science*, *251*(4998), 1243–1246. <https://doi.org/10.1126/science.2006412>
- Barrière, A., & Félix, M. A. (2005). High local genetic diversity and low outcrossing rate in *Caenorhabditis elegans* natural populations. *Current Biology*, *15*(13), 1176–1184. <https://doi.org/10.1016/j.cub.2005.06.022>
- Barrington, E. J. W. (2020). Hormone. Retrieved November 15, 2020, from <https://www.britannica.com/science/hormone>
- Baugh, L. R. (2013). To grow or not to grow: Nutritional control of development during *Caenorhabditis elegans* L1 Arrest. *Genetics*. <https://doi.org/10.1534/genetics.113.150847>
- Blázquez, E., Velázquez, E., Hurtado-Carneiro, V., & Ruiz-Albusac, J. M. (2014). Insulin in the brain: Its pathophysiological implications for states related with central insulin resistance, type 2 diabetes and alzheimer's disease. *Frontiers in Endocrinology*. <https://doi.org/10.3389/fendo.2014.00161>
- Bretscher, A. J., Kodama-Namba, E., Busch, K. E., Murphy, R. J., Soltesz, Z., Laurent, P., & de Bono, M. (2011). Temperature, oxygen, and salt-sensing neurons in *C. elegans* are carbon dioxide sensors that control avoidance behavior. *Neuron*, *69*(6), 1099–1113. <https://doi.org/10.1016/j.neuron.2011.02.023>
- Butcher, R. A., Fujita, M., Schroeder, F. C., & Clardy, J. (2007). Small-molecule pheromones that control dauer development in *Caenorhabditis elegans*. *Nature Chemical Biology*, *3*(7), 420–422. <https://doi.org/10.1038/nchembio.2007.3>
- Chan, S. J., & Steiner, D. F. . (2000). Insulin through the Ages: Phylogeny of a Growth Promoting and Metabolic Regulatory Hormone. *American Zoologist*, *40*(2), 213–222.
- Chao, W., & D'Amore, P. A. (2008). IGF2: Epigenetic regulation and role in development and disease. *Cytokine and Growth Factor Reviews*, *19*(2), 111–120. <https://doi.org/10.1016/j.cytogfr.2008.01.005>

- Claeys, I., Simonet, G., Poels, J., Van Loy, T., Vercammen, L., De Loof, A., & Vanden Broeck, J. (2002, April 1). Insulin-related peptides and their conserved signal transduction pathway. *Peptides*. Elsevier. [https://doi.org/10.1016/S0196-9781\(01\)00666-0](https://doi.org/10.1016/S0196-9781(01)00666-0)
- Conlon, J. M. (2001). Evolution of the insulin molecule: Insights into structure-activity and phylogenetic relationships. *Peptides*, 22(7), 1183–1193. [https://doi.org/10.1016/S0196-9781\(01\)00423-5](https://doi.org/10.1016/S0196-9781(01)00423-5)
- Cook, S. J., Jarrell, T. A., Brittin, C. A., Wang, Y., Bloniarz, A. E., Yakovlev, M. A., ... Emmons, S. W. (2019). Whole-animal connectomes of both *Caenorhabditis elegans* sexes. *Nature*, 571(7763), 63–71. <https://doi.org/10.1038/s41586-019-1352-7>
- Cornils, A., Gloeck, M., Chen, Z., Zhang, Y., & Alcedo, J. (2011). Specific insulin-like peptides encode sensory information to regulate distinct developmental processes. *Development*, 138(6), 1183–1193. <https://doi.org/10.1242/dev.060905>
- Corsi, A. K., Wightman, B., & Chalfie, M. (2015). A transparent window into biology: A primer on *Caenorhabditis elegans*. *Genetics*, 200(2), 387–407. <https://doi.org/10.1534/genetics.115.176099>
- Csaba, G. (2013). Insulin at a unicellular eukaryote level. *Cell Biology International*, 37(4), 267–275. <https://doi.org/10.1002/cbin.10054>
- Duarte, A. I., Moreira, P. I., & Oliveira, C. R. (2012). Insulin in central nervous system: More than just a peripheral hormone. *Journal of Aging Research*, 2012. <https://doi.org/10.1155/2012/384017>
- Duret, L., Guex, N., Peitsch, M. C., & Bairoch, A. (1998). New insulin-like proteins with atypical disulfide bond pattern characterized in *Caenorhabditis elegans* by comparative sequence analysis and homology modeling. *Genome Research*, 8(4), 348–353. <https://doi.org/10.1101/gr.8.4.348>
- Ebberink, R. H. M., Smit, A. B., & Van Minnen, J. (1989). The Insulin Family: Evolution of Structure and Function in Vertebrates and Invertebrates. *The Biological Bulletin*, 177(2), 176–182. <https://doi.org/10.2307/1541928>
- Edwards, S. L., Mergan, L., Parmar, B., Cockx, B., De Haes, W., Temmerman, L., & Schoofs, L. (2019, February 1). Exploring neuropeptide signalling through proteomics and peptidomics. *Expert Review of Proteomics*. Taylor and Francis Ltd. <https://doi.org/10.1080/14789450.2019.1559733>
- Evans, E. A., Chen, W. C., & Tan, M. W. (2008). The DAF-2 insulin-like signaling pathway independently regulates aging and immunity in *C. elegans*. *Aging Cell*, 7(6), 879–893. <https://doi.org/10.1111/j.1474-9726.2008.00435.x>
- Fernandes de Abreu, D. A., Caballero, A., Fardel, P., Stroustrup, N., Chen, Z., Lee, K. H., ... Ch'ng, Q. L. (2014a). An Insulin-to-Insulin Regulatory Network Orchestrates Phenotypic Specificity in Development and Physiology. *PLoS Genetics*, 10(3), 17–19. <https://doi.org/10.1371/journal.pgen.1004225>
- Fernandes de Abreu, D. A., Caballero, A., Fardel, P., Stroustrup, N., Chen, Z., Lee, K. H., ... Ch'ng, Q. L. (2014b). An Insulin-to-Insulin Regulatory Network Orchestrates Phenotypic Specificity in Development and Physiology. *PLoS Genetics*, 10(3), 1004225. <https://doi.org/10.1371/journal.pgen.1004225>
- Fernandes de Abreu, D. A., Caballero, A., Fardel, P., Stroustrup, N., Chen, Z., Lee, K. H., ... Ch'ng, Q. L. (2014c). An Insulin-to-Insulin Regulatory Network Orchestrates Phenotypic Specificity in Development and Physiology. *PLoS Genetics*, 10(3). <https://doi.org/10.1371/journal.pgen.1004225>
- Fielenbach, N., & Antebi, A. (2008). *C. elegans* dauer formation and the molecular basis of plasticity. *Genes and Development*. <https://doi.org/10.1101/gad.1701508>

- Frézal, L., & Félix, M. A. (2015). *C. elegans* outside the Petri dish. *ELife*, 4, 1–14. <https://doi.org/10.7554/eLife.05849>
- Gerozissis, K. (2003). Brain Insulin : Regulation , Mechanisms of Action and Functions. *Cellular and Molecular Neurobiology*, 23(1), 1–25.
- Grishanin, R. N., Klenchin, V. A., Loyet, K. M., Kowalchuk, J. A., Ann, K., & Martin, T. F. J. (2002). Membrane Association Domains in Ca²⁺-dependent Activator Protein for Secretion Mediate Plasma Membrane and Dense-core Vesicle Binding Required for Ca²⁺-dependent Exocytosis*. *Journal of Biological Chemistry*, 277(24), 22025–22034. <https://doi.org/10.1074/jbc.M201614200>
- Guo, Z. Y., Qiao, Z. S., & Feng, Y. M. (2008). The in vitro oxidative folding of the insulin superfamily. *Antioxidants and Redox Signaling*, 10(1), 127–139. <https://doi.org/10.1089/ars.2007.1860>
- Hall, D. H., & Hedgecock, E. M. (1991). *Kinesin-Related Gene uric-104 Is Required for Axonal Transport of Synaptic Vesicles in C. elegans*. *Cell* (Vol. 65).
- Honda, Y., Tanaka, M., & Honda, S. (2008). Modulation of longevity and diapause by redox regulation mechanisms under the insulin-like signaling control in *Caenorhabditis elegans*. *Experimental Gerontology*, 43(6), 520–529. <https://doi.org/10.1016/j.exger.2008.02.009>
- Hossain, M. A., & Wade, J. D. (2017). Novel Methods for the Chemical Synthesis of Insulin Superfamily Peptides and of Analogues Containing Disulfide Isosteres. *Accounts of Chemical Research*, 50(9), 2116–2127. <https://doi.org/10.1021/acs.accounts.7b00288>
- Hu, P. J. (2007). Dauer. In *WormBook* (pp. 1–19). <https://doi.org/10.1895/wormbook.1.144.1>
- Hunt-Newbury, R., Viveiros, R., Johnsen, R., Mah, A., Anastas, D., Fang, L., ... Moerman, D. G. (2007). High-throughput in vivo analysis of gene expression in *Caenorhabditis elegans*. *PLoS Biology*, 5(9), 1981–1997. <https://doi.org/10.1371/journal.pbio.0050237>
- Ino, Y., & Yoshida, K. (2009). Parallel use of two behavioral mechanisms for chemotaxis in *Caenorhabditis elegans*. *Journal of Neuroscience*, 29(17), 5370–5380. <https://doi.org/10.1523/JNEUROSCI.3633-08.2009>
- Ishii, D. N. (1993). Neurobiology of Insulin and Insulin-Like Growth Factors. In *Neurotrophic Factors* (pp. 415–442). Elsevier. <https://doi.org/10.1016/b978-0-08-057132-4.50018-6>
- Jacob, T. C., & Kaplan, J. M. (2003). The EGL-21 Carboxypeptidase E Facilitates Acetylcholine Release at *Caenorhabditis elegans* Neuromuscular Junctions. *The Journal of Neuroscience*, 23(6), 2122–2130.
- Jorgensen, E. M., & Mango, S. E. (2002). The art and design of genetic screens: *Caenorhabditis elegans*. *Nature Reviews Genetics*, 3(5), 356–369. <https://doi.org/10.1038/nrg794>
- Kao, G., Nordenson, C., Still, M., Rönnlund, A., Tuck, S., & Naredi, P. (2007). ASNA-1 Positively Regulates Insulin Secretion in *C. elegans* and Mammalian Cells. *Cell*, 128(3), 577–587. <https://doi.org/10.1016/j.cell.2006.12.031>
- Kawano, T., Nagatomo, R., Kimura, Y., Gengyo-Ando, K., & Mitani, S. (2006). Disruption of *ins-11*, a *Caenorhabditis elegans* insulin-like gene, and phenotypic analyses of the gene-disrupted animal. *Bioscience, Biotechnology and Biochemistry*, 70(12), 3084–3087. <https://doi.org/10.1271/bbb.60472>
- Kimura, K. D., Riddle, D. L., & Ruvkun, G. (2011). The *C. Elegans* DAF-2 insulin-like receptor is abundantly expressed in the nervous system and regulated by nutritional status. *Cold Spring Harbor Symposia on Quantitative Biology*, 76, 113–120. <https://doi.org/10.1101/sqb.2011.76.010660>

- Kosinski, R. A., & Zaremba, M. (2007). Dynamics of the model of the caenorhabditis elegans neural network. *Acta Physica Polonica B*, 38(6), 2201–2210.
- Laron, Z. (2001). Insulin-like growth factor 1 (IGF-1): A growth hormone. *Journal of Clinical Pathology - Molecular Pathology*, 54(5), 311–316. <https://doi.org/10.1136/mp.54.5.311>
- Lázár, B. A., Jancsó, G., & Sántha, P. (2020). Modulation of sensory nerve function by insulin: Possible relevance to pain, inflammation and axon growth. *International Journal of Molecular Sciences*, 21(7). <https://doi.org/10.3390/ijms21072507>
- Lee, D., Lee, H., Kim, N., Lim, D. S., & Lee, J. (2017). Regulation of a hitchhiking behavior by neuronal insulin and TGF- β signaling in the nematode *Caenorhabditis elegans*. *Biochemical and Biophysical Research Communications*, 484(2), 323–330. <https://doi.org/10.1016/j.bbrc.2017.01.113>
- Lee, H., Choi, M. K., Lee, D., Kim, H. S., Hwang, H., Kim, H., ... Lee, J. (2012). Nictation, a dispersal behavior of the nematode *Caenorhabditis elegans*, is regulated by IL2 neurons. *Nature Neuroscience*, 15(1), 107–112. <https://doi.org/10.1038/nn.2975>
- Lee, R. Y. N., Hench, J., & Ruvkun, G. (2001). Regulation of *C. elegans* DAF-16 and its human ortholog FKHL1 by the *daf-2* insulin-like signaling pathway. *Current Biology*, 11(24), 1950–1957. [https://doi.org/10.1016/S0960-9822\(01\)00595-4](https://doi.org/10.1016/S0960-9822(01)00595-4)
- Lee, S. H., Zabolotny, J. M., Huang, H., Lee, H., & Kim, Y. B. (2016). Insulin in the nervous system and the mind: Functions in metabolism, memory, and mood. *Molecular Metabolism*, 5(8), 589–601. <https://doi.org/10.1016/j.molmet.2016.06.011>
- Li, C. (2005). The ever-expanding neuropeptide gene families in the nematode *Caenorhabditis elegans*. *Parasitology*. Cambridge University Press. <https://doi.org/10.1017/S0031182005009376>
- Li, Chris, Kim, K., & Colledge, C. (2008). Neuropeptides. In *WormBook* (pp. 1–36). <https://doi.org/10.1895/wormbook.1.142.1>
- Li, W., Kennedy, S. G., & Ruvkun, G. (2003). *daf-28* encodes a *C. elegans* insulin superfamily member that is regulated by environmental cues and acts in the DAF-2 signaling pathway. *Genes and Development*, 17(7), 844–858. <https://doi.org/10.1101/gad.1066503>
- Lim, J. P., & Brunet, A. (2013). Bridging the transgenerational gap with epigenetic memory. *Trends in Genetics*, 29(3), 176–186. <https://doi.org/10.1016/j.tig.2012.12.008>
- Lin, K., Hsin, H., Libina, N., & Kenyon, C. (2001). Regulation of the *Caenorhabditis elegans* longevity protein DAF-16 by insulin/IGF-1 and germline signaling. *Nature Genetics*, 28(june), 139–145.
- Matsunaga, Y. (2017). Diverse insulin-like peptides in *Caenorhabditis elegans*. *International Biology Review*, 1(1). <https://doi.org/10.18103/ibr.v1i1.1276>
- Matsunaga, Y., Gengyo-Ando, K., Mitani, S., Iwasaki, T., & Kawano, T. (2012). Physiological function, expression pattern, and transcriptional regulation of a *Caenorhabditis elegans* insulin-like peptide, INS-18. *Biochemical and Biophysical Research Communications*, 423(3), 478–483. <https://doi.org/10.1016/j.bbrc.2012.05.145>
- Matsunaga, Y., Honda, Y., Honda, S., Iwasaki, T., Qadota, H., Benian, G. M., & Kawano, T. (2016). Diapause is associated with a change in the polarity of secretion of insulin-like peptides. *Nature Communications*, 7. <https://doi.org/10.1038/ncomms10573>
- Matsunaga, Y., & Kawano, T. (2018). The *C. elegans* insulin-like peptides (ILPs). *AIMS Biophysics*, 5(4), 217–

230. <https://doi.org/10.3934/biophy.2018.4.217>
- Matsunaga, Y., Nakajima, K., Gengyo-Ando, K., Mitani, S., Iwasaki, T., & Kawano, T. (2012). A caenorhabditis elegans insulin-like peptide, INS-17: Its physiological function and expression pattern. *Bioscience, Biotechnology and Biochemistry*, 76(11), 2168–2172. <https://doi.org/10.1271/bbb.120540>
- McCulloch, K. A., Zhou, K., & Jin, Y. (2020). Neuronal transcriptome analyses reveal novel neuropeptide modulators of excitation and inhibition imbalance in *C. elegans*. *PLoS ONE*, 15(6). <https://doi.org/10.1371/journal.pone.0233991>
- Murphy, C. T., & Hu, P. J. (2013). Insulin/insulin-like growth factor signaling in *C. elegans*. In *WormBook : the online review of C. elegans biology* (pp. 1–43). <https://doi.org/10.1895/wormbook.1.164.1>
- Nagamatsu, S., Chan, S. J., Falkmers, S., & Steiner, D. F. (1991). Evolution of the Insulin Gene Superfamily.
- Nagasawa, H., Kataoka, H., Isogai, A., Tamura, S., Suzuki, A., Mizoguchi, A., ... Takahashi, S. Y. (1986). Amino acid sequence of a prothoracicotropic hormone of the silkworm *Bombyx mori* (insulin/relaxin). *Biochemistry*, 83, 5840–5843.
- Norris, D. O., & Carr, J. A. (2013). *Vertebrate Endocrinology* (fifth edit). Elsevier Inc.
- Obsil, T., & Obsilova, V. (2008). Structure/function relationships underlying regulation of FOXO transcription factors. *Oncogene*. <https://doi.org/10.1038/onc.2008.20>
- Pierce, S. B., Costa, M., Wisotzkey, R., Devadhar, S., Homburger, S. A., Buchman, A. R., ... Ruvkun, G. (2001). Regulation of DAF-2 receptor signaling by human insulin and ins-1, a member of the unusually large and diverse *C. elegans* insulin gene family. *Genes and Development*, 15(6), 672–686. <https://doi.org/10.1101/gad.867301>
- Ritter, A. D., Shen, Y., Bass, J. F., Jeyaraj, S., Deplancke, B., Mukhopadhyay, A., ... Walhout, A. J. M. (2013). Complex expression dynamics and robustness in *C. elegans* insulin networks. *Genome Research*, 23(6), 954–965. <https://doi.org/10.1101/gr.150466.112>
- Rosoff, M. L., Bürglin, T. R., & Li, C. (1992). Alternatively Spliced Transcripts of the f/p-I Gene Encode Distinct FMRFamide-like Peptides in *Caenorhabditis elegans*. *The Journal of Neuroscience*, 12(6), 2356–2361.
- Russo, A. F. (2017). Overview of Neuropeptides: Awakening the Senses? *Headache*, 57, 37–46. <https://doi.org/10.1111/head.13084>
- Ryle, A. P., Sanger, F., Smith, L. F., & Kitai, R. (1955). The disulphide bonds of insulin. *The Biochemical Journal*, 60(4), 541–556. <https://doi.org/10.1042/bj0600541>
- Salio, C., Lossi, L., Ferrini, F., & Merighi, A. (2006). Neuropeptides as synaptic transmitters. *Cell Tissue Res*, 326(583–598). <https://doi.org/10.1007/s00441-006-0268-3>
- Schechter, R., Whitmire, J., Holtzclaw, L., George, M., Harlow, R., & Devaskar, S. U. (1992). Developmental regulation of insulin in the mammalian central nervous system. *Brain Research*, 582(1), 27–37. [https://doi.org/10.1016/0006-8993\(92\)90313-X](https://doi.org/10.1016/0006-8993(92)90313-X)
- Schulinkamp, R. J., Pagano, T. C., Hung, D., & Raffa, R. B. (2000). Insulin receptors and insulin action in the brain: Review and clinical implications. *Neuroscience and Biobehavioral Reviews*, 24(8), 855–872. [https://doi.org/10.1016/S0149-7634\(00\)00040-3](https://doi.org/10.1016/S0149-7634(00)00040-3)
- Schwabe, C., & McDonald, J. K. (1977). Relaxin: A disulfide homolog of insulin. *Science*, 197(4306), 914–915.

<https://doi.org/10.1126/science.887933>

- Separovic, F., Wade, J. D., & Shabanpoor, F. (2009). The Human Insulin Superfamily of Polypeptide Hormones. In *Vitamines and hormones* (pp. 1–31).
- Sieburth, D., Madison, J. M., & Kaplan, J. M. (2006). PKC-1 regulates secretion of neuropeptides. *Nature Neuroscience*. <https://doi.org/10.1038/nn1810>
- Sossin, W. S., Sweet-Cordero, A., & Scheller, R. H. (1990). Dale's hypothesis revisited: Different neuropeptides derived from a common prohormone are targeted to different processes. *Proceedings of the National Academy of Sciences of the United States of America*, *87*(12), 4845–4848. <https://doi.org/10.1073/pnas.87.12.4845>
- Steiner, D. F., Cunningham, D., Spigelman, L., & Aten, B. (1967). Insulin biosynthesis: Evidence for a precursor. *Science*, *157*(3789), 697–700. <https://doi.org/10.1126/science.157.3789.697>
- Stiernagle, T. (2006). Maintenance of *C. elegans*. In *WormBook : the online review of C. elegans biology* (pp. 1–11). <https://doi.org/10.1895/wormbook.1.101.1>
- Taylor, S. R., Santpere, G., Weinreb, A., Barrett, A., Reilly, M. B., Xu, C., ... Miller, D. M. (2020). *Molecular topography of an entire nervous system*. *bioRxiv*. <https://doi.org/10.1101/2020.12.15.422897>
- Thoemke, K., Yi, W., Ross, J. M., Kim, S., Reinke, V., & Zarkower, D. (2005). Genome-wide analysis of sex-enriched gene expression during *C. elegans* larval development. *Developmental Biology*, *284*(2), 500–508. <https://doi.org/10.1016/j.ydbio.2005.05.017>
- Thomas, J. H., Birnby, D. A., & Vowels, J. J. (1993). Evidence for parallel processing of sensory information controlling dauer formation in *Caenorhabditis elegans*. *Genetics*, *134*(4), 1105–1117.
- Utiger, R. D. (2011). Insulin-like growth factor. Retrieved December 10, 2020, from <https://www.britannica.com/science/insulin-like-growth-factor>
- Utiger, R. D. (2020). Insulin. Retrieved November 15, 2020, from <https://www.britannica.com/science/insulin>
- Van Bael, S., Watteyne, J., Boonen, K., De Haes, W., Menschaert, G., Ringstad, N., ... Temmerman, L. (2018). Mass spectrometric evidence for neuropeptide-amidating enzymes in *Caenorhabditis elegans*. *Journal of Biological Chemistry*, *293*(16), 6052–6063. <https://doi.org/10.1074/jbc.RA117.000731>
- Van Bael, S., Zels, S., Boonen, K., Beets, I., Schoofs, L., & Temmerman, L. (2018). A *Caenorhabditis elegans* Mass Spectrometric Resource for Neuropeptidomics. *Journal of the American Society for Mass Spectrometry*, *29*(5), 879–889. <https://doi.org/10.1007/s13361-017-1856-z>
- Viney, M. E., Gardner, M. P., & Jackson, J. A. (2003). Variation in *Caenorhabditis elegans* dauer larva formation. *Development Growth and Differentiation*, *45*(4), 389–396. <https://doi.org/10.1046/j.1440-169X.2003.00703.x>
- Watts, D. J., & Strogatz, S. H. (1998). Collective dynamics of “small-world” networks. *Nature*, *393*(June), 440–442. Retrieved from <https://www.ncbi.nlm.nih.gov/pubmed/9623998>
- Weiss, M., Steiner, D. F., & Philipson, L. H. (2014). Insulin Biosynthesis, Secretion, Structure, and Structure-Activity Relationships. In K. R. Feingold, B. Anawalt, A. Boyce, & E. Al. (Eds.), *Endotext [Internet]*. South Dartmouth (MA): MDText.com, Inc.; 2000-. Retrieved from <https://www.ncbi.nlm.nih.gov/books/NBK279029/>

- White, J. G., Southgate, E., Thomson, J. N., & Brenner, S. (1986). The structure of the nervous system of the nematode *Caenorhabditis elegans*. *Philosophical Transactions of the Royal Society of London. Series B, Biological Sciences*, 314(1165), 1–340.
- Wolkow, C. A., & Hall, D. H. (2015). Introduction to the Dauer Larva, Overview. In *WormAtlas*. <https://doi.org/doi:10.3908/wormatlas.3.10>
- Wrigley, S., Arafa, D., & Tropea, D. (2017). Insulin-like growth factor 1: At the crossroads of brain development and aging. *Frontiers in Cellular Neuroscience*, 11(14), 1–15. <https://doi.org/10.3389/fncel.2017.00014>
- Yang, H., Lee, B. Y., Yim, H., & Lee, J. (2020). Neurogenetics of nictation, a dispersal strategy in nematodes. *Journal of Neurogenetics*, 1–8. <https://doi.org/10.1080/01677063.2020.1788552>
- Yokoyama, M. (2020). *C. elegans* as a model organism. Retrieved November 20, 2020, from <https://www.news-medical.net/life-sciences/C-elegans-as-a-Model-Organism.aspx#:~:text=Caenorhabditis elegans is a species,organism to study human diseases.&text=elegans has been used as,as studying the immune system.>
- Zheng, S., Chiu, H., Boudreau, J., Papanicolaou, T., Bendena, W., & Chin-Sang, I. (2019). A functional study of all 40 *Caenorhabditis elegans* insulin-like peptides. *Journal of Biological Chemistry*, 293(43), 16912–16922. <https://doi.org/10.1074/jbc.RA118.004542>
- Zwaal, R. R., Mendel, J. E., Sternberg, P. W., & Plasterk, R. H. A. (1997). Two neuronal G proteins are involved in chemosensation of the *Caenorhabditis elegans* dauer-inducing pheromone. *Genetics*, 145(3), 715–727.

APPENDICES

1. Risk Analysis

All experiments are conducted in laboratories with safety level 1, as only non-pathogenic organisms *C. elegans* and *E. coli* OP50 are used. General laboratory rules according to the Good Laboratory Practice are followed throughout this project. Protective gear such as gloves and a lab coat are worn during the experimental work as a precautionary measure. Eating, drinking, and storing food in the lab is prohibited. Volatile organic solvents are handled in the fume hood. Upon leaving the laboratory environment, hands are washed properly with soap and disinfected with an alcohol gel if necessary. After employing reusable equipment, it is decontaminated by autoclavation. Surfaces are disinfected with ethanol when exposed to harmful substances. Laminar flow cabinets are always disinfected with 70% ethanol before and after use. Materials that are used in the flow are first disinfected with 70% ethanol, as are gloved hands. Biohazardous waste is deposited in the specific containers intended for it, be it for solid, liquid, or sharp material. Low-risk solid biological waste is disposed of in cardboard cordi boxes. High-risk waste is disposed of in PE containers. Organic solvents are collected in (non-) halogenated organic waste. Machines and equipment are always used correctly as written in the equipment user's manual. When using the autoclave, extra attention is needed. The autoclave may never be opened when it is operating under pressure and heat resistant gloves are worn when handling materials coming out of the autoclave. When using the centrifuge, extra attention is paid to correctly balance the samples in the rotor and that the rotor is secured. Some specific products used during the experimental setup needed extra safety measures and are discussed below.

When performing gel electrophoresis, the reagent GelRed is employed. Although safer than its predecessor, ethidium bromide, the exact risks are still unclear, and thus it should be handled with additional caution. A separate zone is used for gel electrophoresis and no contaminated material is transferred from inside the room to the rest of the laboratory. When entering, a specific lab coat for this zone is put on. This coat is again taken off when leaving the zone. Gloves are disposed of before leaving the room, and any external equipment entering remains there or is disposed of appropriately as biohazardous waste. Contact with skin or eyes should always be prevented.

Calcium chloride (CaCl₂) causes severe eye irritation. In case of contact, rinse with water.

Cholesterol is harmful when swallowed. When ingested, the mouth should be rinsed thoroughly.

Disodium Ethylenediaminetetraacetic acid (EDTA) is harmful by inhalation and there is danger of serious damage to health by prolonged exposure through inhalation. Avoid contact by handling it under a local exhaust or with respiratory protection.

Ethanol (EtOH) is highly flammable. Keep the substance out of the vicinity of open flames. It causes light to moderate irritation to respiratory system, eyes, and skin.

Sodium hydroxide (NaOH) is corrosive. It causes severe burns, eye injury and is harmful when swallowed. Avoid contact by wearing gloves, otherwise rinse thoroughly with water.

Sodium hypochlorite (NaOCl) is an inflammable and explosive chemical. It causes severe burns, eye injury and respiratory problems. It must be stored near other flammable substances. Avoid contact by wearing gloves, otherwise rinse thoroughly with water. After swallowing, rinse the mouth thoroughly.

2. Buffers and solutions

Bleach solution: volume 3mL

- Add 2mL of 5% NaOCl (common household bleach, Honeywell) to a 15mL Falcon tube.
- Add 1mL 5M NaOH and swirl to homogenise.

Always prepare fresh bleaching solution.

Bleach solution for handling contamination: volume 2mL

- Add 1mL of 5% NaOCl (common household bleach, Honeywell) to a 15mL Falcon tube.
- Add 1mL of 5M NaOH and swirl to homogenise.

Always prepare fresh bleaching solution.

CaCl₂: concentration 1M; volume 1L

- Weigh 147g of 147.01g/mol CaCl₂ (Sigma-Aldrich) and add to a Duran bottle.
- Add Milli-Q water to a volume of 800mL and swirl to homogenise.
- Autoclave the solution.
- Add 200mL of autoclaved Milli-Q water under the laminar flow to a final volume of 1L.

Cholesterol in ethanol: concentration 5mg/mL; volume 1L

- Weigh 5g of 386.65g/mol cholesterol (Sigma-Aldrich) and add to a Duran bottle.
- Add 200mL of 100% ethanol absolute (VWR Prolabo Chemicals) and swirl to homogenise.

LB medium: volume 1L

- Weigh 20g of LB broth (Sigma-Aldrich) and add to a Duran bottle.
- Add AD water to a volume of 800mL and swirl to homogenise.
- Autoclave the solution.
- Add 200mL of autoclaved AD water under the laminar flow to a final volume of 1L.

MgSO₄: concentration 1M; volume 1L

- Weigh 246.4g of 246.48g/mol MgSO₄ (Sigma-Aldrich) and add to a Duran bottle.
- Add Milli-Q to a volume of 800mL and swirl to homogenise.
- Autoclave the solution.
- Add 200mL of autoclaved Milli-Q under the laminar flow to a final volume of 1L.

NaOH: concentration 5M; volume 100mL

- Weigh 20g of NaOH pellets (Sigma-Aldrich) and add to a Duran bottle.
- Add Milli-Q to a final volume of 100mL and stir until fully dissolved.

Phosphate buffer: concentration 1M; Volume 1L

- Weigh KH_2PO_4 and K_2HPO_4 and add them to a Duran bottle:
 - 108.87g KH_2PO_4 (136.09g/mol, Sigma-Aldrich)
 - 34.84g K_2HPO_4 (174.18g/mol, Sigma-Aldrich)
- Add Milli-Q to a volume of 800mL and swirl bottle to homogenise.
- Autoclave the solution.
- Add 200mL of autoclaved Milli-Q under the laminar flow to the final volume of 1L.

S basal medium: volume 1L

- Weigh NaCl, KH_2PO_4 and K_2HPO_4 and add them to a Duran bottle:
 - 5.85g NaCl (58.44g/mol, Sigma-Aldrich)
 - 6g KH_2PO_4 (136.09g/mol, Sigma-Aldrich)
 - 1g K_2HPO_4 (174.18g/mol, Sigma-Aldrich)
- Add Milli-Q to a volume of 800mL and swirl bottle to homogenise.
- Autoclave the solution.
- Add 200mL of autoclaved Milli-Q under the laminar flow to the final volume of 1L.

TAE buffer (50x): volume 1L

- Weigh Trizma base and Disodium EDTA and add to a Duran bottle.
 - 242g Trizma Base (121.14g/mol, Sigma-Aldrich)
 - 18.61g EDTA (372.24 g/mol, Sigma-Aldrich)
- Add AD water to a volume of 700mL and put on a stirrer until dissolved.
- Add 57.1mL of 60.05g/mol acetic acid (Sigma-Aldrich) and swirl bottle to homogenise.
- Fill up to 1L with AD water.

3. Insulin expression patterns

3.1. Neuron expression expressed in percentages

These insulin expression patterns were acquired via Cengen database's online tool. The data is unfiltered, as there was no threshold selected. The table shows the percentage of overall expression found in each neuron. There were no data available for *ins-8*, *ins-31*, and *ins-38*.

Gene	ADA	ADE	ADF	ADL	AFD	AIA	AIB	AIM	AIN	AIY	AIZ	ALA	ALM	ALN	AOR	AS	ASEL	ASER	ASG	ASH	ASI	ASJ	ASK	AUA	AVA	AVB	AVD	AVE	AVF	AVG
<i>ins-1</i>	0%	0%	0%	0%	0%	28%	0%	3%	6%	1%	5%	0%	0%	1%	0%	0%	0%	2%	0%	0%	2%	5%	0%	0%	0%	0%	0%	0%	2%	0%
<i>ins-2</i>	0%	0%	3%	0%	0%	0%	0%	0%	0%	1%	0%	0%	0%	0%	0%	0%	0%	8%	0%	0%	0%	59%	0%	0%	0%	0%	0%	0%	2%	0%
<i>ins-3</i>	0%	0%	7%	0%	0%	0%	0%	0%	0%	0%	0%	0%	0%	0%	0%	0%	0%	14%	0%	0%	35%	12%	0%	0%	0%	0%	0%	0%	0%	
<i>ins-4</i>	0%	0%	0%	0%	0%	0%	0%	0%	0%	0%	0%	0%	0%	0%	0%	0%	0%	27%	0%	0%	50%	6%	0%	0%	0%	0%	0%	0%	0%	
<i>ins-5</i>	0%	0%	0%	0%	0%	0%	0%	0%	1%	0%	0%	0%	0%	0%	0%	0%	0%	1%	0%	0%	30%	60%	0%	0%	0%	0%	0%	0%	0%	
<i>ins-6</i>	0%	0%	0%	0%	0%	0%	0%	0%	0%	0%	0%	0%	0%	0%	0%	0%	0%	0%	0%	0%	46%	51%	0%	0%	0%	0%	0%	0%	0%	
<i>ins-7</i>	0%	0%	0%	12%	0%	0%	0%	1%	0%	0%	0%	73%	0%	0%	0%	0%	1%	0%	0%	0%	0%	0%	0%	0%	0%	1%	0%	0%	0%	
<i>ins-8</i>																														
<i>ins-9</i>	0%	0%	0%	0%	0%	0%	0%	0%	0%	0%	0%	0%	0%	0%	0%	0%	0%	0%	0%	0%	68%	21%	0%	0%	0%	0%	0%	0%	0%	
<i>ins-10</i>	0%	0%	0%	0%	0%	6%	0%	0%	0%	0%	0%	0%	0%	0%	0%	0%	0%	0%	0%	0%	0%	0%	0%	0%	0%	0%	0%	0%	0%	
<i>ins-11</i>	0%	0%	0%	29%	0%	0%	0%	0%	0%	1%	0%	0%	0%	0%	0%	0%	0%	0%	0%	23%	0%	0%	0%	0%	0%	0%	0%	1%	1%	0%
<i>ins-12</i>	0%	0%	0%	0%	0%	0%	0%	0%	0%	0%	0%	0%	0%	0%	0%	0%	0%	0%	0%	21%	0%	0%	0%	0%	0%	0%	0%	0%	4%	0%
<i>ins-13</i>	0%	0%	0%	0%	0%	0%	0%	0%	0%	0%	0%	0%	0%	0%	0%	0%	0%	0%	0%	0%	0%	0%	0%	0%	0%	0%	0%	0%	0%	0%
<i>ins-14</i>	0%	0%	0%	1%	7%	0%	0%	0%	0%	0%	0%	0%	0%	0%	0%	0%	20%	8%	0%	2%	0%	2%	6%	0%	0%	0%	0%	0%	0%	0%
<i>ins-15</i>	0%	0%	0%	2%	5%	0%	0%	0%	0%	0%	0%	0%	0%	0%	0%	0%	33%	9%	0%	1%	0%	2%	4%	0%	0%	0%	0%	0%	0%	0%
<i>ins-16</i>	0%	0%	0%	21%	21%	15%	0%	0%	0%	0%	0%	0%	0%	0%	8%	0%	0%	0%	0%	1%	0%	0%	0%	0%	0%	0%	0%	1%	0%	0%
<i>ins-17</i>	1%	0%	0%	0%	0%	0%	0%	0%	4%	0%	41%	0%	0%	3%	0%	0%	0%	0%	0%	0%	0%	0%	0%	0%	0%	0%	0%	2%	0%	2%
<i>ins-18</i>	0%	0%	2%	0%	0%	20%	0%	0%	0%	0%	0%	0%	0%	2%	0%	0%	6%	2%	0%	0%	0%	2%	0%	0%	0%	0%	0%	0%	0%	0%
<i>ins-19</i>	0%	0%	0%	0%	0%	0%	0%	0%	68%	0%	0%	0%	0%	0%	0%	0%	0%	0%	0%	0%	0%	0%	10%	0%	0%	0%	0%	0%	0%	0%
<i>ins-20</i>	0%	0%	0%	0%	0%	0%	0%	0%	0%	0%	0%	0%	0%	0%	0%	0%	0%	0%	0%	3%	3%	20%	0%	0%	0%	0%	0%	0%	0%	0%
<i>ins-21</i>	0%	0%	0%	0%	1%	0%	0%	0%	0%	0%	0%	0%	0%	0%	0%	0%	2%	17%	0%	0%	2%	0%	0%	0%	0%	0%	0%	0%	0%	0%
<i>ins-22</i>	0%	0%	0%	0%	0%	0%	0%	0%	0%	0%	0%	0%	0%	0%	0%	0%	32%	40%	0%	0%	4%	0%	0%	0%	0%	0%	0%	0%	0%	0%
<i>ins-23</i>	0%	0%	0%	0%	1%	0%	0%	0%	0%	0%	0%	0%	0%	0%	0%	0%	40%	24%	0%	0%	0%	0%	0%	0%	0%	0%	0%	0%	0%	0%
<i>ins-24</i>	0%	0%	27%	0%	0%	0%	0%	0%	0%	1%	0%	0%	0%	0%	0%	0%	0%	0%	0%	0%	3%	36%	1%	0%	0%	0%	0%	0%	0%	0%
<i>ins-25</i>	5%	0%	0%	0%	0%	32%	0%	0%	0%	5%	0%	0%	1%	0%	0%	0%	0%	0%	0%	0%	0%	0%	0%	0%	0%	0%	0%	0%	0%	0%
<i>ins-26</i>	0%	0%	0%	0%	0%	0%	0%	0%	0%	0%	0%	0%	0%	0%	0%	0%	3%	10%	0%	0%	63%	4%	0%	0%	0%	0%	0%	0%	0%	0%
<i>ins-27</i>	1%	0%	6%	0%	0%	0%	0%	0%	3%	2%	0%	0%	0%	0%	0%	0%	6%	1%	0%	2%	0%	1%	2%	1%	0%	0%	0%	0%	0%	0%
<i>ins-28</i>	0%	0%	0%	0%	0%	25%	0%	0%	29%	0%	0%	0%	0%	0%	0%	0%	0%	0%	0%	0%	0%	0%	0%	0%	0%	0%	0%	0%	0%	0%
<i>ins-29</i>	0%	0%	0%	0%	0%	39%	0%	0%	1%	3%	0%	0%	1%	0%	0%	0%	0%	0%	0%	0%	0%	0%	0%	0%	0%	0%	0%	0%	0%	0%
<i>ins-30</i>	0%	0%	1%	0%	0%	0%	0%	0%	0%	0%	0%	0%	0%	0%	0%	0%	4%	2%	0%	0%	9%	48%	10%	0%	0%	0%	0%	0%	0%	0%
<i>ins-31</i>																														
<i>ins-32</i>	0%	0%	0%	3%	0%	0%	0%	0%	0%	0%	0%	0%	0%	0%	0%	0%	2%	5%	0%	1%	3%	71%	0%	0%	0%	0%	0%	0%	0%	0%
<i>ins-33</i>	0%	0%	0%	0%	0%	0%	0%	0%	0%	0%	0%	0%	0%	0%	0%	0%	0%	0%	0%	2%	0%	0%	1%	1%	0%	0%	2%	1%	0%	0%
<i>ins-34</i>	0%	0%	0%	0%	0%	0%	0%	0%	0%	0%	0%	0%	0%	0%	0%	0%	0%	0%	0%	0%	0%	0%	0%	0%	0%	0%	0%	0%	10%	0%
<i>ins-35</i>	0%	0%	0%	0%	0%	0%	0%	0%	0%	0%	0%	0%	0%	0%	0%	0%	9%	16%	0%	0%	0%	0%	4%	0%	0%	0%	0%	0%	0%	0%
<i>ins-36</i>	0%	0%	3%	3%	0%	0%	0%	0%	0%	0%	0%	0%	0%	0%	0%	1%	0%	9%	6%	6%	6%	0%	0%	13%	0%	0%	0%	0%	0%	0%
<i>ins-37</i>	0%	0%	3%	0%	0%	0%	0%	1%	0%	0%	0%	0%	0%	0%	0%	0%	0%	0%	0%	0%	10%	0%	1%	0%	1%	0%	0%	0%	0%	3%
<i>ins-38</i>																														
<i>ins-39</i>	0%	0%	1%	1%	30%	0%	0%	0%	0%	0%	0%	0%	0%	0%	0%	0%	0%	5%	0%	0%	0%	17%	21%	0%	0%	0%	0%	0%	0%	0%
<i>daf-28</i>	0%	0%	7%	0%	6%	0%	0%	0%	11%	0%	0%	0%	0%	0%	0%	0%	0%	5%	0%	0%	25%	15%	0%	0%	0%	0%	0%	0%	0%	0%

Gene	AVH	AVJ	AVK	AVL	AVM	AWA	AWB	AWC_OFF	AWC_ON	BAG	BDU	CAN	CEP	DA	DA9	DB	DB01	DVA	DVB	DVC	FLP	HSN	I1	I2	I3	I4	I5	I6	IL1	IL2_DV	
ins-1	0%	0%	0%	0%	0%	1%	1%	0%	0%	1%	0%	0%	0%	0%	0%	0%	0%	0%	0%	1%	0%	0%	0%	0%	0%	0%	5%	0%	0%	0%	
ins-2	0%	0%	0%	0%	0%	2%	0%	0%	2%	0%	0%	0%	0%	0%	0%	0%	0%	0%	0%	0%	10%	0%	0%	0%	0%	0%	0%	0%	0%	0%	
ins-3	0%	0%	0%	0%	0%	6%	0%	0%	0%	0%	0%	0%	0%	0%	0%	0%	0%	0%	0%	0%	0%	0%	0%	0%	0%	0%	0%	0%	0%	0%	
ins-4	0%	0%	0%	0%	0%	2%	0%	0%	0%	0%	0%	0%	0%	0%	0%	0%	0%	0%	0%	0%	0%	0%	0%	0%	0%	0%	0%	0%	0%	0%	
ins-5	0%	0%	0%	0%	0%	2%	1%	0%	0%	0%	0%	0%	0%	0%	0%	0%	0%	0%	0%	0%	0%	0%	0%	0%	0%	0%	0%	0%	0%	0%	
ins-6	0%	0%	0%	0%	0%	0%	0%	0%	0%	0%	0%	0%	0%	0%	0%	0%	0%	0%	0%	0%	0%	0%	0%	0%	0%	0%	0%	0%	0%	0%	
ins-7	0%	0%	6%	0%	0%	0%	0%	0%	0%	0%	0%	0%	0%	0%	0%	0%	0%	0%	0%	4%	0%	0%	0%	0%	0%	0%	0%	0%	0%	0%	
ins-8																															
ins-9	0%	0%	0%	0%	0%	7%	0%	0%	0%	0%	0%	0%	0%	0%	0%	0%	0%	0%	0%	0%	0%	0%	0%	0%	0%	0%	0%	0%	0%	1%	
ins-10	0%	0%	0%	0%	0%	0%	0%	0%	0%	0%	0%	0%	0%	0%	0%	0%	0%	0%	0%	0%	0%	0%	0%	1%	9%	1%	24%	0%	0%	0%	0%
ins-11	2%	0%	0%	0%	0%	0%	0%	1%	0%	0%	0%	1%	0%	0%	0%	0%	0%	0%	0%	0%	0%	0%	0%	0%	0%	0%	0%	0%	0%	0%	
ins-12	0%	0%	0%	0%	0%	12%	0%	6%	3%	0%	0%	0%	0%	0%	0%	0%	0%	0%	1%	0%	0%	0%	0%	0%	0%	0%	0%	0%	0%	0%	
ins-13	0%	0%	0%	0%	0%	0%	0%	0%	0%	0%	0%	0%	0%	0%	0%	0%	0%	0%	0%	0%	0%	0%	0%	0%	0%	0%	0%	0%	0%	0%	
ins-14	0%	0%	0%	0%	0%	10%	0%	19%	12%	11%	0%	0%	0%	0%	0%	0%	0%	0%	0%	0%	0%	0%	0%	0%	0%	0%	0%	0%	0%	0%	
ins-15	0%	0%	0%	0%	0%	14%	0%	17%	5%	5%	0%	0%	0%	0%	0%	0%	0%	0%	0%	0%	0%	0%	0%	0%	0%	0%	0%	0%	0%	2%	
ins-16	0%	0%	0%	0%	0%	0%	0%	0%	0%	0%	0%	1%	1%	0%	0%	1%	0%	0%	0%	0%	0%	0%	0%	0%	0%	0%	1%	0%	0%	0%	
ins-17	0%	0%	0%	0%	0%	0%	0%	0%	0%	0%	0%	0%	0%	0%	0%	0%	0%	0%	0%	0%	0%	2%	0%	0%	0%	1%	0%	0%	0%	0%	
ins-18	0%	0%	0%	0%	0%	4%	1%	6%	3%	0%	0%	0%	0%	0%	0%	0%	0%	0%	0%	0%	0%	0%	0%	0%	0%	0%	0%	0%	0%	1%	
ins-19	0%	0%	0%	0%	0%	0%	0%	0%	0%	0%	0%	0%	0%	0%	0%	6%	0%	0%	0%	0%	0%	0%	0%	0%	0%	0%	0%	0%	0%	0%	0%
ins-20	0%	0%	0%	0%	0%	0%	0%	0%	0%	0%	0%	0%	0%	0%	0%	0%	2%	0%	0%	0%	0%	0%	0%	0%	0%	0%	0%	0%	0%	0%	0%
ins-21	0%	0%	0%	0%	0%	1%	20%	22%	32%	0%	0%	0%	0%	0%	0%	0%	0%	0%	0%	0%	0%	0%	0%	0%	0%	0%	0%	0%	0%	0%	
ins-22	0%	0%	0%	0%	0%	2%	0%	9%	10%	0%	0%	0%	0%	0%	0%	0%	0%	0%	0%	0%	0%	0%	0%	0%	0%	0%	0%	0%	0%	0%	0%
ins-23	0%	0%	0%	0%	0%	0%	0%	16%	17%	0%	0%	0%	0%	0%	0%	0%	0%	0%	0%	0%	0%	0%	0%	0%	0%	0%	0%	0%	0%	0%	0%
ins-24	0%	0%	0%	0%	0%	15%	0%	1%	1%	0%	0%	0%	0%	0%	0%	0%	0%	0%	0%	0%	0%	0%	0%	1%	0%	0%	0%	0%	0%	0%	0%
ins-25	0%	0%	0%	0%	0%	1%	0%	0%	0%	3%	1%	0%	0%	0%	0%	0%	0%	0%	0%	0%	0%	0%	0%	0%	0%	0%	0%	0%	0%	0%	0%
ins-26	0%	0%	0%	0%	0%	18%	0%	0%	0%	0%	0%	0%	0%	0%	0%	0%	0%	0%	0%	0%	0%	0%	0%	0%	0%	0%	0%	0%	0%	0%	0%
ins-27	0%	0%	0%	0%	0%	0%	4%	8%	2%	1%	1%	0%	1%	0%	0%	0%	0%	0%	0%	0%	1%	0%	0%	0%	0%	1%	2%	0%	0%	0%	0%
ins-28	0%	0%	0%	0%	0%	4%	0%	0%	0%	0%	0%	0%	0%	0%	0%	0%	0%	0%	0%	0%	0%	0%	0%	0%	0%	0%	0%	0%	0%	0%	0%
ins-29	0%	0%	0%	0%	0%	2%	0%	0%	0%	22%	0%	0%	0%	0%	0%	0%	0%	0%	0%	0%	0%	0%	0%	0%	0%	0%	1%	0%	0%	0%	0%
ins-30	0%	0%	0%	0%	0%	18%	0%	1%	0%	0%	0%	3%	0%	0%	0%	0%	0%	0%	0%	0%	0%	0%	0%	0%	0%	0%	0%	0%	0%	0%	0%
ins-31																															
ins-32	0%	0%	0%	0%	0%	9%	0%	0%	2%	0%	0%	0%	0%	0%	0%	0%	0%	0%	0%	0%	0%	0%	0%	0%	0%	0%	0%	0%	0%	0%	0%
ins-33	0%	0%	0%	0%	1%	0%	0%	0%	0%	0%	1%	0%	0%	0%	0%	1%	0%	0%	0%	0%	0%	0%	0%	0%	0%	0%	0%	50%	0%	0%	0%
ins-34	0%	0%	0%	0%	0%	0%	0%	0%	0%	0%	0%	0%	4%	0%	5%	0%	0%	0%	0%	0%	0%	14%	16%	0%	0%	0%	6%	0%	0%	0%	0%
ins-35	0%	0%	0%	0%	2%	3%	0%	20%	25%	0%	0%	0%	0%	0%	0%	0%	0%	0%	0%	0%	0%	0%	0%	0%	0%	0%	0%	0%	0%	0%	0%
ins-36	0%	0%	0%	0%	0%	0%	0%	0%	0%	2%	0%	0%	0%	0%	0%	0%	0%	0%	0%	0%	0%	0%	0%	0%	0%	0%	0%	0%	0%	0%	6%
ins-37	0%	8%	0%	0%	0%	4%	0%	3%	0%	0%	0%	1%	0%	8%	0%	19%	1%	0%	0%	0%	0%	0%	0%	0%	0%	0%	0%	0%	0%	0%	0%
ins-38																															
ins-39	0%	0%	0%	0%	0%	0%	0%	1%	19%	0%	0%	0%	0%	0%	0%	0%	0%	0%	0%	0%	0%	0%	0%	0%	0%	0%	0%	0%	0%	0%	0%
daf-28	0%	0%	0%	0%	0%	0%	1%	8%	10%	0%	0%	0%	0%	0%	0%	0%	0%	0%	0%	0%	0%	0%	0%	0%	0%	0%	0%	0%	0%	0%	0%

Gene	IL2_LR	LUA	M1	M2	M3	M4	M5	MC	MI	NSM	OLL	OLQ	PDA	PDB	PDE	PHA	PHB	PHC	PLM	PLN	PQR	PVC	PVD	PVM	PVN	PVP	PVQ	PVR	PVT	PVW
<i>ins-1</i>	5%	0%	0%	0%	0%	0%	0%	0%	0%	2%	0%	0%	0%	0%	0%	0%	0%	0%	0%	0%	0%	2%	0%	0%	0%	0%	0%	0%	0%	15%
<i>ins-2</i>	0%	0%	0%	0%	0%	0%	0%	0%	0%	0%	0%	0%	0%	0%	0%	0%	0%	0%	0%	0%	0%	0%	0%	0%	0%	0%	0%	0%	0%	0%
<i>ins-3</i>	0%	0%	0%	0%	0%	0%	0%	0%	0%	0%	0%	1%	0%	0%	0%	0%	0%	0%	0%	0%	0%	0%	0%	0%	0%	0%	0%	0%	0%	0%
<i>ins-4</i>	0%	0%	0%	0%	0%	0%	0%	0%	0%	0%	0%	0%	0%	0%	0%	0%	0%	0%	0%	0%	0%	0%	0%	0%	0%	0%	0%	0%	0%	0%
<i>ins-5</i>	0%	0%	0%	0%	0%	0%	0%	0%	0%	0%	0%	0%	0%	0%	0%	0%	0%	0%	0%	0%	0%	0%	0%	0%	0%	0%	0%	0%	0%	0%
<i>ins-6</i>	0%	0%	0%	0%	0%	0%	0%	0%	0%	0%	0%	0%	0%	0%	0%	0%	1%	0%	0%	0%	0%	0%	0%	0%	0%	0%	0%	0%	0%	0%
<i>ins-7</i>	0%	0%	0%	1%	0%	0%	0%	0%	0%	0%	0%	0%	0%	0%	0%	0%	0%	0%	0%	0%	0%	0%	0%	0%	0%	0%	0%	0%	0%	0%
<i>ins-8</i>																														
<i>ins-9</i>	0%	0%	0%	0%	0%	0%	0%	0%	0%	0%	0%	0%	0%	0%	0%	0%	0%	0%	0%	0%	0%	0%	0%	0%	0%	0%	0%	0%	0%	0%
<i>ins-10</i>	0%	0%	1%	1%	1%	26%	0%	25%	0%	0%	0%	0%	3%	0%	0%	0%	0%	0%	0%	0%	0%	0%	0%	1%	0%	0%	0%	0%	0%	0%
<i>ins-11</i>	1%	0%	0%	0%	0%	0%	0%	0%	0%	0%	0%	0%	0%	3%	0%	2%	0%	0%	0%	0%	0%	0%	0%	0%	0%	0%	0%	0%	0%	0%
<i>ins-12</i>	0%	0%	0%	0%	0%	0%	0%	0%	0%	0%	0%	0%	0%	0%	19%	28%	0%	0%	0%	0%	0%	0%	0%	0%	0%	0%	4%	0%	0%	0%
<i>ins-13</i>	0%	0%	0%	0%	0%	0%	0%	0%	0%	0%	0%	0%	0%	0%	0%	0%	0%	0%	0%	0%	0%	0%	0%	0%	0%	0%	0%	0%	0%	0%
<i>ins-14</i>	0%	0%	0%	0%	0%	0%	0%	0%	0%	0%	0%	0%	0%	0%	0%	0%	0%	0%	0%	0%	0%	0%	0%	0%	0%	0%	0%	0%	0%	0%
<i>ins-15</i>	0%	0%	0%	0%	0%	0%	0%	0%	0%	0%	0%	0%	0%	0%	0%	0%	0%	0%	0%	0%	0%	0%	0%	0%	0%	0%	0%	0%	0%	0%
<i>ins-16</i>	0%	0%	0%	0%	0%	0%	0%	0%	0%	0%	0%	0%	0%	0%	0%	0%	0%	0%	0%	0%	0%	0%	0%	0%	0%	0%	0%	0%	0%	0%
<i>ins-17</i>	0%	2%	0%	2%	0%	1%	1%	0%	3%	0%	0%	0%	0%	0%	0%	1%	1%	0%	0%	6%	0%	0%	0%	0%	0%	0%	0%	0%	0%	0%
<i>ins-18</i>	1%	4%	6%	3%	0%	2%	0%	0%	0%	0%	0%	0%	0%	0%	10%	9%	0%	2%	0%	1%	0%	0%	0%	0%	0%	0%	0%	6%	0%	0%
<i>ins-19</i>	0%	0%	0%	0%	0%	0%	0%	0%	0%	16%	0%	0%	0%	0%	0%	0%	0%	0%	0%	0%	0%	0%	0%	0%	0%	0%	0%	0%	0%	0%
<i>ins-20</i>	0%	0%	0%	0%	0%	0%	0%	0%	0%	0%	0%	0%	0%	0%	0%	0%	26%	0%	0%	0%	0%	27%	0%	9%	0%	0%	0%	0%	0%	0%
<i>ins-21</i>	0%	0%	0%	0%	0%	0%	0%	0%	0%	0%	0%	0%	0%	0%	0%	0%	1%	0%	0%	0%	0%	0%	0%	0%	0%	0%	0%	0%	0%	0%
<i>ins-22</i>	0%	0%	0%	0%	0%	0%	0%	0%	0%	0%	0%	0%	0%	0%	0%	0%	0%	0%	0%	0%	0%	0%	0%	0%	0%	0%	0%	0%	0%	0%
<i>ins-23</i>	0%	0%	0%	0%	0%	0%	0%	0%	0%	0%	0%	0%	0%	0%	0%	0%	0%	0%	0%	0%	0%	0%	0%	0%	0%	0%	0%	0%	0%	0%
<i>ins-24</i>	0%	0%	0%	0%	0%	0%	0%	0%	0%	0%	0%	0%	0%	0%	0%	0%	1%	0%	0%	0%	0%	0%	0%	0%	0%	0%	0%	0%	0%	0%
<i>ins-25</i>	0%	0%	19%	0%	0%	0%	0%	0%	0%	0%	0%	0%	0%	0%	0%	0%	0%	0%	0%	0%	0%	0%	0%	0%	0%	0%	0%	0%	0%	0%
<i>ins-26</i>	0%	0%	0%	0%	0%	0%	0%	0%	0%	0%	0%	0%	0%	0%	0%	0%	0%	0%	0%	0%	0%	0%	0%	0%	0%	0%	0%	0%	0%	0%
<i>ins-27</i>	0%	2%	0%	3%	0%	1%	0%	0%	0%	0%	0%	0%	0%	0%	0%	1%	0%	0%	0%	0%	0%	0%	0%	2%	0%	0%	0%	0%	0%	0%
<i>ins-28</i>	0%	0%	28%	0%	0%	12%	0%	0%	0%	0%	0%	0%	0%	0%	0%	0%	0%	0%	0%	0%	0%	0%	0%	0%	0%	0%	0%	0%	0%	0%
<i>ins-29</i>	0%	0%	5%	0%	0%	1%	0%	0%	0%	1%	0%	0%	0%	0%	0%	0%	0%	0%	0%	0%	0%	0%	0%	0%	0%	0%	0%	0%	0%	0%
<i>ins-30</i>	0%	0%	0%	0%	0%	0%	0%	0%	0%	0%	0%	0%	0%	0%	0%	0%	0%	0%	0%	0%	0%	0%	0%	0%	0%	0%	0%	0%	0%	0%
<i>ins-31</i>																														
<i>ins-32</i>	0%	0%	0%	0%	0%	0%	1%	0%	0%	0%	0%	0%	0%	0%	0%	0%	0%	0%	0%	0%	0%	0%	0%	0%	0%	0%	0%	0%	0%	0%
<i>ins-33</i>	0%	0%	0%	1%	0%	0%	0%	0%	0%	0%	0%	0%	0%	0%	0%	0%	0%	0%	0%	1%	0%	0%	0%	0%	0%	1%	0%	2%	0%	0%
<i>ins-34</i>	0%	0%	0%	4%	0%	0%	0%	0%	0%	0%	0%	0%	0%	0%	0%	0%	0%	0%	0%	0%	0%	0%	0%	0%	0%	0%	0%	0%	0%	0%
<i>ins-35</i>	0%	0%	0%	0%	0%	0%	0%	0%	0%	0%	0%	0%	0%	0%	0%	0%	0%	0%	0%	0%	0%	0%	0%	0%	0%	0%	0%	0%	0%	0%
<i>ins-36</i>	2%	0%	0%	0%	0%	0%	0%	0%	0%	0%	0%	0%	0%	0%	2%	11%	17%	0%	1%	0%	0%	0%	0%	0%	0%	0%	0%	0%	0%	0%
<i>ins-37</i>	0%	0%	0%	0%	0%	0%	1%	2%	0%	1%	0%	0%	0%	0%	0%	0%	0%	0%	0%	0%	0%	1%	0%	0%	0%	0%	0%	0%	0%	0%
<i>ins-38</i>																														
<i>ins-39</i>	0%	0%	0%	0%	0%	0%	0%	0%	0%	0%	0%	0%	0%	0%	0%	0%	3%	0%	0%	0%	0%	0%	0%	0%	0%	0%	0%	0%	0%	0%
<i>daf-28</i>	0%	0%	0%	0%	0%	0%	0%	0%	0%	0%	0%	0%	0%	0%	0%	0%	0%	0%	0%	0%	0%	0%	0%	0%	0%	0%	0%	0%	0%	0%

Gene	RIA	RIB	RIC	RID	RIF	RIG	RIH	RIM	RIP	RIR	RIS	RIV	RMD_DV	RMD_LR	RME_DV	RME_LR	RMF	RMG	RMH	SAA	SAB	SDQ	SIA	SIB	SMB	SMD	URA	URB	URX	URY
ins-1	2%	0%	0%	4%	0%	0%	0%	0%	0%	0%	0%	0%	0%	0%	0%	0%	0%	0%	0%	0%	0%	0%	0%	0%	0%	0%	0%	0%	0%	0%
ins-2	0%	0%	0%	0%	0%	0%	0%	0%	0%	5%	0%	0%	0%	0%	0%	0%	0%	0%	0%	0%	0%	0%	0%	0%	0%	0%	9%	2%	2%	0%
ins-3	0%	0%	0%	0%	0%	0%	0%	0%	0%	17%	0%	0%	0%	0%	0%	0%	0%	0%	0%	0%	0%	0%	0%	0%	0%	0%	2%	2%	0%	0%
ins-4	0%	0%	0%	0%	0%	0%	0%	0%	0%	2%	0%	0%	0%	0%	0%	0%	0%	0%	0%	0%	1%	0%	0%	0%	0%	0%	8%	3%	0%	0%
ins-5	0%	0%	0%	0%	0%	0%	0%	0%	0%	0%	0%	0%	0%	2%	0%	0%	0%	0%	0%	0%	0%	0%	0%	0%	0%	0%	0%	0%	0%	0%
ins-6	0%	0%	0%	0%	0%	0%	0%	0%	0%	0%	0%	0%	0%	0%	0%	0%	0%	0%	0%	0%	0%	0%	0%	0%	0%	0%	0%	0%	0%	0%
ins-7	0%	0%	0%	0%	0%	0%	0%	0%	0%	0%	0%	0%	0%	0%	0%	0%	0%	0%	0%	0%	0%	0%	0%	0%	0%	0%	0%	0%	0%	0%
ins-8																														
ins-9	0%	0%	0%	0%	0%	0%	0%	0%	0%	0%	0%	0%	0%	0%	0%	0%	0%	0%	0%	0%	0%	0%	0%	0%	0%	0%	0%	0%	0%	0%
ins-10	0%	0%	0%	0%	0%	0%	0%	0%	0%	0%	0%	0%	0%	0%	0%	0%	0%	0%	0%	0%	0%	0%	0%	0%	0%	0%	0%	0%	0%	0%
ins-11	0%	0%	0%	0%	0%	0%	0%	2%	0%	0%	0%	0%	0%	0%	31%	1%	0%	0%	0%	0%	0%	0%	0%	0%	0%	0%	0%	0%	0%	0%
ins-12	0%	0%	0%	0%	0%	0%	0%	0%	0%	0%	0%	0%	0%	0%	0%	1%	0%	0%	0%	0%	0%	0%	0%	0%	0%	0%	0%	0%	0%	0%
ins-13	0%	0%	0%	0%	0%	0%	0%	0%	0%	0%	0%	0%	0%	99%	0%	0%	0%	0%	0%	0%	0%	0%	0%	0%	0%	0%	0%	0%	0%	0%
ins-14	0%	0%	0%	0%	0%	0%	0%	0%	0%	0%	0%	0%	0%	0%	0%	0%	0%	0%	0%	0%	0%	0%	0%	0%	0%	0%	0%	0%	0%	0%
ins-15	0%	0%	0%	0%	0%	0%	0%	0%	0%	0%	0%	0%	0%	0%	0%	0%	0%	0%	0%	0%	0%	0%	0%	0%	0%	0%	0%	0%	0%	0%
ins-16	0%	0%	0%	0%	0%	0%	0%	0%	0%	0%	0%	0%	0%	0%	0%	0%	0%	0%	0%	0%	0%	2%	0%	15%	1%	0%	0%	0%	0%	0%
ins-17	0%	0%	0%	3%	5%	0%	0%	0%	0%	0%	0%	0%	0%	0%	0%	1%	0%	3%	0%	0%	0%	0%	0%	8%	0%	0%	0%	0%	0%	0%
ins-18	0%	0%	0%	0%	0%	0%	0%	0%	0%	2%	0%	0%	0%	0%	0%	0%	0%	3%	0%	0%	0%	0%	0%	0%	0%	0%	1%	0%	0%	
ins-19	0%	0%	0%	0%	0%	0%	0%	0%	0%	0%	0%	0%	0%	0%	0%	0%	0%	0%	0%	0%	0%	0%	0%	0%	0%	0%	0%	0%	0%	0%
ins-20	0%	0%	0%	0%	0%	0%	0%	0%	0%	0%	0%	3%	0%	0%	0%	0%	0%	0%	0%	0%	0%	0%	0%	0%	0%	7%	0%	0%	0%	0%
ins-21	0%	0%	0%	0%	0%	0%	0%	0%	0%	0%	0%	0%	0%	0%	0%	0%	0%	0%	0%	0%	0%	0%	0%	0%	0%	0%	0%	0%	0%	1%
ins-22	0%	0%	0%	0%	0%	0%	0%	0%	0%	0%	0%	0%	0%	0%	0%	0%	0%	0%	0%	0%	0%	0%	0%	0%	0%	0%	0%	0%	0%	0%
ins-23	0%	0%	0%	0%	0%	0%	0%	0%	0%	0%	0%	0%	0%	0%	0%	0%	0%	0%	0%	0%	0%	0%	0%	0%	0%	0%	0%	0%	0%	0%
ins-24	0%	10%	0%	0%	0%	0%	0%	0%	0%	0%	0%	0%	0%	0%	0%	0%	0%	0%	0%	0%	0%	0%	0%	0%	0%	0%	0%	0%	0%	0%
ins-25	0%	0%	9%	0%	0%	1%	8%	0%	1%	10%	0%	0%	0%	0%	0%	0%	0%	0%	0%	0%	0%	0%	0%	0%	0%	0%	0%	0%	0%	0%
ins-26	0%	0%	0%	0%	0%	0%	0%	0%	0%	0%	0%	0%	0%	0%	0%	0%	0%	0%	0%	0%	0%	0%	0%	0%	0%	0%	0%	0%	0%	0%
ins-27	0%	9%	3%	0%	0%	1%	10%	0%	3%	1%	6%	0%	0%	0%	1%	0%	0%	0%	0%	0%	0%	0%	0%	0%	0%	0%	0%	0%	4%	0%
ins-28	0%	0%	0%	0%	0%	0%	0%	0%	0%	0%	0%	0%	0%	0%	0%	0%	0%	0%	0%	0%	0%	0%	0%	0%	0%	0%	0%	0%	0%	0%
ins-29	0%	0%	5%	0%	0%	0%	3%	0%	0%	10%	0%	0%	0%	0%	0%	0%	0%	0%	0%	0%	0%	0%	0%	0%	0%	0%	0%	0%	1%	0%
ins-30	0%	1%	0%	0%	0%	0%	0%	0%	0%	0%	0%	0%	0%	0%	0%	0%	0%	0%	0%	0%	0%	0%	0%	0%	0%	0%	0%	0%	0%	0%
ins-31																														
ins-32	0%	0%	0%	0%	0%	0%	0%	0%	0%	0%	0%	0%	0%	0%	0%	0%	0%	0%	0%	0%	0%	0%	0%	0%	0%	0%	0%	0%	0%	0%
ins-33	0%	0%	0%	0%	0%	0%	0%	0%	0%	0%	0%	1%	2%	0%	0%	1%	0%	1%	5%	0%	0%	0%	0%	0%	1%	0%	0%	3%	15%	0%
ins-34	0%	0%	0%	4%	0%	3%	0%	0%	0%	0%	0%	15%	0%	0%	0%	0%	0%	0%	0%	0%	0%	2%	0%	1%	0%	12%	0%	2%	0%	0%
ins-35	0%	0%	0%	0%	0%	0%	0%	0%	0%	0%	0%	0%	0%	0%	0%	0%	0%	0%	0%	0%	0%	15%	0%	0%	0%	0%	0%	0%	0%	3%
ins-36	0%	0%	0%	0%	0%	0%	2%	0%	0%	0%	0%	0%	0%	0%	0%	0%	0%	0%	0%	0%	0%	0%	0%	0%	0%	10%	0%	1%	0%	0%
ins-37	0%	0%	0%	0%	0%	1%	0%	0%	0%	0%	0%	0%	0%	0%	0%	0%	5%	0%	0%	1%	12%	0%	0%	0%	0%	0%	0%	0%	0%	0%
ins-38																														
ins-39	0%	0%	0%	0%	0%	0%	0%	1%	0%	0%	0%	0%	1%	0%	0%	0%	0%	0%	0%	0%	0%	0%	0%	0%	0%	0%	0%	0%	0%	0%
daf-28	0%	0%	0%	0%	0%	0%	0%	0%	0%	4%	0%	0%	0%	0%	0%	0%	0%	0%	0%	0%	0%	0%	0%	0%	0%	0%	2%	2%	0%	0%

Gene	VA	VA12	VB	VB01	VB02	VC	VC_4_5	VD_DD	
<i>ins-1</i>	0%	0%	0%	0%	0%	0%	0%	0%	100%
<i>ins-2</i>	0%	0%	0%	0%	0%	0%	0%	0%	100%
<i>ins-3</i>	0%	0%	0%	0%	0%	0%	0%	0%	100%
<i>ins-4</i>	0%	0%	0%	0%	0%	0%	0%	0%	100%
<i>ins-5</i>	0%	0%	0%	0%	0%	0%	0%	0%	100%
<i>ins-6</i>	0%	0%	0%	0%	0%	0%	0%	0%	100%
<i>ins-7</i>	0%	0%	0%	0%	0%	0%	0%	0%	100%
<i>ins-8</i>									
<i>ins-9</i>	0%	0%	0%	0%	0%	0%	0%	0%	100%
<i>ins-10</i>	0%	0%	0%	0%	0%	0%	0%	0%	100%
<i>ins-11</i>	1%	0%	0%	0%	0%	0%	0%	0%	100%
<i>ins-12</i>	0%	0%	0%	0%	0%	0%	0%	0%	100%
<i>ins-13</i>	0%	0%	0%	0%	0%	0%	0%	0%	100%
<i>ins-14</i>	0%	0%	0%	0%	0%	0%	0%	0%	100%
<i>ins-15</i>	0%	0%	0%	0%	0%	0%	0%	0%	100%
<i>ins-16</i>	0%	0%	0%	8%	2%	0%	0%	0%	100%
<i>ins-17</i>	0%	0%	0%	0%	0%	0%	0%	0%	100%
<i>ins-18</i>	0%	0%	0%	0%	0%	0%	0%	0%	100%
<i>ins-19</i>	0%	0%	0%	0%	0%	0%	0%	0%	100%
<i>ins-20</i>	0%	0%	0%	0%	0%	0%	0%	0%	100%
<i>ins-21</i>	0%	0%	0%	0%	0%	0%	0%	0%	100%
<i>ins-22</i>	0%	0%	0%	0%	0%	0%	0%	0%	100%
<i>ins-23</i>	0%	0%	0%	0%	0%	0%	0%	0%	100%
<i>ins-24</i>	0%	0%	0%	0%	0%	0%	0%	0%	100%
<i>ins-25</i>	0%	0%	0%	0%	0%	0%	0%	0%	100%
<i>ins-26</i>	0%	0%	0%	0%	0%	0%	0%	0%	100%
<i>ins-27</i>	0%	1%	0%	0%	0%	0%	0%	0%	100%
<i>ins-28</i>	0%	0%	0%	0%	0%	0%	0%	0%	100%
<i>ins-29</i>	0%	0%	0%	0%	0%	0%	0%	0%	100%
<i>ins-30</i>	0%	0%	0%	0%	0%	0%	0%	0%	100%
<i>ins-31</i>									
<i>ins-32</i>	0%	0%	0%	0%	0%	0%	0%	0%	100%
<i>ins-33</i>	2%	0%	2%	1%	1%	0%	0%	1%	100%
<i>ins-34</i>	0%	0%	0%	1%	1%	0%	0%	0%	100%
<i>ins-35</i>	0%	0%	0%	0%	0%	0%	0%	1%	100%
<i>ins-36</i>	0%	0%	0%	0%	0%	0%	0%	1%	100%
<i>ins-37</i>	3%	0%	5%	0%	1%	0%	0%	0%	100%
<i>ins-38</i>									
<i>ins-39</i>	0%	0%	0%	0%	0%	0%	0%	0%	100%
<i>daf-28</i>	0%	0%	0%	0%	0%	0%	0%	0%	100%

4. Post-hoc analysis p-values of nictation assays

Table 1: Post-hoc analysis p-values of ILP mutant strains after 3 nictation assays. Significant values are indicated with an asterisks ($p < 0.05$).

	Nictation ratio	Nictation ratio only nictating	Initiation index	Average duration
<i>Ins-17 OE</i>	0.55328	0.5203	0.8186	0.77541
<i>Ins-39 OE</i>	0.00989*	0.0301*	0.0898	0.39912
<i>Ins-15 OE</i>	0.63641	0.6571	0.5957	0.99847
<i>Ins-36 OE</i>	0.34847	0.7311	0.1304	0.99926
<i>Ins-21 OE</i>	0.99360	1.0000	0.6323	0.99790
<i>Ins-37 OE</i>	0.94135	0.8499	1.00000	0.83039
<i>Ins-38 OE</i>	0.98979	0.6978	0.9999	0.85249
<i>Ins-19 OE</i>	0.02773*	0.1019	0.0724	0.68387
<i>Ins-19 KO</i>	0.48516	0.5674	0.3262	0.99999
<i>Ins-17 KO</i>	0.04976*	0.0233*	0.4348	0.04171*
<i>Ins-4 KO</i>	1.00000	1.0000	1.0000	1.00000
<i>Ins-1 KO</i>	0.34085	0.4658	0.9998	<1e-04*
<i>Ins-6 KO</i>	1.00000	0.9631	0.9999	0.00133*

Table 2: Post-hoc analysis p-values of ILP mutant strains after 5 nictation assays. Significant values are indicated with an asterisks ($p < 0.05$).

	Nictation ratio	Nictation ratio only nictating	Initiation index	Average duration
<i>Ins-17 OE</i>	0.0239*	0.0287*	0.0724	0.0981
<i>Ins-39 OE</i>	0.6367	0.8733	0.9968	0.5817
<i>Ins-36 OE</i>	0.1568	0.1535	0.0345*	0.9427
<i>Ins-19 OE</i>	0.0838	0.1345	0.0391*	0.6427
<i>Ins-17 KO</i>	0.4480	0.1635	0.8415	0.1669
<i>Ins-19 KO</i>	0.0659	0.1101	0.0892	0.2960

AFDELING
Straat nr bus 0000
3000 LEUVEN, BELGIË
tel. + 32 16 00 00 00
fax + 32 16 00 00 00
www.kuleuven.be

